UNIVERSITY OF TRENTO - ITALY

INTERNATIONAL DOCTORATE SCHOOL IN INFORMATION AND COMMUNICATION TECHNOLOGIES

PHD THESIS

to obtain the title of

PhD in ICT

of the University of Trento - Italy

Speciality : Telecommunication

Defended by

Karina Mabell Gomez Chavez

Energy Efficiency in Wireless Access Networks: Measurements, Models and Algorithms

Thesis Advisor: Prof. Imrich Chlamtac

prepared at CREATE-NET Trento–Italy, iNSPIRE Team

defended on April, 2013

Jury :

Advisor:	Prof. Imrich Chlamtac	-	CREATE-NET (Italy)
Co–Advisor:	Prof. Fabrizio Granelli	-	University of Trento (Italy)
	Dr. Daniele Miorandi	-	CREATE-NET (Italy)
Examinators:	Prof. Khaldoun Al Agha	-	Universite Paris-Sud (France)
	Prof. Jose Moreno	-	Carlos III University (Spain)
	Prof. Cigdem Sengul	-	Brookes University (United Kingdom)

Energy Efficiency in Wireless Access Networks: Measurements, Models and Algorithms

Abstract:

Wireless Telecommunication networks have become fundamental to daily activities. Today, people have access to at least one type of wireless telecommunication network. In this context, optimizing the energy consumption of wireless telecommunications infrastructure has become a new challenge for the research community, governments and industries in order to reduce CO_2 emission and operational energy costs. This thesis investigates the power consumption of indoor/outdoor Wireless Access Devices (WADs, specifically WiFi and WiMAX access points) and provides novel techniques for improving the energy efficiency of wireless access networks. Our approach focuses on monitoring and analyzing the power consumption of WADs using real–testbed and experimental measurements in order to understand the fundamental limits and trade-offs involved. This, in turn, will be used to propose efficient techniques to reduce power consumption and to maximize the energy efficiency of wireless access networks. We introduce *energino* a novel hardware and software solution for real–time energy consumption monitoring in wireless networks. We also propose an experimentally–driven approach to (i) characterize typical WADs from a power consumption standpoint, (ii) develop simple and accurate power consumption models and metrics for such WADs, and (iii) design techniques to tune the power consumption of a wireless infrastructure to the actual network conditions in terms of both users density and traffic patterns. Our measurements from several real–life deployments show that (a) the power consumption of such WADs exhibits a linear dependence on the traffic until a saturation point is reached and (b) the developed techniques can deliver significant energy savings with minimal degradation in terms of the quality of service provided.

Keywords: Energy Efficiency, Wireless Access Networks, *energino*, Power Consumption Models, WiFi, WiMAX, *morfeo*

This page is intentionally left blank

Esta tesis esta dedicada al ser maravilloso de la tierra, a quien dedico mi primer pensamiento en la mañana y en ultimo pensamiento de la noche. Por darme el amor mas puro y maravilloso, y por ser mi todo en todos los momentos de mi vida.

Para mi madre Zoila Hilda Chavez

This page is intentionally left blank

Acknowledgments

This dissertation would not have been possible without the guidance and the help of several individuals who in one way or another contributed and extended their valuable assistance in the preparation and completion of this study.

First at all, I would like to take the opportunity to thank my advisor Prof. Imrich Chlamtac and co–advisor Prof. Fabrizio Granelli for helping to improve my work through their advice and ideas.

I would like also to thank Dr. Daniele Miorandi and Dr. Tinku Rasheed for their kind, responsible and understanding advises during the process of this thesis giving some advice and ideas to accomplish this thesis. I am grateful to Dr. Roberto Riggio for the valuable comments, discussions and support related to the topics investigated in this Thesis. Without their continuous support all this would have been not possible.

Furthermore, I would like to thank Dr. Cigdem Sengul for the valuable comments and discussions related to the power model and *morfeo* algorithm and for allowing to use the BOWL Testbed infrastructure for the measurements of IEEE 802.11n Indoor presented in Chapter 4, 5 and 6.

I would like also to thank Dr. Nico Bayer for the valuable comments and discussions related to *morfeo* algorithm and for allowing to use the outdoor testbed deployed at Telekom Innovation Laboratories in Berlin, Germany, for the measurements of IEEE 802.11g Outdoor presented in Chapter 4 and 6.

I would like to express my gratitude to my colleagues and friends from the CREATE–NET Research Centre for the moral support. Last but not the least, my family, Andrea and friends for their support and encouragement during this years of study, thank you so much.

Karina Mabell Gomez Chavez

Italy, April 2013

This page is intentionally left blank

Contents

List of Figures

List of Tables

List of Equations

List of Algorithms

This page is intentionally left blank

Chapter 1

Introduction

Contents

1.1 Motivations

According to a number of climate studies [gw1 , Watanabe 2012, gw3], the 20th century's last two decades were the hottest in 400 years and possibly the warmest for several millenniums, so behavior of the past human generations cannot be the cause of the current global warming. However, this is not the case of the new human generation behavior which have huge impact on global warming mainly due to the technological boom occurred across the last century. *Global warming* is a hot topic, the projected impact of global warming often makes headlines [gw2]. The potentially disastrous effects of even a few degree temperature rise may cause the disappearance of island countries into the ocean, polar ice melts, sea level rises and hurricanes and tropical storms may intensify, to name a few [gw1 , Watanabe 2012, gw3 , gw2].

In other hand, the cost of the electricity is increasing every year, authors in [**?**] concluded that, in USA, the history of coal–fired electricity suggests that there is a fluctuating floor to its future costs, which is determined by coal prices. Since coal is a limited natural resource then the coal prices will increase in the future [iee]. Similar tendency is observed in the European countries, a statistical study regarding electricity and natural gas price supported by the European Commission [ec] reports that electricity increased in the last three years, from 2010 to 2012, and it will continue increasing in the coming years. It will have a dramatic impact on the communication service prices specially on those countries that are importing their energy such as Italy and Cyprus, which actually have the highest industries electricity prices in the Europe Union [ec]. Therefore, considering the environmental and economical motivations explained before, one of the most urgent challenges in the new century for current and future human generations is to investigate and introduce new energy efficiency technologies that can enable a transition towards a more sustainable society with a reduced CO_2 footprint.

We all know that modern society is more dependent on strong and efficient communication means; several daily activities has been planned using communication infrastructure. Social networks, such as Facebook and twitter, Software applications and Internet in general are the most attractive and instantaneous access media to be used for common individuals in order to communicate human feelings, news, sharing pictures-files and hundreds of others services. This tendency is increasing exponentially the traffic volumes, i.e. the amount of traffic volumes in wireless network increases from 300% to 700% annually [Micallef 2010]. The recent smartphone, tablet and laptop revolution are also contributing to this phenomena. For instance, the number of WiFi APs deployed are increasing exponentially [Jardosh 2009] due to the necessity of provided Internet connectivity for users anywhere and anytime mainly for business scope.

Energy efficiency in Information and Communication Technology (ICT) infrastructures is becoming a top priority for industries, governments and scientific communities alike. Although, due to the number of variables involved, it is hard to find definitive figures on the impact of the ICT sector on the global CO_2 emissions, it is widely accepted that such impact is non–negligible and that by 2020 it could range from 2% up to 10% of the worldwide carbon emissions [RFG 2008, sma 2010, GAP 2012]. Isolating the impact of the Telecoms is even more problematic. In [sma 2010] it is estimated that by 2020 the Telecom infrastructure and devices alone would account for about the 25% of the ICT sector's CO_2 emissions and that mobile networks will be responsible for about half of those emissions. In [RFG 2008], a relevant analysis of the electricity consumption of the ICT sector is reported, for the reference year 2005 by the European Union (EU), where the total electricity consumption related to ICT infrastructure and ICT end–user–equipment was 216,0 TWh/year. This is equivalent to 7.8% of the total electricity consumption in the EU. Additionally, [RFG 2008] reports a forecast for the year 2020 of the total electricity consumption related to ICT sector. It will be 433.1 TWh/year, which will represent 10.9% total electricity consumption in the EU. Therefore, the challenge of the European Commission is to reduce at least 20% of Europe's energy consumption by 2020. In order to achieve the challenge, the EC has financed more than 30 research projects working on energy efficiency in ICT [EUF]. The research community is also collaborating to save energy consumption. In the last three years, green technologies became the new topic including in several conferences and initiatives[1] in order to research solutions.

1.2 Research Questions

Network topology, transmission media, packet processing and coverage considerations are some of the key aspects governing energy efficiency at the network and device level. However, data reveals a large expenditure of energy on the radio access network. The paradigm shift from "*always on*" network to "*always available*" under similar time constraints is gaining importance. This is due to the fact that, the periods of extended underutilization can be predictable, detected and utilized for additional energy savings. At this point, the use of different operation modes in Wireless Access Devices (WAD) (referred as WAD, which can be an Access Point or Base Station) are mandatory for energy saving in wireless access networks. However, the achievable savings are not easily quantifiable and there are some open questions in this field (i) which *metric* to use in order to decide which network is more energy efficient compared to another network?, and (ii) how to understand *how much energy* is consumed by a specific network for specific operations? Accordingly, it is important both to define energy efficiency metrics as well as power consumption trends in order to migrate toward the new green technologies generation. In this Thesis we address the following questions:

(a) *Where is the power used in WADs?*

(b) *How is the power consumed in WADs? How much of the power is wasted?*

(c) *How much of the wasted power could be saved?*

(d) *What are future trends (that affect energy use and waste)?*

(e) *Which are the critical aspects of standards with respect to power consumption?*

(f) *Which is the relationship between power consumption and performance in the network?*

(g) *Under which conditions it is possible to put the WADs in different operation modes?*

(h) *How the time for switching between the different operation modes affect the network performance?*

(i) *Which network architectures allows to introduce different operation modes?*

It is the Author's standpoint that the answers to these questions are very important since they would provide us with an increased insight into the network behaviour, paving the way to the development of (i) experimental–methods for understanding the network behavior in terms of power consumption (see Chapter 3

[1]Green Touch Industry–driver Initiative. Available at: http://www.greentouch.org

and Chapter 4), (ii) realistic metrics and models for power consumption in wireless access networks (see Chapter 5) and (iii) energy efficiency protocols and algorithms for their operations (see Chapter 6).

1.3 Research Methodology

In order to answer the research questions outlined previously, we apply the *quantitative experimental method* for understanding the power consumption behavior of WADs and the reasons that govern such behavior in order to identify **where** and **how** the power of WADs is consumed. Our *quantitative experimental method* aims to investigate the outlined research questions looking at potential relationships between variables including the power consumption, the transmission power level, the datagram size and the modulation and coding schemes, and specially the traffic load.

In our *quantitative experimental method*, *energino* power meter is used as the data collection instrument. Energino is an hardware and software solution for real–time power consumption monitoring of WADs (see Chapter 3). Using this data collection instrument, we create a real testing environment and performed several experiments, which are explained in detail in the Chapter 4 for producing results used for summarizing, comparing, and generalizing the power consumption behavior of WADs. Statistics derived from *quantitative experimental method* results are used to establish the existence of associative or causal relationships between variables (see Chapter 5). Finally, the *quantitative experimental method* results and outputs help us to propose efficient techniques for reducing energy wastage and improving the energy efficiency of the wireless access networks (see Chapter 5).

1.4 Contributions and Outline

The main contributions of this Thesis are:

(i) Design and development of *energino*, a novel hardware and software solution for real–time energy consumption monitoring in wireless access networks.

(ii) Propose a methodology to characterize energy consumption of WADs as a function of (a) the traffic load, (b) the modulation and coding schemes, (c) the size of the datagram used and (d) different transmission power levels.

(iii) Identify and develop meaningful metrics in order to evaluate network energy efficiency in wireless access networks.

(iv) Propose a simple and accurate power consumption model for the WADs which is validated by experimental measurements with real WADs using different parameter settings.

(v) Design and implement energy–saving architectures, techniques and algorithms for reducing the energy consumption of wireless access networks.

The rest of the Thesis is organized as follows. Chapter 2 discusses the state of the art of the related topic to this Thesis while Chapter 3 introduces energino an hardware and software solution for power consumption monitoring of DC-devices. In Chapter 4 the power consumption behavior of WADs working with WiFi and WiMAX technologies are presented and Chapter 5 describes several energy and power consumption metrics and models for wireless access devices. Then, Chapter 6 summarizes the proposed energy–saving solutions for wireless access networks discussed in this Thesis. Finally, Chapter 7 draws conclusions and describes the future work.

Below we will provide a more detailed overview of each Chapter. List of Author's Publications and Abbreviations are provided in the appendix of this Thesis.

1.4.1 Chapter 2: State of the Art

In Chapter 2, we discuss the state of the art. We present an overview of the related work on tools and methodologies for power consumption measurements, the power consumption models and the energy efficiency improvements proposed for WADs.

1.4.2 Chapter 3: Hardware and Software Solution for Power Consumption Monitoring of Wireless Access Networks

In Chapter 3, we introduce *energino* a scalable and affordable solution for energy consumption monitoring in wireless networks. The *energino* power meter is a standalone plug–load meter based on the Arduino platform providing high resolution and sampling rate capabilities. We evaluate the capabilities and distinctive features of the *energino* power meter in real–circuits. Results show that *energino* is capable of isolating high resolution/frequency dynamics that can not be analyzed using commercially available tools.

The main contents of this Chapter have been published in paper [Gomez 2012b]. The prototype of *energino* was implemented and evaluated by the author of this Thesis under the supervision of Dr. Roberto Riggio. We also release both the hardware schematics and the software with a permissive license in order to encourage the research community to use and extend it.

1.4.3 Chapter 4: Power Consumption Behavior of Wireless Access Devices (WiFi and WiMAX Technologies)

In Chapter 4 the power consumption behavior of WADs working with different technologies is presented. We propose an experimentally–driven approach to characterize typical indoor/outdoor WADs from an energy consumption standpoint. We focused our attention on the monitoring, measurement and analysis of the energy consumption patterns of WiFi and WiMAX WADs. We target the characterization of the power consumption of WiFi and WiMAX WADs in terms of (i) the amount of traffic sent/received by the WAD, (ii) the modulation and coding schemes used, (iii) the size of the session level data units and (iv) transmission power levels. The analysis and comparison of the power consumption behavior between IEEE 802.11g–IEEE 802.11n Indoor WAD is also presented in this Chapter. Our measurements show that the power consumption of such WADs exhibits a linear dependence on the traffic until a saturation point is reached.

The contributions of this Chapter have been previously published in paper [Gomez 2012a]. The author of this Thesis was responsible for the design, implementation and evaluation of the measurements campaign using *energino*.

1.4.4 Chapter 5: Energy and Power Consumption Metrics and Models for Wireless Access Devices

In Chapter 5, we describe several energy and power consumption metrics and models for WADs. We propose specific power consumption models and metrics for application level estimation of energy consumption for designing energy–aware wireless network. In particular, we implement a simple and realistic power consumption models for WADs, which reflect the power consumption in various functioning states and during transitions between states of the WAD. By applying the power consumption models, we are able to evaluate and analyze the energy efficiency of various WADs. Experimental measurements with real WADs validated the proposed metrics and models.

The models and results of this Chapter have been published in [Gomez 2011, Gomez 2012a]. The author of this Thesis formulated the models, carried out all the measurements and analyzed of results.

1.4.5 Chapter 6: Energy–Saving Solutions for Wireless Access Networks

In Chapter 6, we summarize the proposed energy–saving solutions for WADs discussed in this Thesis. We present *morfeo* a flexible energy–saving decision algorithm to tune the energy consumption of a wireless infrastructure to the actual network conditions in terms of both user density and traffic patterns. Experimental results from a real–life deployment shows that our solution can deliver significant energy savings with minimal degradation in terms of the quality of service provided.

Part of the content of this Chapter have been published in paper [Riggio , Gomez 2013]. The solution algorithms were devised, implemented and evaluated by the author of this Thesis.

This page is intentionally left blank

Chapter 2

State of the Art

Contents

In this Chapter, we present an overview of the related work on (i) tools and methodologies for power consumption measurements, (ii) the power consumption models and (iii) the energy efficiency improvements proposed for WADs.

2.1 Power Consumption Measurements: Tools and Methodologies

Energy consumption measurements of complete devices have been performed mainly for mobile phones [Rice 2010] and Network Interface Cards (NICs) [Feeney 2001, Ebert 2002, Halperin 2010]. In this section, we focus on the tools and methodologies used in order to perform real–time power consumption measurements while the power consumption models and main observations of these works will be explained in the next section.

In [Carroll 2010], a detailed analysis of the power consumption of a recent mobile phone, the Openmoko Neo Freerunner is presented. The authors measure the overall system power as well as the exact breakdown of power consumption by the main hardware components of the device. In order to calculate the power consumed by the phone, both the supply voltage and current are measured experimentally. Firstly, the authors measure the current inserting a sensing resistor on the power supply rails of the relevant components–this is relatively simple on the device–under–test selected, since most of them have been designed with placeholders for sense resistors. Authors used a current-sense resistor selected such that the peak voltage drop did not exceed 10mV, which in all cases is less than 1% of the supply voltage and therefore presents an acceptably small perturbation. With a known resistance and measured voltage drop, current is determined by Ohm's law. In order to measure the voltages, a National Instruments PCI–6229 Data Acquisition Module[1] is used. Using the experimental testbed, the real traffic logs are collected together with the power consumption of the phone.

[1] Available at: http://sine.ni.com/nips/cds/view/p/lang/en/nid/14136

In [Halperin 2010], measurements of the power consumption of an 802.11n NIC across a broad set of operating states (channel width, transmit power, rates, antennas, Multiple–Input/Multiple–Output (MIMO) streams, sleep, and active modes) are reported. The NIC used in the experiments is available in a mini-PCI Express form factor, which was connected to the desktop–testbed–node via an adapter that converts to a PCI Express interface. To measure the power consumption, the authors placed a resistor (40Ω) on the 3.3V power supply to the wireless interface. A National Instruments 6218 Data Acquisition Module (NIDAM)[2] was used in order to measure and record the voltage drop across the resistor. Thus, the power consumed by the wireless interface was calculated using the data recorded with NIDAM. In order to inject traffic in the experimental testbed, packets with 1500 bytes are generated and logged several times. Then, the average of multiple collecting samples was used for estimating the instantaneous power consumption of the NIC (i) during transmission or reception, and (ii) for sleep and idle modes.

In [Rice 2010], authors ran a large number of automated tests using Google Android G1, Magic, Hero and Nexus handsets and present results for the average energy consumption of connection and data transmission over 802.11 wireless networks. The phone's power consumption is measured by inserting a high-precision 0.02Ω measurement resistor in series between a battery terminal and its connector on the phone. A National Instruments PCI-MIO-16E-4[3] sampling board is used in order to measure the voltage across the phone battery and also the voltage drop across the measurement resistor at 250 kHz. Inserting the measurement resistor increases the circuit resistance, and therefore its power consumption. This is not a problem for measurements purposes as this is typically less than 1% of the total power. Then the current is determined by Ohm's law.

The tools and methodologies used by [Carroll 2010, Halperin 2010, Rice 2010] for measuring the energy consumption of wireless devices are similar and suitable to be used in laboratory tests. However, these solutions are not suitable at moment to scale the experiments to real–time power monitoring in deployed testbed. Other similar approaches for energy consumption monitoring suitable to be used in laboratory tests are explained in [Feeney 2001, Ebert 2002]. These works perform high resolution and high frequency sampling using a digital oscilloscope. However such solution is expensive and hard to integrate in distributed networks due to typically bulky laboratory equipments. On the other hand, for battery–powered devices the energy consumption of the such devices can be derived from the battery discharge as explained in [Rantala 2009, Lochin 2003, Pathak 2011]. However, this solution cannot be applied for the majority of the wireless networking devices since these devices are often not battery–powered.

In order to measure the whole power consumption of devices, commercial products can be used. In particular, several plug–load power meters are available as off–the–shelf solutions, they are all characterized by low frequency and low reso-

[2]Available at: http://sine.ni.com/nips/cds/view/p/lang/en/nid/203484

[3]Available at: http://sine.ni.com/nips/cds/view/p/lang/en/nid/10795

lution sampling capabilities. The *Watts Up!* [wat] and Expert Power Controller (EPC) [EPC] power meters are an example of commercial solutions. *Watts Up!* and EPC are "plug load" power meters that measures the amount of electricity used by whatever electrical appliance is plugged into it. Such measurements, taken with a granularity of 0.1W and a sampling period of 1s, can be logged into the device's internal memory or they can be exported using either an Ethernet port or a serial interface. Nevertheless, such specifications proved to be insufficient to catch dynamics occurring at the transition point between linear and saturation power consumption regimes are shown in our previous works [Gomez 2011, Gomez 2012a].

2.2 Power Consumption Models of Wireless Access Devices

Real–world energy consumption measurements of wireless networking devices have not been performed often in the past. This, in turn, led to unrealistic and/or over–simplified models being used in simulations.

In [Feeney 2001], the authors present several measurements for an IEEE 802.11a–based wireless network interface operating in idle, sleep, receive and transmit modes. Such measurements are obtained using an oscilloscope. In the work, the per–packet energy consumption E is approximated using a linear model given by:

$$E = m \cdot S + b \tag{2.1}$$

Where,

- S is the length of the packet,
- m represent the values of the linear coefficients,
- b is a constant and it must be determined experimentally for various operation modes,

The authors conclude that the energy consumption of an IEEE 802.11a wireless interface has a complex range of behaviors according to several factors such as relative proportions of broadcast and point-to-point traffic, packet size and reliance on promiscuous mode operations. The behavior of power consumption as a function of packet size is shown to follow a linear behavior. However, the model does not consider the case of link–layer fragmentation and the impact of the different amount of traffic on power consumption figures.

Similar work in terms of methodology is presented in [Ebert 2002]. The paper presents several results for power consumption of an IEEE 802.11b wireless network interface. The scenario was built using two laptops with WLAN interfaces and an oscilloscope in order to monitor power consumption on the wireless interface. The authors do not provide a power consumption model but they derive a novel metric from their measurements. The metric is the energy per bit goodput $E_{bit-good}$ given by:

$$E_{bit-good} = \frac{Average_{CP}}{Goodput} \tag{2.2}$$

Where,

- $Goodput$ indicates the (MAC) goodput (expressed in [Bit/s]), it must be recorded simultaneously with the power consumption measurements ($Average_{CP}$);

- $Average_{CP}$ indicates the power consumption measurements (expressed in [W]);

- $E_{bit-good}$ indicates the amount of energy expenditure in order to transmit one bit of payload data successfully (expressed in [J/Bit]);

The authors also conclude that large packets use energy more efficiently than small ones as well as high modulation schemes are more energy efficient. In contrast to our work, the impact of traffic on power consumption figures is not considered for the Authors.

In [Halperin 2010], the authors focus their analysis on the new IEEE 802.11n standard using a wide range of experiments. Each experiment is aimed at assessing the impact that a certain feature (e.g. channel width, transmission power, modulation and coding scheme, etc.) has on the global energy consumption figures. The testbed used for the power consumption measurements was composed of two nodes placed close to each other in order to have good link quality, which allowed the authors to effectively exploit all the IEEE 802.11n modulation and coding schemes. The main conclusions of this work are that (i) for optimizing energy consumption, it is imperative to use the fastest single-stream rate possible, especially for shorter packets and (ii) the optimal device settings will also depend on channel conditions and workload. The authors also observed that transmit power levels have very little effect on the power consumed by the interface.

In [Xiao 2010], the authors present a power consumption model for IEEE 802.11g WLANs exploiting the power saving mode. The authors also show the power consumption model accuracy w.r.t. physical data measured from three popular mobile platforms, namely Maemo, Android and Symbian. The model aims at estimating the energy usage based on the flow characteristics which are easily available on all the platforms without modifications to low–level software components or hardware. The authors conclude that energy is wasted by the idle status between packet intervals, in line with our results.

A theoretical energy consumption model is also presented in [Ergen 2007]. In their work, the authors aims at assessing the amount of energy spent by an IEEE 802.11 station in order to transmit 1 MByte of data. In contrast to our work, the scenario considered is based on an IEEE 802.11 network with N stations rather than 1 station. The authors assume that the power consumption depends on five physical radio states which are transmit, receive, listen, sleep, and off. The resulting model estimates the total energy (in Joules) consumed by a station in order to transmit/receive 1 MByte of data based on (i) the energy consumed by the station in a specific state and (ii) the energy consumed by the station for transmitting/receiving 1 MByte. Based on calculations, the author concludes that energy usage for the station grows approximately linearly with N and as N increases, the energy wastage also increases. Such behavior is mainly due to passive overhearing of packets intended for another station. The power consumption is analyzed only for a fixed amount of traffic.

The results reported by the authors in [Feeney 2001, Xiao 2010, Ebert 2002, Halperin 2010, Ergen 2007] provides us with insights on the power consumption of the single wireless interface rather than of the system as a whole, ignoring the energy expenditures related to other functions such as operations for packet forwarding and reception, fragmentation and reassembling etc. On the other hand, in this Thesis, we focus our attention on the overall energy expenditure in that it is useful to (i) model the real power consumption behavior for WWAN and WLAN WADs and (ii) determine *where* and *how* the energy is wasted in wireless access network gateways.

In [Tauber 2011], the authors focus on the energy consumption of a wireless network as a whole. The authors present a joint experimental evaluation of energy consumption and performance in a IEEE 802.11–based WLAN using both 802.11a and 802.11n operating modes. The testbed consisted of an AP communicating with a single station. The power consumption measurements are taken using a suitable power meter and traffic is injected using the iperf traffic generator. The authors have exploited an application–level approach, varying the packet size and transmission rate and evaluating the energy consumption across a wide transmission rates. They also perform a comparison of the energy consumed by popular Internet applications such as YouTube and Skype. A metric for energy usage namely Effective Application–specific energy–usage (E_A) was defined, as follows:

$$E_A = \frac{P}{T} \tag{2.3}$$

Where,

- P is the mean power used during transmission of flow (expressed in [J]);
- T is the mean throughput of flow (expressed in [Mb/s]);

The authors also observed that both the application's transmission rate and the packet size have an impact on power consumption when the device is acting as transmitter. In contrast to our work, the case when the device is acting as receiver is not considered, and no power consumption model is provided.

In [Garcia-Saavedra 2011], the authors investigate the case of IEEE 802.11-based WLANs and first show that, given the existing diversity of power consumption figures among mobile devices, performing a fair allocation of resources among devices is challenging. The authors propose a criterion to objectively balance between the most energy-efficient configuration and the throughput-optimal allocation and derive a closed-form expression for the optimal configuration of WLANs with respect to the energy-efficiency criteria.

In [Deruyck 2010], the authors present a power consumption model for wireless access networks and, in particular, for mobile WiMAX, HSPA and LTE networks. The scenario is a suburban area and a physical bit rate of 10 Mb/s is used. The authors compare wireless technologies for one SISO system and three MIMO systems considering a ranking of the wireless technologies as a function of their power consumption, range and energy efficiency. To compare the different technologies, the authors define models in order to calculate the total power consumption per user and the power consumption of the base station. In contrast to our work, the model provided by the authors is based in the amount of power consumed by each part of the system separately rather than the power consumption of the system as a whole. The authors also present relevant analysis to (i) determine which technology is the best solution for the specified area, and (ii) compare the power consumption of the wireless access networks with the power consumption of the wired access networks. In order to compare the different technologies, the authors define:

- The total power consumption Pu_{tot} per user (expressed in W) given by:

$$Pu_{tot} = P_{home} + P_{access} + P_{core} \tag{2.4}$$

  Where,

  - P_{home} is the power consumption of the CPE (Customer Premises Equipment)(in W);
  - P_{access} is the power consumption of the access network (expressed in W);
  - P_{core} is the power consumption of the core network (expressed in W);

- The power consumption Pb of the base station (expressed in W) given by:

$$Pb = n_{sector} \cdot (n_{Tx} \cdot P_{amp} + P_{trans} + P_{proc} + P_{conv} + P_{gen}) + P_{micro} + P_{airco} \tag{2.5}$$

  Where,

  - n_{sector} is the number of sectors in the cell;
  - n_{Tx} is the number of transmitting antennas per sector;
  - P_{amp} is the power consumption of the power amplifier;
  - P_{trans} is the power consumption of the transceiver;
  - P_{proc} is the power consumption of the digital signal processing unit;
  - P_{conv} is the power consumption of the AC-DC converter;
  - P_{gen} is the power consumption of the signal generator;
  - P_{micro} is the power consumption of the microwave link;
  - P_{airco} is the power consumption of the air conditioning;

The most relevant conclusion of the paper is that with a pre–defined bit rate of 10 Mb/s, the mobile WiMAX is the most energy–efficient solution compared with HSPA and LTE. However, the investigation is limited to a fixed amount of traffic consequently the scenarios of low traffic load and high traffic load are not considered leaving the question "how the traffic affects the power consumption of the WiMAX, HSPA and LTE devices" unanswered.

2.3 Energy Efficiency Improvements in Wireless Access Networks

In this section, we present an overview of the related work on energy efficiency improvements proposed for cellular and enterprise WiFi networks.

From the beginning, cellular networks are designed to optimize the energy consumption of mobile devices. Recently, the focus has moved towards the optimization of energy consumption of fixed infrastructure. The article [Pentikousis 2010] gives an overview of the evolution of mobile devices, from the first until the latest generation of mobile technologies, and its implication on power management. The article shows that power management plays a very important role in mobile devices and mobile networking. Therefore, the design of novel ways to deliver network services in mobile communication networks without resorting to always–on connectivity, combining with a suitable service management, is mandatory in order to increase the energy efficiency of mobile networks. Techniques for energy saving on mobile devices are discussed in [Perrucci 2008]. Authors present a possible solution introducing a secondary air interface with lower energy consumption. It is used as a signaling channel to wake up mobile devices in the presence of wireless networks.

From WADs point of view, the majority of the works investigate the most efficient ways to turn off cells/networks or put them in sleep mode, while maintaining good quality of service [Marsan 2010, Saker 2009, Marsan 2009, Micallef 2010, Elayoubi 2011, Dufkova 2010]. In [Marsan 2010], a cooperative approach between two operators, offering service over the same area, is used in order to reduce energy consumption. The technique used is energy-aware cooperative management of the cellular access networks. It works in two different conditions (i) in high traffic conditions, both networks are used (ii) in low traffic conditions, one network is switched off and the second network supports all the traffic in a transparent mode to the users. Several alternatives as regards to the switch-off pattern are discussed such as switch-off frequencies and balanced roaming costs. However, this solution has several administrative implications because it requires operator cooperation. Similar approach is used in [Saker 2009] but using heterogeneous 2G/3G networks of the same operator. The paper [Saker 2009], proposes energy–efficient radio resource management algorithms for heterogeneous networks. These algorithms allow finding the optimal traffic allocation in cooperative 2G/3G network in order to power on/off an entire system (2G or 3G) for high or low traffic scenarios respectively. This proposed solution decreases the power consumption while guaranteeing the quality of service (QoS) for the offered traffic.

The same approach, putting resources in sleep mode, is also used in [Marsan 2009, Micallef 2010, Elayoubi 2011] but in a more efficient way. These papers introduce models for the energy–aware management of cellular access networks. The idea is to reduce the number of active cells in low traffic conditions. Consequently, when some cells are switched off, the traffic is taken by the cells that remain active in order to guarantee the availability of the service over the whole area. This solution implies changes on antenna tilt configuration in order to guarantee the coverage area. In [Dufkova 2010] a methodology for saving energy in Mobile Communications Networks is presented. It is based on re–arranging the user–cell association in order to allow shutting down of under–utilized parts of the network. These set of solutions have an approach focusing on minimizing the idle time of the network, taking advantage of low traffic, in order to maximize the energy savings.

Similar sleeping approaches also exist for WLANs [Jardosh 2009, Lorincz 2010]. In the papers, the authors affirm that the most of energy consumed in a wireless network is wasted because of the large period of idle network resources in the absence of traffic. Therefore, the paper [Jardosh 2009] proposes SEAR, a resource on–demand strategy to power on or off resources in high–density WLANs. SEAR strategy analyses the volume and location of user demand in order to power on/off WLAN access points (APs) dynamically according to the user demand. As similar approach is used in [Lorincz 2010], focusing mainly on wireless access. The proposed technique analyses traffic in different hours, days and weeks in order to optimize the management of on/off state (idle or sleep) and transmission power of access stations. The paper [Lorincz 2010] considers as example the energy consumption of IEEE 802.11b/g WLAN networks, remarking that similar considerations can be done also for other wireless technologies (3G, WiMAX, LTE systems).

Other approaches to save energy include exploiting the heterogeneity of the access technologies and the interaction with wired networks, and adapting transmission power based on energy and coverage trade-offs [Al-Hazmi]. For example, one of the proposals is to decrease the number of active APs by increasing the transmission power and relay messages using ad hoc networking to increase coverage. We also present a pioneer works in techniques for reducing network energy consumption. In [Nedevschi 2008] the techniques are investigated in wired network. Nevertheless, the approach can be applied to wireless networks taking account the limitations of wireless communications. The paper [Nedevschi 2008] investigates two forms of power management schemes for energy savings. The first scheme explores putting components in sleep mode and the second scheme explores adapting the rate of "network operation" to workload in order to reduce the energy consumed in the absence of packets and when actively processing packets. The authors also determine when sleeping is best and under which conditions rate adaptation is best. Both sleeping and rate adaptation are performed showing improvements in energy with small increase in latency and packet loss.

In [Armour], the authors describe a set of challenges in order to minimize power consumption in the whole cellular network architecture. The future solutions are mainly focusing on energy metrics, energy efficient architectures, multi-hop routing and frequency management. In [Fehske 2009], the authors propose the deployment of small, low-power base stations together with conventional macro sites. The same approach is used in [Richter 2010] for homogeneous and heterogeneous wireless networks, where the utilization of low-power micro sites instead of macro sites is considered to enhance throughput, energy efficiency and network coverage. The micro sites are low power base stations thus the energy efficiency of the network is improved. The technique adapts the power transmissions of micro sites to take traffic load conditions into account. These proposed methods uses the current cellular network infrastructure adding micro sites as a solution in order to improve the power consumption by area. However, this implies major changes to the hardware and software in the cellular network deployments, and as a consequence, will affect the current cellular network infrastructure.

Finally, a different approach is presented in [J.-M. 2010]. The technique optimizes the transmission power of the base stations in order to reduce the global energy consumption in the network. The optimization technique takes into account (i) the effect of shadowing (ii) the presence of thermal noise (ii) the impact of the base station transmission power in the coverage and the capacity of mobile cellular networks. Thus, the optimization technique determines the optimal transmitting power to each base station while it maintains the QoS. Similar techniques are also used in [Richter 2010, Lorincz 2010]. These techniques are very interesting because they help to save energy just limiting power transmission without affecting the QoS. These solutions require only minor upgrades to the base station software.

From the literature, it is evident that those schemes that turn off parts of the infrastructure, or put it in sleep mode, have significant potential in terms of reducing energy consumption in wireless networks. In our work, we add to this understanding and show its feasibility in a real network by taking into account hardware and software limitations, the time and energy it takes to switch on and off interfaces and devices, and their impact on network and energy consumption performance.

This page is intentionally left blank

Chapter 3

Energino: Hardware and Software Solution for Power Consumption Monitoring of Wireless Access Networks

Contents

3.1 Introduction

In this Chapter, we introduce *energino* a novel hardware and software solution for real–time energy consumption monitoring in wireless networks. The development of *energino* was motivated by limitations, especially in terms of sampling resolution and granularity, found in currently available commercial solutions for energy consumption monitoring. As a matter of fact, the available commercial solutions are not able to identify high resolution/frequency power variations in WADs where the variations occur in milliseconds.

To the best of our knowledge, *energino* is the first power meter capable of delivering high performance while remaining an affordable solution for large deployments. We also release both the hardware schematics and the software of *energino* [1] with a permissive license in order to encourage the research community to use and extend it. We evaluated the distinctive features of *energino* power meter in a realistic setting in Chapter 4.

[1] Available at: http://www.energino-project.org/

3.2 Requirements

The *energino* power meter has been designed around the following set of requirements:

- **High sampling rate:** Ideally, in order to isolate MAC–layer features such as RTS/CTS handshakes and acknowledgments in WiFi networks a millisecond precision is needed. Therefore, if high frequencies dynamics, such as these MAC–level protocol transients are to be caught, an high frequency sampling rate is required.

- **High resolution:** In order to develop realistic models capable of capturing the correlation between different traffic patterns and energy consumption, it is mandatory to collect samples with a very fine granularity, ideally in the order of 10 mW or less.

- **Low–cost/Low–power:**.The fraction of devices that can be actively monitored in a wireless network is clearly limited by the cost to deploy *and* run such energy monitoring infrastructure. As a result, having a device that is both cheap to produce/assemble and that require very low power in order to operate is mandatory if a significant number of wireless devices have to be monitored.

- **Manageability:** Supporting basic management functions, such as being able to selectively turn on/off network devices or radio interfaces, enables the development of novel protocols and algorithms capable of adapting power consumption to the real network conditions (i.e., number of users and traffic patterns).

- **Autonomous:** Being able to operate as a stand–alone monitor without requiring the connectivity to either the device being monitored or to a third device is of capital importance in a highly distributed deployment. Such requirements mandate both a dedicated power supply and the support of networking functionality (i.e. Ethernet, WiFi, ZigBee).

3.3 Design Choices

Covering the entire spectrum of requirements with a single commercial product proved to be unfeasible. In particular, albeit several plug–loads meters are available as off–the–shelf solutions, they are all characterized by low frequency and low resolution sampling capabilities. Moreover, their prices range between 80 €, for devices without network connectivity and very limited storage capabilities, up to 200 € for devices with full network connectivity (Ethernet or ZigBee).

The *Watts Up!* [wat] meters are an example of devices belonging to this family. *Watts Up!* is a "plug load" meter that measures the amount of electricity used by whatever electrical appliance is plugged into it. Such measurements, taken with a

Table 3.1: Approaches to power consumption monitoring.

	Resolution	Sampling Rate	Price	Ease of Deployment
Plug-load meters	Low	Low	Average	High
Oscilloscopes	Very High	Very High	Very High	Low

granularity of 0.1W and a sampling period of 1s, can be logged into the device's internal memory or they can be exported using either an Ethernet port or a serial interface. Nevertheless, such specifications proved to be insufficient to catch dynamics occurring at the transition point between linear and saturation power consumption regimes [Gomez 2011, Gomez 2012a]. It is the Author's opinion that, a sampling period in the order of tens of times per second and a resolution of 10 mW is required in order to properly investigate such high resolution/frequency power consumption dynamics.

High resolution and high frequency sampling can be easily obtained using a digital oscilloscope as done in [Feeney 2001]. However such a solution is expensive with a cost ranging from 500 € up to several thousand of euros. Moreover, meant to serve as laboratory equipment, oscilloscopes are typically bulky and hard to integrate in an highly distributed network.

A summary of the advantages and disadvantages of both family of solutions is reported in Table 3.1. As it can be seen, there is a clear space for novel energy consumption monitoring solutions. It is worth noticing that, albeit the design presented in this chapter is primarily addressed towards the needs of the experimentally driven research, it can be easily extended to support also use cases coming from the industry such as monitoring of deployments powered using renewable sources and/or validation and characterization of the energy budget of metropolitan wireless networks.

3.4 Architecture: Hardware and Software

energino is a plug–load meter designed to monitor the energy consumption of DC devices. It consists of an hardware and a software components both based on the Arduino platform. A management backend written in Python is used to configure *energino*'s operating parameters, i.e. sampling rate and resolution, and to gather the energy consumption statistics. We release both the hardware schematics and the software with a permissive license[2] in order to encourage the research community to use and extend it.

[2] Available at: http://www.energino-project.org

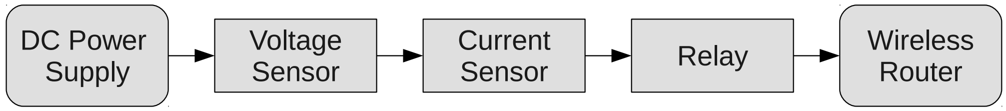

Figure 3.1: Energino system architecture details.

3.4.1 Hardware Details

The need for a programmable and extensible platform drove us toward the Arduino platform. Arduino [ard] is an open–source fast prototyping platform which, at its core, consists of a programmable micro–controller that can sense the environment using a variety of sensors and can affect its surroundings by controlling lights, motors, and other actuators. Additional modules, called "shields", can be used in order to extend the Arduino capabilities. Particularly relevant for our prototype are the extensions providing networking functionality (Ethernet, WiFi, and ZigBee).

The Arduino board supports 6 input channels using a 10–bit analog to digital converter. In particular, it maps input voltages between 0 V and 5 V to integer values between 0 and 1023. The ensuing resolution is thus 4.9 mV per unit. Each input can be sampled with a period of 100 μs which results in a maximum sampling rate of 10kHz. Such a sampling rate is not high enough to catch MAC-level events such as acknowledgments however, we accepted it as a reasonable trade–off between cost/complexity and performance.

The Arduino has been extended with a custom module integrating a voltage sensor (based on a voltage divider), a current sensor (based on the Hall effect), and a solid state relay. A block diagram of the entire system is reported in Fig. 3.1. In the rest of this section we shall describe in details these three subsystems.

3.4.1.1 Voltage Sensor

The voltage sensor is implemented using a resistive voltage divider which produces an output voltage (V_{out}) that is a fraction of its input voltage (V_{in}). The divider consist of a series of two resistors R_1 and R_2. The relationship between input voltage, V_{in}, and output voltage, V_{out}, is given by:

$$V_{out} = V_{in} \cdot \frac{R2}{R1 + R2} \tag{3.1}$$

The divider has been dimensioned to support input voltages up to 55 V. The rationale behind this choice is that standard Power–Over–Ethernet injectors typically used to power networking devices are characterized by an output voltage of 48 V. In particular, $R_1 = 10\ K\Omega$ and $R_2 = 100\ K\Omega$, which result in an output voltage of 4.3 V when an input voltage of 48 V is applied. This is within the Arduino constraints even if slight fluctuations of the input voltage occur.

3.4.1.2 Current Sensor

The current sensor consists of a linear Hall–effect[3] circuit capable of measuring currents between −5 A and +5 A. An applied current flowing through this circuit generates a magnetic field which is sensed by the integrated Hall IC and converted into a proportional voltage. The output of the device when no current is flowing through the sensor is 2.5 V. The sensitivity of the device is 185 mV/A, i.e. for each ampere flowing through the current sensor the voltage on its output linearly increases of 185 mV. For example when a 5 A current is applied, the corresponding voltage read on the output is 3.425 V. Reversely, if a negative current of −5 A is applied, the output will read 1.575 V.

3.4.1.3 Relay

Finally, a solid state relay (SSR) is used in order to turn on/off the network device being monitored. An SSR is an electronic switching device where a small control signal controls a larger load. It comprises a voltage or current sensor which responds to an appropriate input (control signal), a solid–state electronic switching device which switches power to the load circuitry either on or off, and some coupling mechanism to enable the control signal to activate this switch without mechanical parts. The device used in our system is a Crydom MPDCD3-B[4]. This SSR relay can switch loads up to 3A@60VDC using a control voltage of 3 to 32 volts direct current (VDC).

3.4.2 Software Details

The Arduino hardware[ard] is programmed using the C/C++ programming language with some simplifications and modifications. A library, called *Wiring*, is provided in order to make common input/output operations easier. Finally, a cross–platform Integrated Development Environment (IDE) written in Java is made available. Such IDE supports basic editing capabilities (syntax highlighting, and automatic indentation) and is also capable of compiling and uploading programs to the board effectively supporting the entire application life–cycle.

The software which manages *energino* periodically transmits over the USB interface (i) the average power , (ii) the actual voltage and (iii) actual current consumed by the monitored device during the last observation period. The actual input voltage is given by:

$$V_{real} = 0.0049 \cdot V_{raw} \frac{R1 + R2}{R2} = 0.0293 \cdot V_{raw} \tag{3.2}$$

Where,

[3] The Hall effect is the generation of an electric potential perpendicular to both an electric current flowing along a conducting material and an external magnetic field.

[4] Available at: http://www.crydom.com/en/Products/Catalog/m_p.pdf

Figure 3.2: **Energino:** Hardware and software solution for power consumption monitoring

- V_{raw} is the outputs of the voltage sensors;
- V_{real} is the the actual converting voltage consumed by the monitored device;

Similarly, the actual input current is given by:

$$I_{real} = \frac{0.0049 \cdot I_{raw} - 2.5}{0.185} = 0.026 \cdot I_{raw} - 13.51 \tag{3.3}$$

Where,

- I_{raw} is the outputs of the current sensors;
- I_{real} is the the actual converting current consumed by the monitored device;

It is worth noticing that during each sampling period the Arduino continuously polls the voltage and the current sensors and accumulates the values into two separate registers. At the end of the polling period the average power consumption is computed and the result is sent over the USB interface. This is done in order to filter–out fluctuations in the values read from the analog inputs.

3.5 Validation of Energino

In this section, we present the experimental evaluation of *energino* power meter in laboratory tests. Here, the current and voltage sensed by *energino* are compared with the current and voltage generated and measured by HAMEG Instrument[5] an AC/DC power supply and current sensor. In Fig. 3.2 the *energino* power meter hardware solution for power consumption monitoring is shown.

Fig. 3.3 a simple circuit used to the validation of *energino* power meter is shown. In this there is a HAMEG Instrument DC power supply (-25 V up to + 25 V),

[5] Available at: `http://www.directindustry.com/`

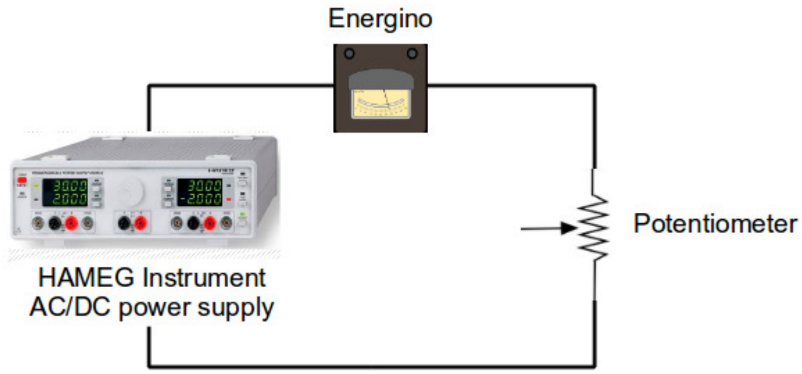

Figure 3.3: Simple circuit used for the validation of *energino* power meter

energino power meter and a potentiometer (50 KΩ-500 KΩ)[6]. To measure the voltage, the authors varied the voltage injected to the circuit from -25 V until 25 V in steps of 5 V. The voltage and current dropped on the potentiometer is monitoring for *energino* power meter during 100s for each sample. In order to change the level of current flowing in the circuit, we fixed the voltage to 5 V and varied the resistance of the potentiometer.

The voltage generated by HAMEG Instrument is compared with the *energino* voltage outputs in Fig. 3.4a while the current measured by HAMEG Instrument and *energino* power meter are shown in Fig. 3.4b, each sample is presented with the 95% confidence interval. As it can been seen in the figures, the empirical voltage and current data–points delivered by HAMEG Instrument are plotted together with the values measured using *energino* power meter, the values measured by the *energino* power meter are matching very well with the data–points generated and measured with HAMEG Instrument.

It is important to note that *energino* power meter is also experimentally evaluated in practical scenarios in Chapter 4, where the power consumption behavior of WADs working with WiFi and WiMAX technologies are presented.

3.6 Conclusions

In this Chapter, we introduced *energino*, an affordable solution for real–time energy consumption monitoring in wireless networks. The hardware schematics and the software architecture were discussed in order to encourage the research community to use and extend *energino*. The main features of *energino* are:

- Arduino–based, a flexible platform with a very active community;

[6]Potentiometer is a three-terminal resistor with a sliding contact that forms an adjustable voltage divider. It acts as a variable resistor or rheostat

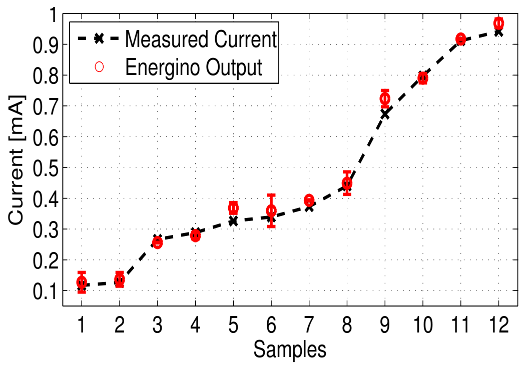

(a) Current Comparison

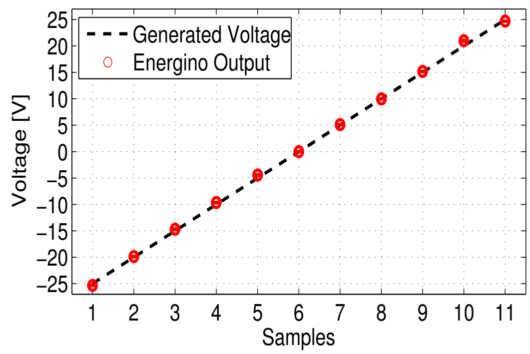

(b) Voltage Comparison

Figure 3.4: Comparison of voltage and current values measured by HAMEG Instrument and *energino* power meter

- High sampling rate, up to 10000 voltage/current samples per second;
- High resolution, configurable from 26 mA down to 1 mA;
- Low cost/low power, it costs about 80 €to assemble an *energino* complete with Ethernet connectivity;
- Manageability, the device being monitored by *energino* can be turned on/off remotely using the embedded RESTful interface;
- Cloud aware, energy consumption statistics can be tracked using COSM.

This page is intentionally left blank

Chapter 4

Power Consumption Behavior of Wireless Access Devices (WiFi and WiMAX Technologies)

Contents

4.1 Introduction

In the last years, wireless local area networks (WLANs) have become the most popular wireless access technology. Due to their rapid evolution in terms of sustained data rates, reduced cost of equipment and ease of deployment, WLANs are nowadays extensively used by corporations, universities and municipalities in order to provide Internet connectivity to end users. Trends analysis reveals that the total amount of WLAN devices deployed has been increasing exponentially over the past few years [Jardosh 2009]. In this context, optimizing the energy consumption of WLAN devices can significantly impact the overall CO_2 footprint of wireless networks [Al-Hazmi].

In such a scenario, two broadband wireless access technologies, WiFi and WiMAX, are witnessing an increasing usage in both metropolitan and rural deployments. The reason behind their adoption lies in the minimal supporting infrastructure required for their operations, which in time enables a high level of flexibility in network deployments, allowing connectivity to be provided only where *and* when needed. Such fluidity in network deployment and operations is made possible by the architectural choices underpinning the standards. However, while energy efficiency trade–offs have been taken into account for the end–users' terminal, which can be mobile or nomadic, less attention has been devoted to the network gateways which, in the case of both WiFi and WiMAX standards, are typically connected to the power grid and, thus, do not pose energy consumption challenges. As a result there is a lack of best practices for designing energy efficient network protocols and architectures for broadband wireless access networks.

The main objective of this Chapter is to experimentally measure and analyze the energy consumption patterns of WiFi and WiMAX WADs[1] at both the component and the network level. In particular, our experiments aim at answering the following questions:

- *Where and how is the power consumed in WiFi and WiMAX WAD? How much of the power is wasted?*
- *What is the relationship between traffic load and power consumption in indoor and outdoor WiFi and WiMAX WAD?*
- *What are the critical aspects of the IEEE 802.11g, IEEE 802.11n and the IEEE 802.16 standards with respect to power consumption?*

The answers to these questions are very important because these help us to (i) model the power consumption of wireless access networks (see Chapter 5) (ii) take good decisions in order to achieve solutions (see Chapter 6). The main contributions of the Chapter are the following:

[1]With a slight abuse of terminology we use the term *WAD* to refer to both the WiMAX Base Station (BS) and to the WiFi Indoor and Outdoor Access Point (AP).

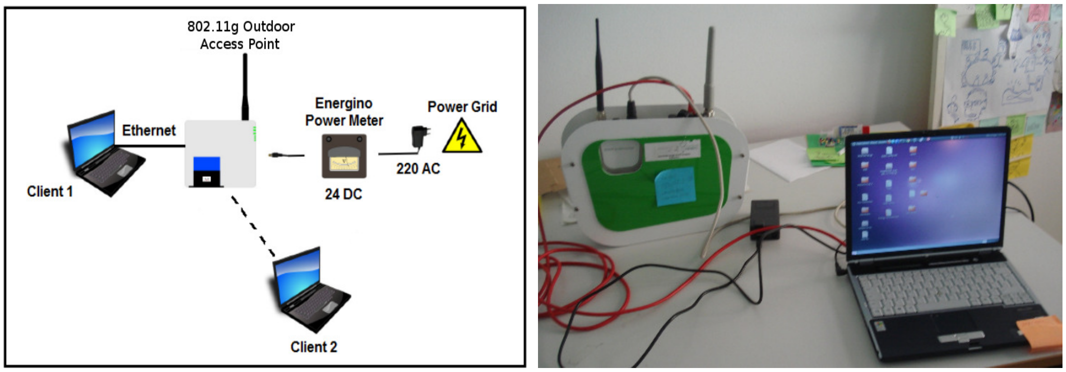

(a) Testing Scenario (b) WiFi Outdoor WAD

Figure 4.1: **WiFi Outdoor WAD:** Network scenario used for the measurement campaign.

- An empirical approach for understanding the energy consumption behavior of WiMAX and indoor–outdoor WiFi WADs. Thereby, we target the characterization of the power consumption of WiFi and WiMAX WADs in terms of (i) the amount of traffic sent/received by the WAD, (ii) the modulation and coding schemes used, (iii) the size of the session level data units and (iv) transmission power levels.
- The analysis and comparison of the power consumption behavior between IEEE 802.11g–IEEE 802.11n Indoor WAD.

4.2 WiFi Outdoor WADs: Power Consumption Behavior of Outdoor IEEE 802.11g Wireless Access Devices

The network setups exploited in the indoor scenario is sketched in Fig. 4.1.

4.2.1 Network Settings

The network is composed of a custom IEEE 802.11g Access Point and two notebooks, the first one Fujiitsu SIEMENS notebook acting as wired *client 1* and the second one DELL Latitude D620 notebook acting as static wireless *client 2*. The testbed is deployed at Telekom Innovation Laboratories in Berlin, Germany. The AP device is a commercially available "saxnet meshnode III" with passive cooling and a robust casing concept thus allowing for operation under extreme conditions. The hardware and software of the meshnode III are described in [Uzun 2012]. It can be equipped with up to four WLAN modules (802.11 a/b, supporting also 11c/i/f, respectively). The node can also be configured as AP nodes using an Ethernet connection for Internet access. The available transmission power is from 80 mW up to 600 mW -

related to indoor or outdoor operation, respectively. The deployed nodes are actually equipped with standard/ High Quality 2.4/5 GHz WiFi–modules with a maximum transmission power of 80/400/600 mW respectively. The used WiFi antennas are omni-directional or of sector type.

The AP's operating frequency was set to 5.18 GHz. It is important to note that, unless otherwise specified, the rate adaptation algorithm has been set to auto and the transmission power has been left to its default value equal to 17 dBm ($\approx$ 50.12 mW) for all experiments. The notebooks *client 1* and *client 2* are regular Fujiitsu SIEMENS and DELL Latitude 6420 respectively, equipped with an Intel PRO/Wireless 3945AB wireless adapter and running Ubuntu 10.04.

4.2.2 Testing Methodology

4.2.2.1 Traffic Generation

Traffic is generated using the Iperf traffic generator [ipe] and is injected into the network through either the *client 1* or the *client 2* so the AP forwards the traffic between both clients. The objective of the experiments is measuring the power consumed by the AP when (i) it is acting as a transmitter, it means *client 1* is generating traffic towards *client 2* and (ii) it is , it means *client 2* is generating traffic towards *client 1*. In both cases the power consumption figures reported in this Section refer to the AP.

4.2.2.2 Power Consumption Monitoring

The power consumption is measured using the *energino* power meter [Gomez 2012b], which was introduced in Chapter 3. The *energino* power meter is interconnected through its USB interface to the *client 1* where a custom data logging software is used in order to log the power consumption statistic, specifically the *energino* power meter logged timestamps, voltage, current and power consumed by the wireless device. The power consumption statistics are logged into the Server with a granularity of 100 mW and a sampling period of 100 ms.

It is important to remark that the power consumption is monitored for the whole device. Therefore, the results reported in this report account for both the power consumed by the processing board for handling the incoming and outgoing traffic (i.e. for segmentation and reassembling, protocol overheads, computing checksums, etc.) as well as for the power consumed to deliver the actual frame over the wireless link (i.e. power amplifiers, modulator/demodulator, etc.).

4.2.2.3 Experimental Details

Synthetic traffic is modelled as single UDP flows. Results reported in this section are the average of measurements collected during 300 seconds. The results are reported in terms average and with 95% confidence interval. The following scenarios have been considered:

Table 4.1: IEEE 802.11g rates and modulation types

Modulation Type	**Data Rate [Mb/s]**
Binary Phase Shift Keying (BPSK)	6/9
Quadrature Phase Shift Keying (QPSK)	12/18
16–Quadrature Amplitude Modulation (16–QAM)	24/36
64–Quadrature Amplitude Modulation (64–QAM)	48/54

i) **Variable Traffic Generation Rate, Fixed Datagram Length.**: In this test, the datagram size is kept constant at 1280 bytes, while the traffic generation rate is progressively increased from 5 Mb/s up to 55 Mb/s in steps of 5 Mb/s.

ii) **Constant Traffic Generation Rate, Variable Datagram Length**: In this test, the traffic generation rate is kept constant at 10 Mb/s while the datagram size is progressively increased from 64 to 1920 bytes in steps of 128 bytes.

iii) **Variable Traffic Generation Rate, Fixed Modulation Type**: In this test, the datagram size is kept constant at 1280 bytes while the message generation rate is progressively increased. The rate control algorithm is disabled and the transmission rate is set manually using the command line interface. The experiment is repeated for each of the transmission rates supported by the wireless adapter (see Table 4.1).

iv) **Variable Traffic Generation Rate, Variable Transmission Power Level**: In this test, the traffic generation rate is progressively increased from 5 Mb/s up to 55 Mb/s in steps of 5 Mb/s. The transmission power level is set manually using the command line interface.

It is worth noticing that, the frame length of 1280 bytes used in the scenario 2 through 4 has been chosen according to the outcomes of the second scenario and this frame length will be used for all the experiments. In fact, it is the length at which the power efficiency of both systems is maximized. In order to calculate this value, we use the *optimal packet size* metric, which is explained in Chapter 5.

4.2.3 Experimental Measurements and Analysis for IEEE 802.11g Wireless Access Devices

Here, the results from the measurements campaign described above are presented. We use the following notation for the figures throughout the section (a) AP_{Rx} is when AP is and (b) AP_{Tx} when AP is acting as a transmitter.

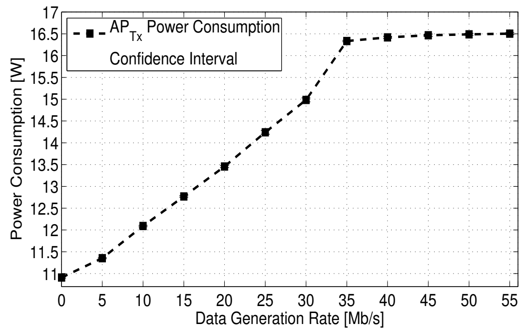

(a) Average Power Consumption (AP in Tx)

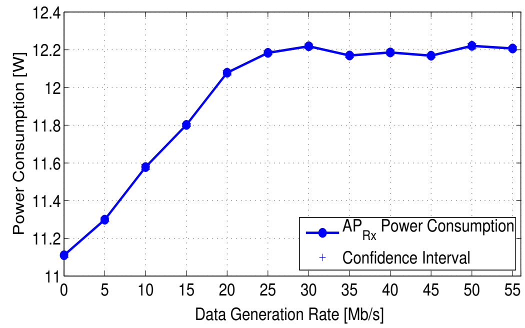

(b) Average Power Consumption (AP in Rx)

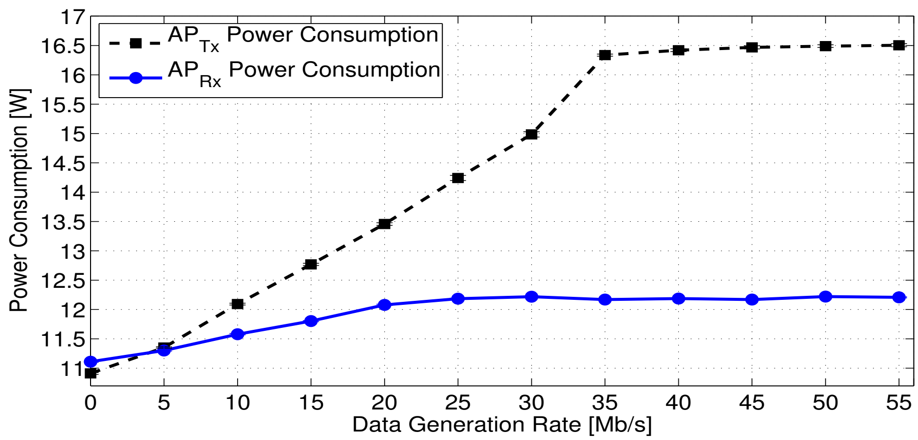

(c) Average Power Consumption (AP in Tx and Rx)

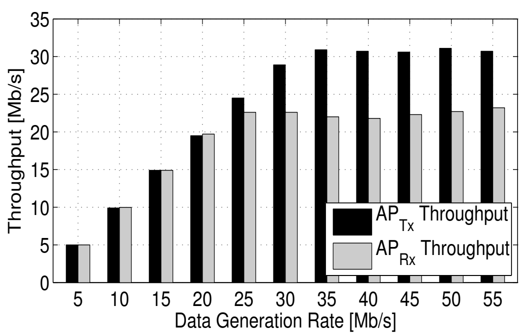

(d) Throughput (AP in Tx and Rx)

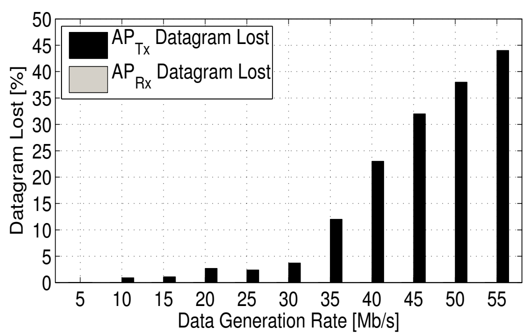

(e) Datagram loss (AP in Tx and Rx)

Figure 4.2: **WiFi Outdoor WADs:** Average power consumption and network performance at the AP as a function of different traffic generation rates for a constant datagram size of 1280 bytes.

4.2.3.1 Traffic Effect on Power Consumption of Wireless Access Devices

In order to study the relationship between traffic load and power consumption, the Fig. 4.2 shows a set of results that summarizes the behavior of AP acting as a transmitter or receiver respectively in terms of power consumption and network performance. The Fig. 4.2c, 4.2a and 4.2b show the average power consumption of the AP as a function of different traffic generation rates, for a fixed datagram size of 1280 bytes. When the AP is acting as a transmitter or receiver, we can observe that:

i) The power consumption of the AP in idle mode is around 11W. The power consumption behavior is similar when the AP is acting as a transmitter or receiver. However, when the AP is is more energy efficient than when the AP is acting as a transmitter. This behavior can be seen in Fig. 4.2c. Similar difference of power consumption for transmission and reception mode is observed in [Feeney 2001]. In this work, the authors investigated the energy consumption of a wireless network interface (802.11a and b) in an Ad Hoc networking environment. They concluded that: *One interesting possibility is that the amount of processing (energy) required to receive a packet depends significantly on received signal strength and/or ambient interference. The relatively high incremental cost of receiving data is partly due to extensive signal processing performed at the receiver. If this requires significant computation, it may also require more energy. This effect may be difficult to quantify without more specialized equipment and a more controlled wireless environment.* In our experiments, the receiver is ≈3 meter away from the transmitter with Line of Sight (LOS) then the received signal is stronger. However, if the received signal strength is weak then the energy consumption in the receiver part can increase due to extensive signal processing performed at the receiver.

ii) The power consumption is monotonically increasing with the traffic load until it reaches a saturation point. However, the saturation point and the power consumption in this point are different when the AP is acting as a transmitter or receiver. The saturation point in terms of power consumption for the AP acting as a transmitter is around 16.5 W while for the AP acting as a receiver is around 12.2 W (see Fig. 4.2a and 4.2b).

iii) Once the AP reaches the saturation point, the maximum throughput remains constant as well as the power consumption. The *saturation* means the data generation rate is higher than the physical link data–rate. The results of throughput are shown in Fig. 4.2d. The saturation point in terms of throughput for the AP acting as a transmitter is around 32 Mb/s while for the AP acting as a receiver is around 23 Mb/s.

iv) When the AP is acting as a transmitter and it reaches the saturation point, the datagram loss increases. In this case, the AP does not have enough memory resource consequently when buffer becomes full, the frames are dropped. Instead, when AP is acting as a receiver the datagram loss is lower than 1%. In this case, the transmitter is the notebook *client 2* and it has enough memory resource for buffering the frames when the wireless interface is saturated. The results of datagram loss are shown in Fig. 4.2e.

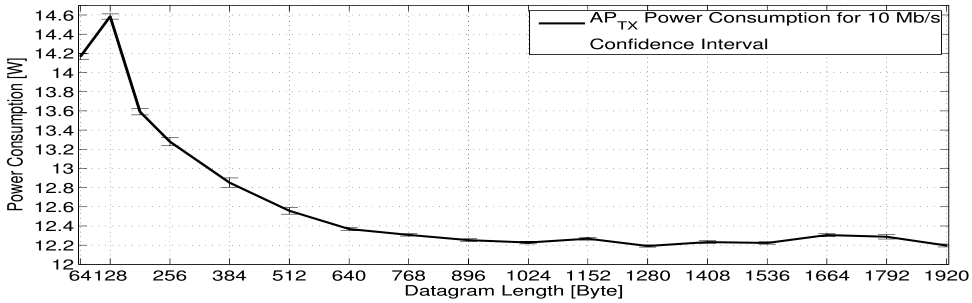

(a) AP acting as a transmitter

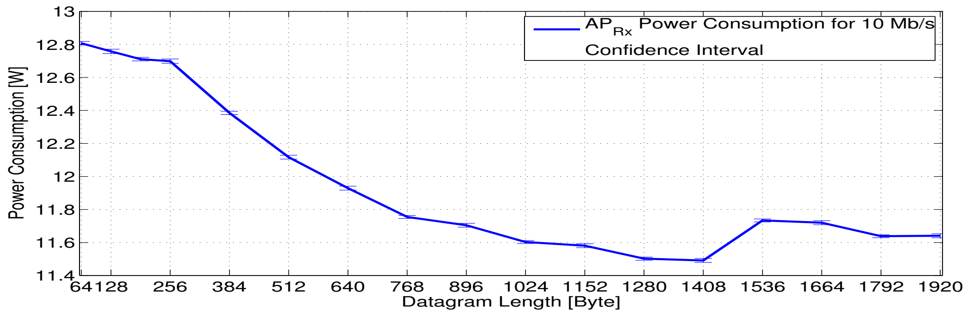

(b) AP

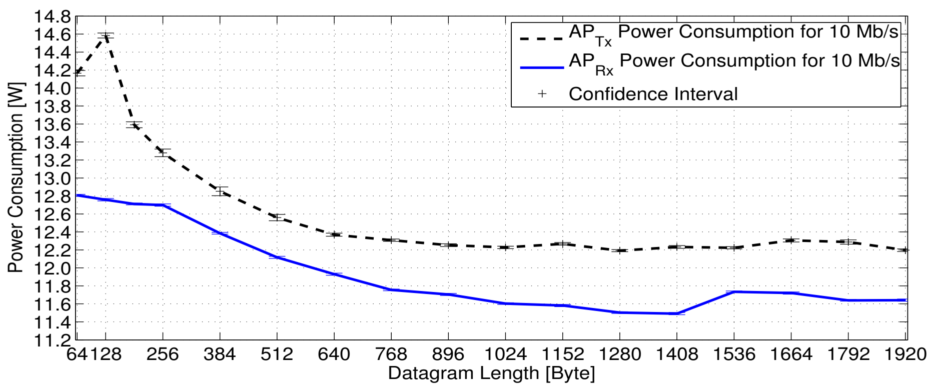

(c) Comparison AP acting as a transmitter/receiver

Figure 4.3: **WiFi Outdoor WADs:** Average power consumption at the AP as a function of the datagram size for a constant traffic generation rate of 10 Mb/s

4.2.3.2 Datagram Size Effect on Power Consumption of Wireless Access Devices

In order to understand the impact of the datagram size on the power consumption of the AP, Fig. 4.3 reports the average power consumption level of the AP as a function of the datagram size for a constant data generation rate of 10 Mb/s. As it can be seen, the datagram size has a considerable impact on power consumption

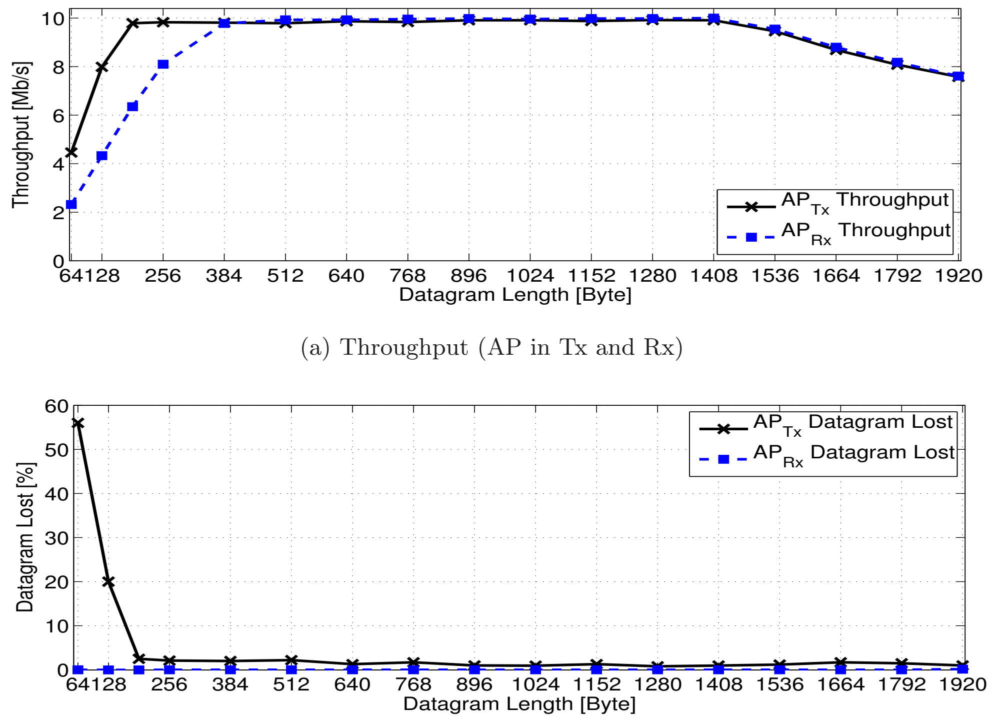

(a) Throughput (AP in Tx and Rx)

(b) Datagram loss (AP in Tx and Rx)

Figure 4.4: **WiFi Outdoor WADs:** Network Performance at the AP as a function of the datagram size for a constant traffic generation rate of 10 Mb/s

when the AP is acting as a transmitter as well as receiver. We can observe that when the AP is acting as a transmitter or receiver:

i) When the datagram size becomes extremely small, the device power is wasted because the AP consumes significantly more power than for large datagram sizes under the same traffic conditions, 10 Mb/s in this case. The power expenditure includes (a) the overhead related to the MAC header and (b) internal operations for generating and buffering all the small datagrams. The results of average power consumption are shown in Fig. 4.3.

ii) When the AP receives a protocol data unit (PDU) larger than the next hop's maximum transmission unit (MTU), the AP fragments the packet. For packets closer to MTU size, the fragmentation creates two packets, one packet with a MTU size and other small packet with the rest of the bytes. Consequently, when fragmentation takes place the throughput utilization decreases and the power consumption increases, especially for high amounts of traffic. The power expenditure includes (a) internal operations for packet fragmentation and packet reassembling, (b) internal operations for buffering packets, (c) the overhead related to the MAC header and (d) the small packets created by fragmentation. Note that the packet reassembling is less energy efficiency that the packet fragmentation, see the results when datagram is 1436 and 1664 bytes(see the Fig. 4.3.a and Fig. 4.3.b).

iii) The impact of the large and small datagrams on the throughput can be seen in Fig. 4.4a. The results show that the throughput decreases when (i) the large datagrams are transmitted/received due to the fragmentation and (ii) small datagrams are transmitted/received due to the high amount of introduced overhead saturates the wireless interface.

iv) The datagram loss increases when the AP is transmitting small datagrams (see Fig. 4.4b). The high amount of overhead introduced by small datagrams saturates the wireless interface. Then, datagram loss increases due to the dropped frames from the buffer (we explained this effect before). The results for datagram loss are shown in Fig. 4.4b.

4.2.3.3 Modulation and Coding Scheme Effect on Power Consumption of Wireless Access Devices

We also study the impact of modulation and coding schemes on power consumption patterns. We forced the different modulation and coding schemes, BPSK 3/4, QPSK 3/4, 16–QAM 3/4, 64–QAM 3/4, to be used by wireless interfaces and measured the power consumption as a function of the traffic generation rate. The results are shown in the next set of figures. The results report the average power consumption at the AP when acting as a transmitter or receiver, as a function of different traffic generation rates. The datagram size is equal to 1280 bytes.

As it can be seen from the results reported in Fig. 4.5 and Fig. 4.6, when the AP is acting as a transmitter or receiver:

i) Lower modulation and coding schemes are less energy efficient than higher modulation and coding schemes.

ii) When the AP reaches the saturation point, the power consumption level is different for each modulation and coding schemes.

4.2.3.4 Transmission Power Level Effect on the Power Consumption of Wireless Access Devices

In the next set of measurements, we report the power consumption statistics relative to the case in which the AP is acting as a transmitter or receiver with different transmission power levels. We considered two different transmission power levels, i.e., 11 dBm and 17 dBm. The results are reported in the next set of figures (see Fig. 4.7). The results show that when the AP is acting as a transmitter or receiver:

i) Different transmission power levels are characterized by different power consumption in saturation. The advantage of decreasing the transmission power

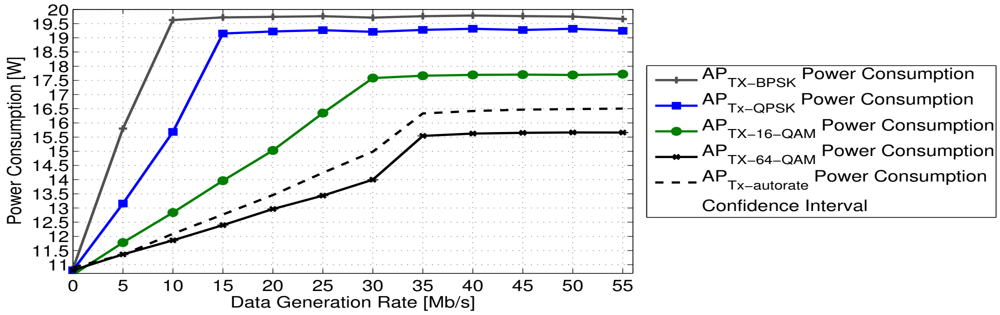

(a) Average Power Consumption (AP in Tx)

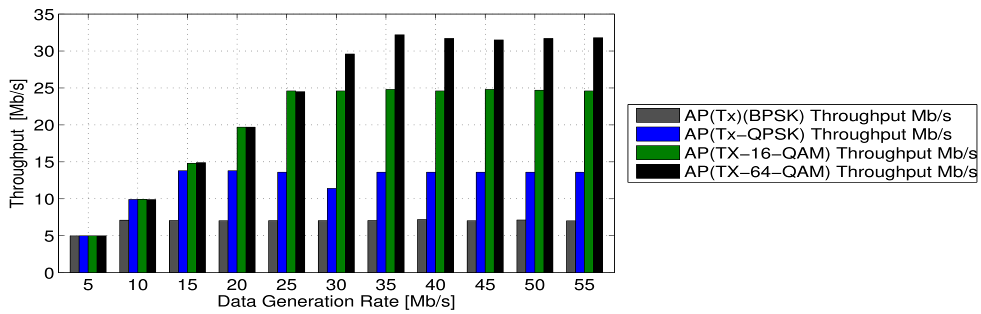

(b) Throughput (AP in Tx)

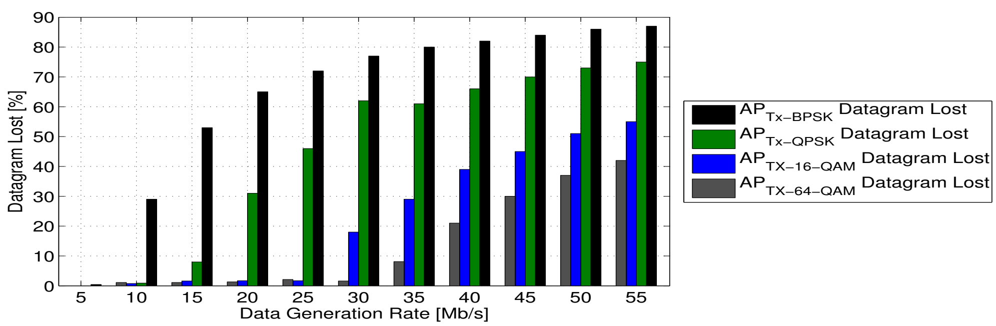

(c) datagram loss (AP in Tx)

Figure 4.5: **WiFi Outdoor WADs:** Average power consumption and network performance at the AP (Tx) as a function of different traffic generation rates for a constant datagram size of 1280 bytes. AP is acting as a transmitter with a fixed modulation and coding scheme.

can be clearly observed when the AP is acting as a transmitter or receiver. The results of average power consumption are shown in Fig. 5.5a and Fig. 5.5b.

ii) It is important to note that the difference in terms of power consumption when the AP is acting as a transmitter or receiver with different transmission power levels is similar.

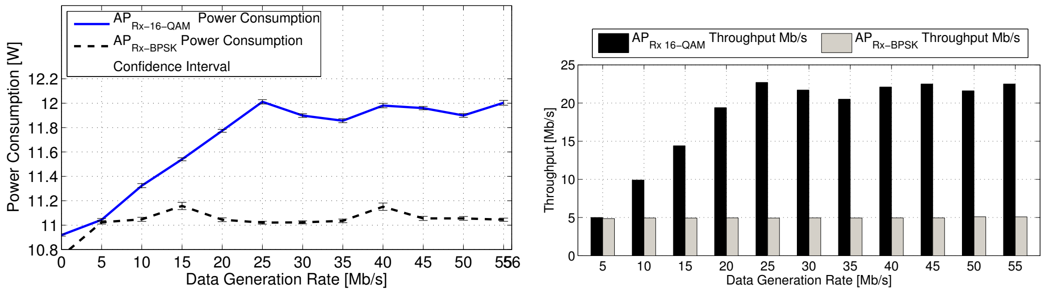

(a) Average Power Consumption (AP in Rx) (b) Throughput (AP in Rx)

Figure 4.6: **WiFi Outdoor WADs:** Average power consumption at the AP as a function of different traffic generation rates for a constant datagram size of 1280 bytes. AP is with a fixed modulation and coding scheme.

iii) The network performance remains basically the same. The results for throughput are shown in Fig. 5.5c and Fig. 5.5d while the results of datagram loss are shown in Fig. 4.7e and Fig. 5.3a.

4.2.4 Measurements of Power Consumption versus Transmissions Power Level

In order to analyze the impact of the variation of transmission power levels on the power consumption of the device, we report the power consumption statistics relative to the case in which the AP is acting as a transmitter with different transmission power levels. We considered 8 different transmission power levels from 0 dBm until 17 dBm. The results are reported in the next set of figures. Results reported in Fig. 4.8 show that when the AP is acting as a transmitter:

i) Different transmitter power levels are characterized by different power consumption. The results of average power consumption of the AP as a function of different traffic generation rates for different transmission power levels for a constant datagram size of 1280 bytes are shown in Fig. 4.8a. In the figure, the advantage of decreasing the transmission power in terms of power consumption can be observed when the AP is acting as a transmitter.

ii) The results for datagram loss are shown in Fig. 4.8b while the results of throughput are shown in Fig. 4.8c. As it can be observed from the results the network performance of the AP remains the same for the transmission power levels from 17 dBm until 5 dBm. Instead, when the AP is working with a transmission power level of 0 dBm the network performance is affected (Datagram loss increases).

iii) The same results are shown in Fig. 4.9 in order to remark the impact of reducing the transmission power level of the AP on the power consumed by the AP.

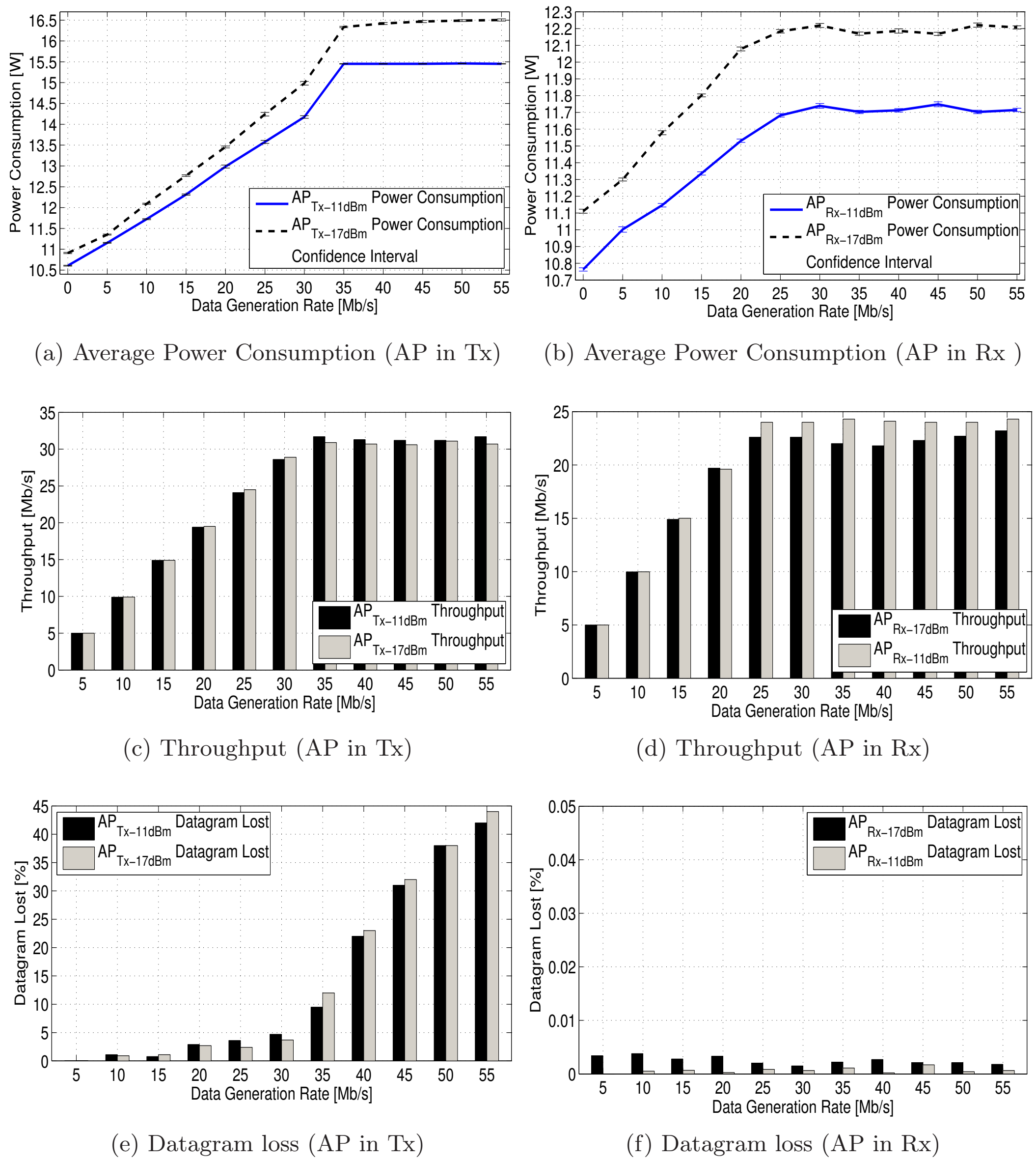

(a) Average Power Consumption (AP in Tx) (b) Average Power Consumption (AP in Rx)

(c) Throughput (AP in Tx) (d) Throughput (AP in Rx)

(e) Datagram loss (AP in Tx) (f) Datagram loss (AP in Rx)

Figure 4.7: **WiFi Outdoor WADs:** Average power consumption and network performance at the AP as a function of different traffic generation rates for different transmission power levels for a constant datagram size of 1280 bytes.

NOTE: It is important to note that, the scenario addressed for this set of measurements is a typical indoor scenario where the distance between AP and *client 2* is around 4 meters.

In order to show clearly the advantage of decreasing the transmission power in terms of power consumption, we calculate the energy cost per bit for each transmission power level. The average energy per bit at AP acting as a transmitter as a function of different traffic generation rates for different transmission power levels

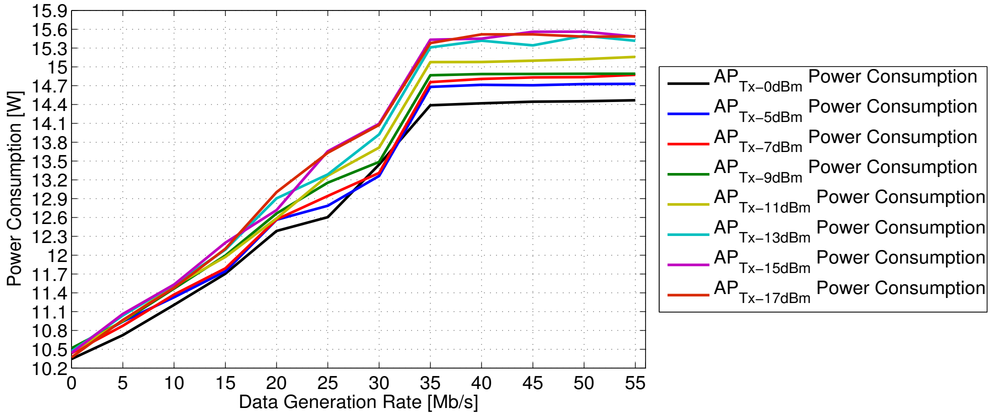

(a) Average Power Consumption (AP in Tx)

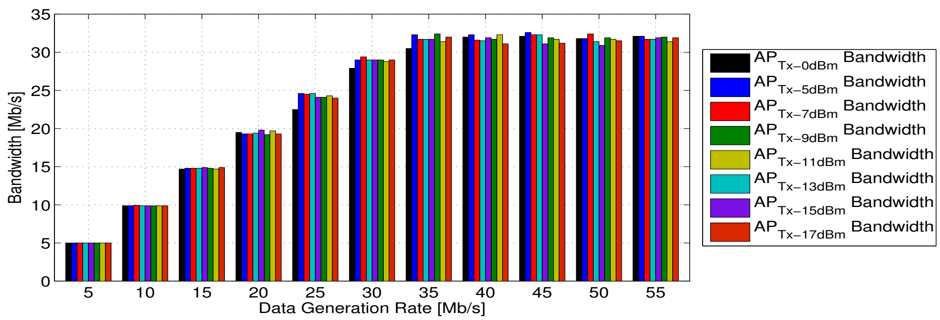

(b) Throughput (AP in Tx)

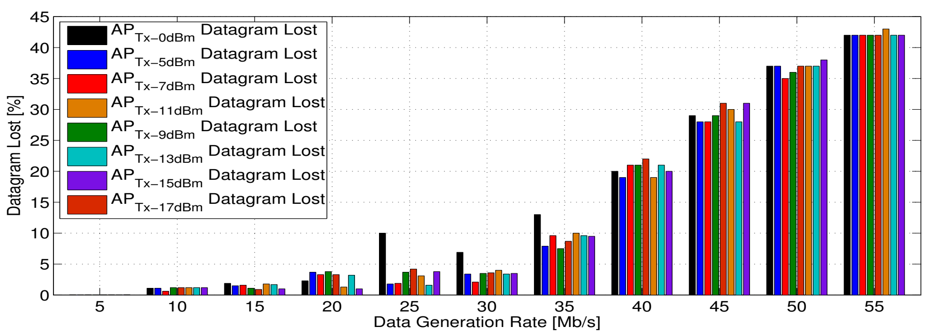

(c) Datagram loss (AP in Tx)

Figure 4.8: **WiFi Outdoor WADs:** Average power consumption at the AP as a function of different traffic generation rates for different transmission power levels for a constant datagram size of 1280 bytes.

are shown in Fig. 4.10.

In Fig. 4.10 are reported the cost of energy per bit for the (i) AP before to archive the saturation point and (ii) AP in the saturation point. As it can be observed in the Fig. 4.10 as well as the transmission power level decreases the energy cost per bit also decreases. The same results are also shown in Table 4.2 with the respective

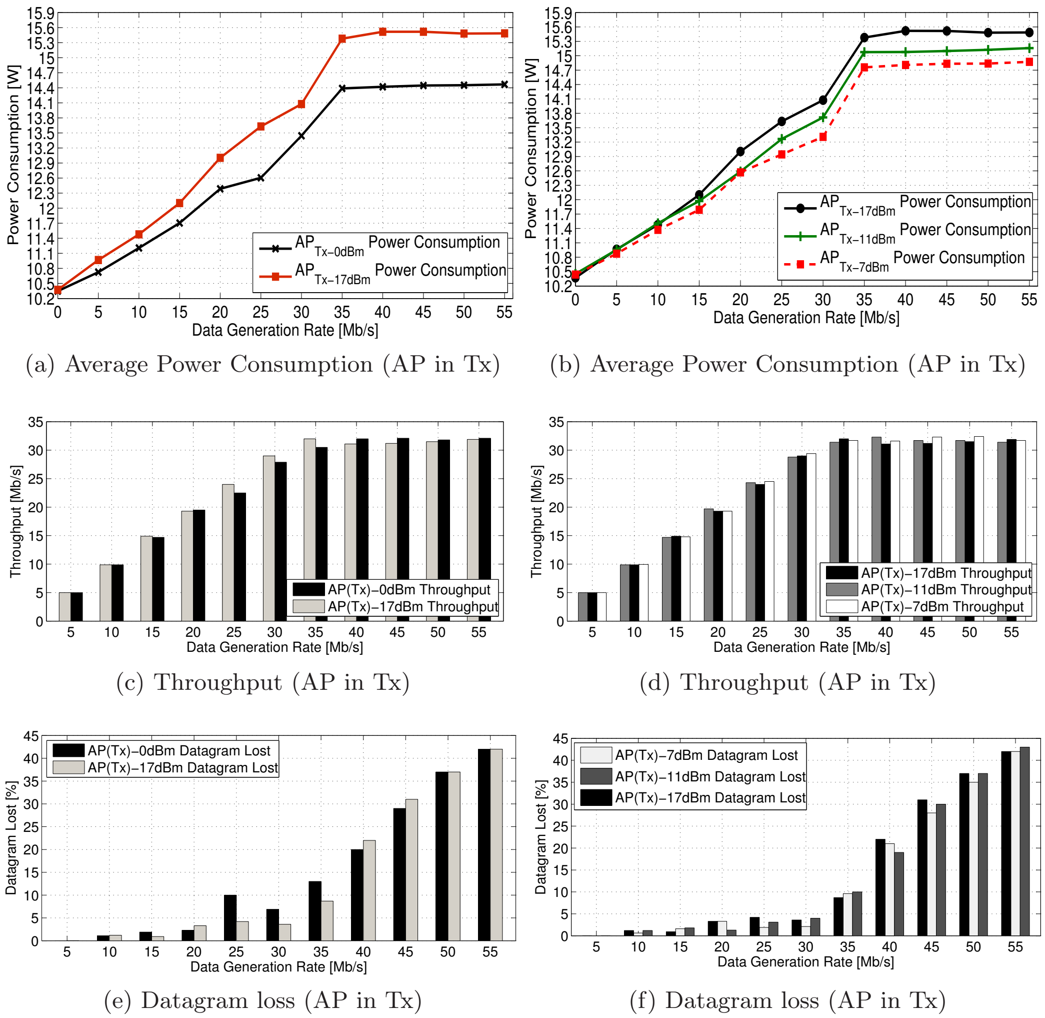

(a) Average Power Consumption (AP in Tx) (b) Average Power Consumption (AP in Tx)

(c) Throughput (AP in Tx) (d) Throughput (AP in Tx)

(e) Datagram loss (AP in Tx) (f) Datagram loss (AP in Tx)

Figure 4.9: **WiFi Outdoor WADs:** Average power consumption at the AP as a function of different traffic generation rates for different transmission power levels for a constant datagram size of 1280 bytes.

95% confidence interval.

4.3 WiFi Indoor WADs: Power Consumption Behavior of Indoor IEEE 802.11g and IEEE 802.11n Wireless Access Devices

Here, the network setups and the methodology used in order to investigate and compare the power consumption of indoor IEEE 802.11g and IEEE 802.11n WADs are described. The network setups exploited in the indoor scenario is sketched in Fig. 4.11.

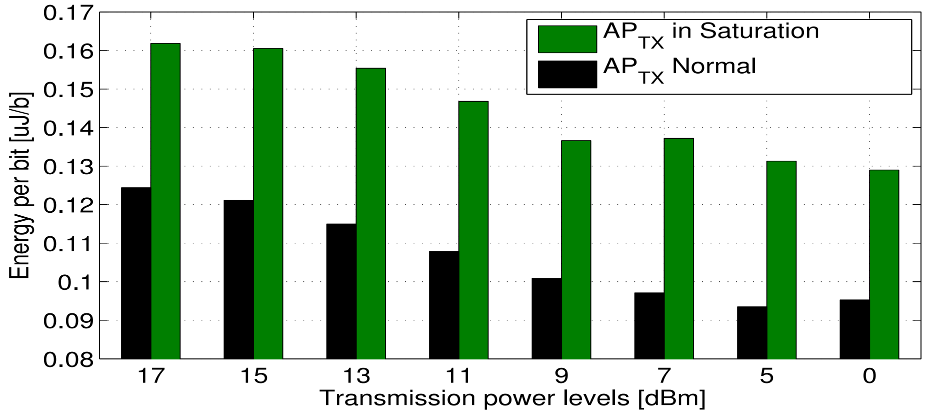

Figure 4.10: **WiFi Outdoor WADs:** Average energy per bit at AP actings as transmitter as a function of different traffic generation rates for different transmission power levels for a constant datagram size of 1280 bytes.

Table 4.2: Average cost energy per bit at WAP acting as a transmitter using different transmission power levels.

Tx Power [dBm]	**Power Consumption in Idle [W]**	**Energy per bit [μJ/s]**	**Energy per bit Saturation [μJ/b]**
17	10.3729 ± 0.0100	0.1244 ± 0.0203	0.1618 ± 0.0072
15	10.4429 ± 0.0099	0.1211 ± 0.0164	0.1605 ± 0.0082
13	10.4679 ± 0.0099	0.1150 ± 0.0130	0.1554 ± 0.0071
11	10.4540 ± 0.0102	0.1079 ± 0.0114	0.1468 ± 0.0047
9	10.5172 ± 0.0117	0.1009 ± 0.0187	0.1366 ± 0.0027
7	10.4385 ± 0.0102	0.0971 ± 0.0163	0.1372 ± 0.0035
5	10.4802 ± 0.0105	0.0935 ± 0.0162	0.1313 ± 0.0031
0	10.3461 ± 0.0108	0.0953 ± 0.0250	0.1290 ± 0.0041

4.3.1 Network settings

The network is composed of a custom IEEE 802.11g/n Access Point (AP) and two notebooks, the first one Fujiitsu SIEMENS notebook acting as wired *client 1* and the second one DELL Latitude D620 notebook acting as a static wireless *client 2* as shown in Fig. 4.11. The AP is part of the Berlin Open Wireless Lab (BOWL)[2] testbed deployed at Deutsche Telekom Laboratories in Berlin, Germany. BOWL [Fischer 2011] is a project of the Intelligent Networks (INET) group at Telekom Innovation Laboratories. The main goal of the BOWL project is to provide an open platform for the wireless networking community. The AP is built around a PCEngines ALIX 3D2 (500MHzx86 CPU, 256MB of RAM) processor board equipped with one IEEE 802.11n wireless interface with RTC/CTS disabled. The Access Point exploits OpenWRT 10.3.01-rc1 as operating system. The ath9k[ath]

[2] Available at: `http://www.bowl.tu-berlin.de/`

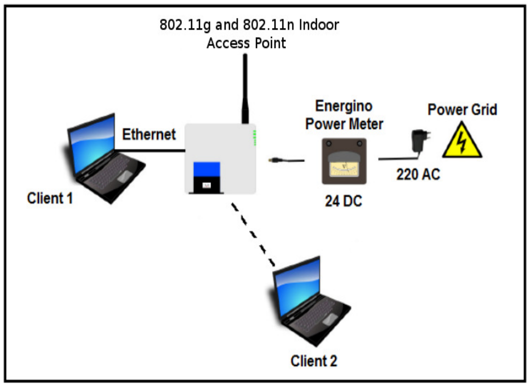

(a) Testing Scenario

(b) WiFi Indoor WAD

Figure 4.11: **WiFi Indoor WAD:** Network scenario used for the measurement campaign.

Wireless NIC driver has been used during the measurements campaign. The AP's operating frequency was set to 2.24GHz (Channel 11). It is important to note that, unless otherwise specified, the rate adaptation algorithm has been set to auto and the transmission power has been left to its default value equal to 19 dBm for all experiments. The notebooks *client 1* and *client 2* are regular Fujiitsu SIEMENS and DELL Latitude 6420 respectively, equipped with an Intel PRO/Wireless 3945AB wireless adapter and running Ubuntu 10.04.

4.3.2 Testing Methodology

The traffic generation and power consumption monitoring follows the same methodology explained in Subsection 4.2.2.1 and 4.2.2.2 respectively.

Synthetic traffic is modeled as single UDP flows. Results reported in this Section are the average of measurements collected during 600 seconds. The results are reported in terms average and with the 95% confidence interval. The following scenarios have been considered:

1) **Variable Traffic Generation Rate, Fixed Datagram Length:** In this test, the datagram size is kept constant at 1280 bytes, while the traffic generation rate is progressively increased from 5 Mb/s up to (i) 55 Mb/s for IEEE 802.11g technology and (ii) 120 Mb/s for IEEE 802.11n technology in steps of 5 Mb/s for both. This experiment is performed twice, firstly the indoor AP is configured with IEEE 802.11g and then the indoor AP is configured with IEEE 802.11n.

2) **Constant Traffic Generation Rate, Variable Datagram Length:** In this test, the traffic generation rate is kept constant at 20 Mb/s while the datagram size is progressively increased from 64 to 1920 bytes in steps of 128 bytes. Here, this experiment is also performed twice, firstly the indoor

AP is configured with IEEE 802.11g and then the indoor AP is configured with IEEE 802.11n.

3) **Variable Traffic Generation Rate, Variable Transmission Power Level:** In this test, the traffic generation rate is progressively increased from 5Mb/s up to 120 Mb/s in steps of 5 Mb/s. The transmission power level is set manually using the command line interface. The experiment is performed only with the indoor AP configured IEEE 802.11n.

4.3.3 Experimental Measurements and Analysis for IEEE 802.11n Wireless Access Devices

Here, the results from the measurements campaign described above are presented. The same notation used for the figures previously is maintained throughout the Section.

4.3.3.1 Traffic effect on Power Consumption of Wireless Access Devices

In order to study the relationship between traffic load and power consumption, the Fig. 4.12 shows a set of results that summarizes the behavior of IEEE 802.11n AP acting as a transmitter or receiver respectively in terms of power consumption and network performance. The Fig. 4.12a shows the average power consumption of the indoor IEEE 802.11n AP as a function of different traffic generation rates, for a fixed datagram size of 1280 bytes. When the AP is acting as a transmitter or receiver, we can observe that:

i) The average power consumption of the indoor IEEE 802.11n AP in idle mode, i.e., without any data but the standard IEEE 802.11n beacons, has been measured as 3.3 W. The results of average power consumption are shown in Fig. 4.12a.

ii) The power consumption behavior of IEEE 802.11g AP is equal to the behavior observed for the power consumption of the IEEE 802.11n AP. This behavior can be seen in Fig. 4.12a.

iii) The power consumption in the saturation point for the indoor IEEE 802.11n AP acting as a transmitter is around 4.9 W while for the indoor IEEE 802.11n AP acting as a receiver is around 3.75 W.

iv) The saturation point in terms of capacity for the AP acting as a transmitter is around 90 Mb/s while for the AP acting as a receiver is around 45 Mb/s. The results of throughput are shown in Fig. 4.12b. Note that the saturation point is determined by the WAD that is transmitting data since it depends on the efficiency of the *auto–modulation* algorithm. The *auto–modulation* algorithm should use the appropriate modulation and coding schemes for each scenario giving priority to higher modulation and coding schemes as much as possible.

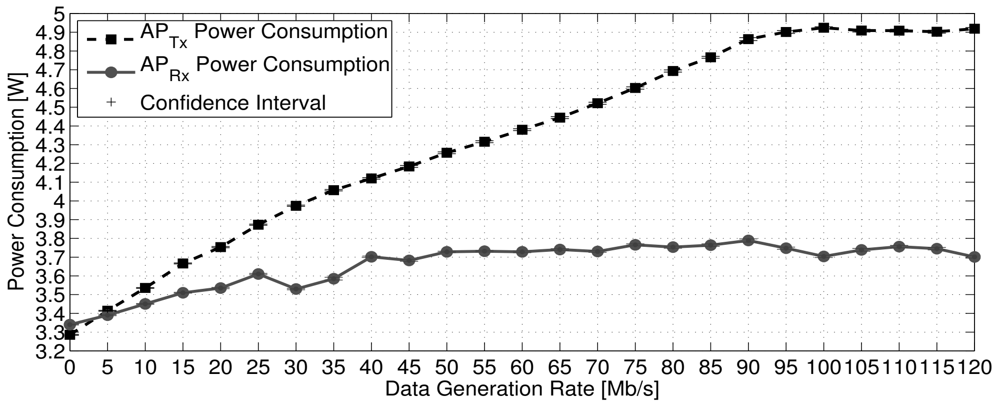

(a) Average Power Consumption (AP in Tx and Rx)

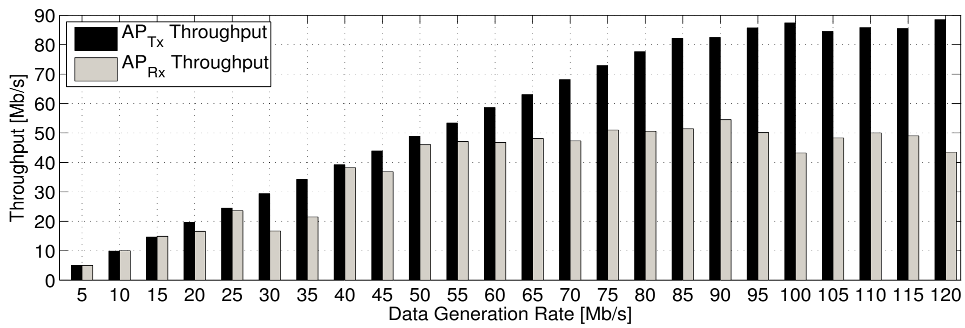

(b) Throughput (AP in Tx and Rx)

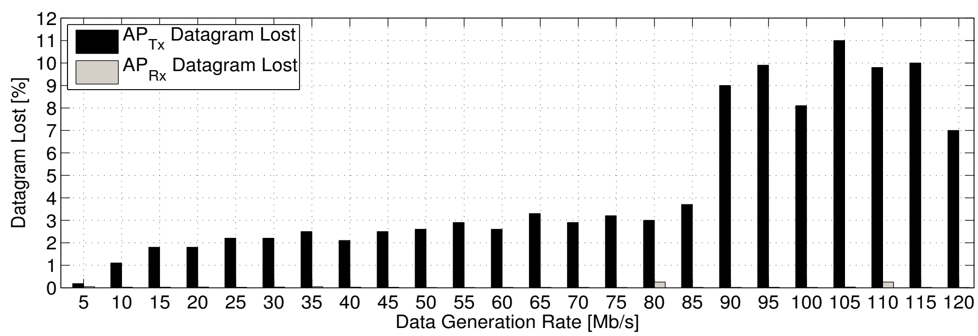

(c) Datagram loss (AP in Tx and Rx)

Figure 4.12: **WiFi Indoor WADs:** Average power consumption and network performance at the IEEE 802.11n AP as a function of different traffic generation rates for a constant datagram size of 1280 bytes

In the case when the indoor IEEE 802.11n AP is acting as a transmitter, we observed that it uses the higher modulation and coding schemes most of the time. Instead, in the case when the *client 2* is acting as a transmitter we observed that it do not use the higher modulation and coding schemes.

v) When the indoor IEEE 802.11n AP is acting as a transmitter and it reaches the saturation point, the datagram loss increases. Instead, when the *client 2* is acting as a transmitter the datagram loss is lower, around 1% (see explanation in the previous section). The results of datagram loss are shown in Fig. 4.12c.

It is important to note that, we observed a similar power consumption behavior for both outdoor 802.11g AP and indoor 802.11g AP. However, there are differences in (i) the amount of power consumed in saturation, (ii) amount of power consumed for transmitting and receiving data and (ii) the amount of traffic that saturates the AP.

4.3.3.2 Datagram Size effect on Power Consumption of Wireless Access Devices

In order to understand the impact of the datagram size on the power consumption of the indoor IEEE 802.11n AP, Fig. 4.13 reports the average power consumption and network performance at indoor IEEE 802.11n AP as a function of the datagram size for a constant data generation rate of 20 Mb/s. As it can be seen, the datagram size has a considerable impact on power consumption of the indoor IEEE 802.11n AP. Note that the power consumption behavior of the IEEE 802.11n AP transmitting and receiving small/large datagrams is equal to the behavior observed for the power consumption of the IEEE 802.11g AP. The observation and remarks regarding small and large datagrams are explained in the previous section.

4.3.3.3 Effect of Transmission Power levels on the Power Consumption of Wireless Access Devices

In the next set of measurements, we report the power consumption statistics related to the case in which the indoor IEEE 802.11n AP is acting as a transmitter or receiver with different transmission power levels. We considered two different transmission power levels, i.e., 12 dBm and 19 dBm (19 dBm is the maximum transmission power supported by the AP). The results are reported in the next set of figures.

When the AP is acting as a transmitter or receiver, results show that the power consumption behavior of the IEEE 802.11n AP using different transmission power levels is equal to the behavior observed for the power consumption of the IEEE 802.11g AP. However, we can observe that the results of power consumption and network performance for IEEE 802.11n AP when are fluctuating. It is because; the *auto–modulation* algorithm in *client 2* is not stable as much is the *auto–modulation* algorithm in IEEE 802.11n AP. We observed that, it is constantly changing from lower to higher modulations and coding schemes. The results of average power consumption are shown in Fig. 4.14a and Fig. 4.15a. While, the results for throughput in percentage are shown in Fig. 4.14b–4.15b and the results of datagram loss are shown in Fig. 4.15c–4.14c.

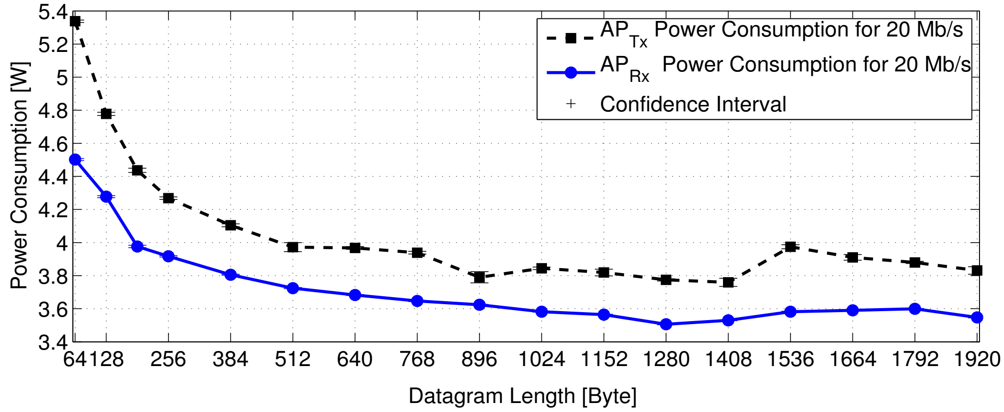

(a) Average Power Consumption (AP in Tx and Rx)

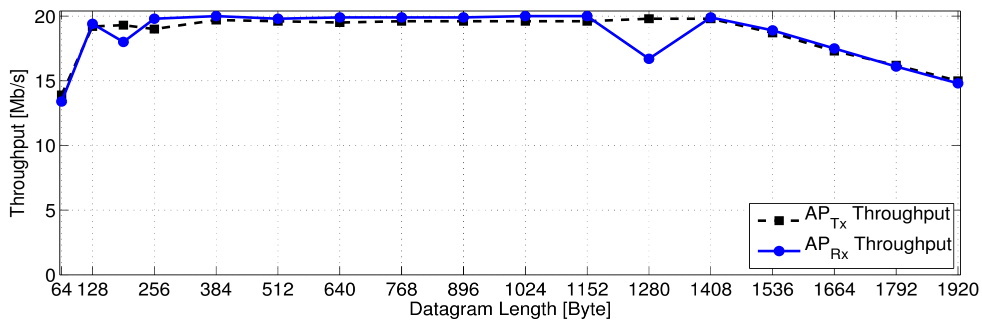

(b) Throughput (AP in Tx and Rx)

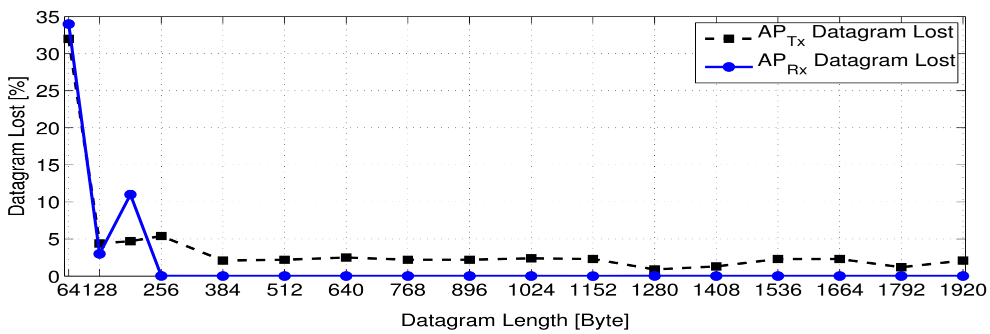

(c) Datagram loss (AP in Tx and Rx)

Figure 4.13: **WiFi Indoor WADs:** Average power consumption and network performance at the IEEE 802.11n AP as a function of the datagram size for a constant traffic generation rate of 20 Mb/s

4.3.4 Power Consumption Behavior Comparison between IEEE 802.11g and IEEE 802.11n Indoor Wireless Access Devices

In this section, we compare the results from the measurement campaign discussed in the previous section. In order to compare the behavior of power consumption of the indoor AP working under IEEE 802.11g and IEEE 802.11n technologies, the

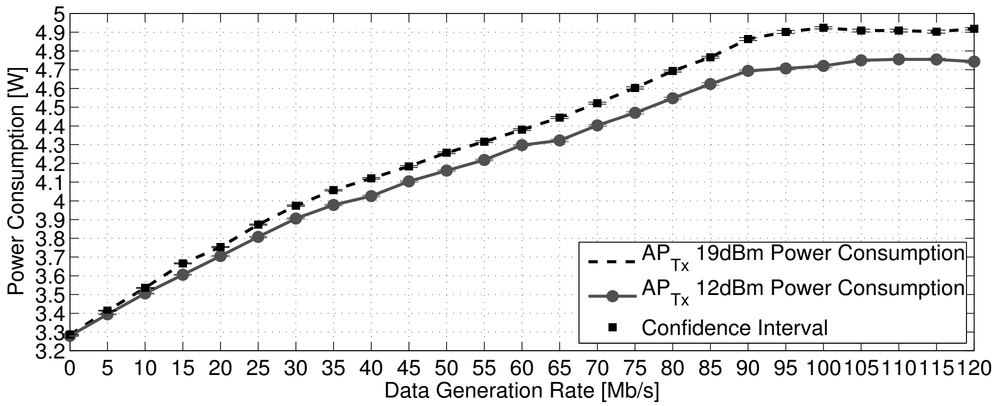

(a) Average Power Consumption (AP in Tx)

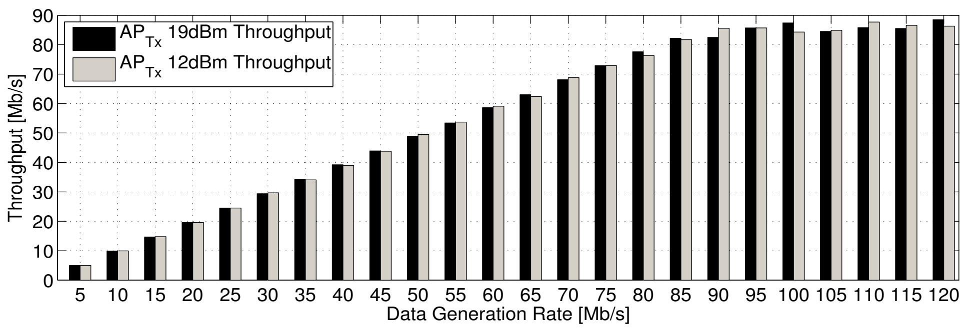

(b) Throughput (AP in Tx)

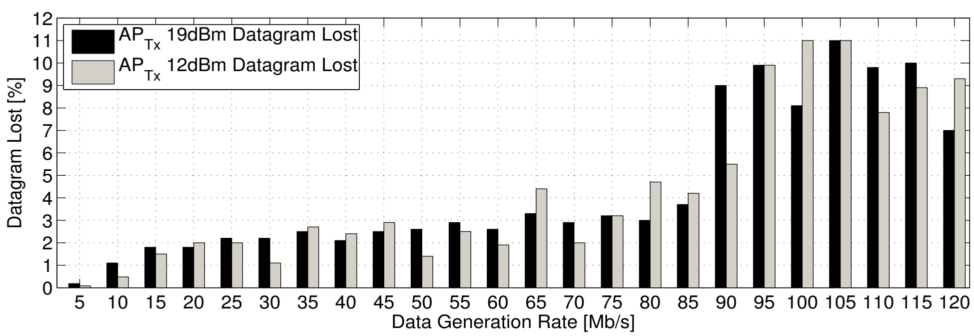

(c) Datagram loss (AP in Tx)

Figure 4.14: **WiFi Indoor WADs:** Average power consumption and network performance at the IEEE 802.11n AP as a function of different traffic generation rates for different transmission power levels rates for a constant datagram size of 1280 bytes

Fig. 4.16 and Fig. 4.17 show a set of results that compare the behavior of AP acting as a transmitter or receiver respectively, in terms of power consumption and network performance. Specifically, the Fig. 4.16a and Fig. 4.17a show the comparison of the average power consumption at the IEEE 802.11g AP and IEEE 802.11n AP

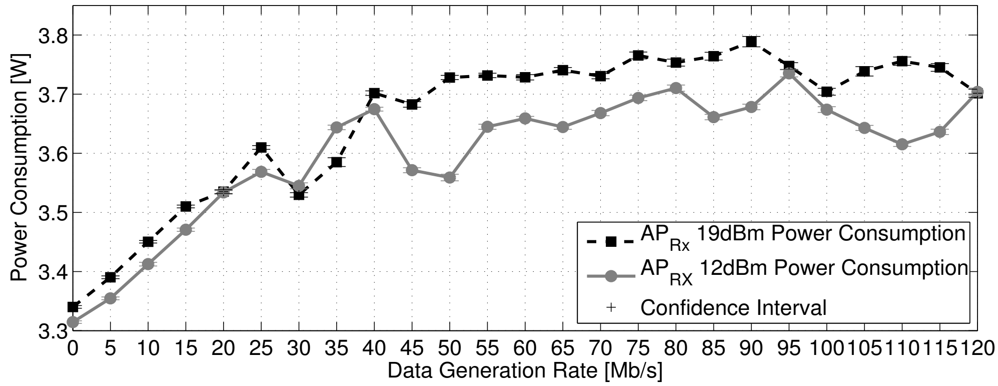

(a) Average Power Consumption (AP in Rx)

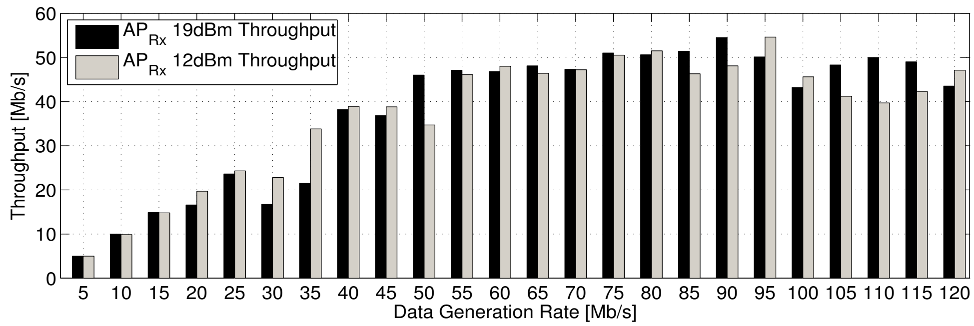

(b) Throughput (AP in Rx)

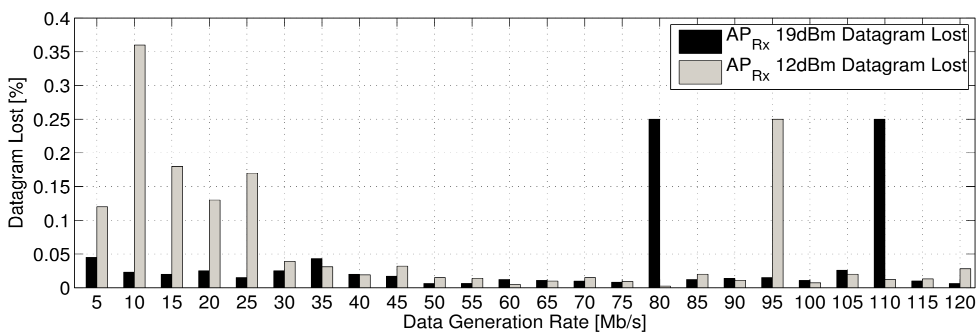

(c) Datagram loss (AP in Rx)

Figure 4.15: **WiFi Indoor WADs:** Average power consumption and network performance at the IEEE 802.11n AP as a function of different traffic generation rates for different transmission power levels rates for a constant datagram size of 1280 bytes

as a function of different traffic generation rates for a constant datagram size of 1280 bytes. We can observe that when the AP is acting as a transmitter or receiver:

i) The average power consumption of the AP in idle mode has been measured as 3.3 W and it is the same for both technologies. The results of average power consumption are shown in Fig. 4.16a and Fig. 4.17a.

ii) The power consumption behavior is similar for both the cases when the AP is configured with IEEE 802.11g and IEEE 802.11n. The power consumption is monotonically increasing with the traffic load until it reaches a saturation point. However, the power consumption at the saturation point and the slope of the curve of power consumption are different when AP configured with IEEE 802.11g and IEEE 802.11n.

iii) The power consumption for the AP acting as a transmitter in the saturation point is around 4.9 W for IEEE 802.11n and 4 W for IEEE 802.11g. The power consumption for the AP acting as a receiver is around 3.75 W for IEEE 802.11n and 3.63 W for IEEE 802.11g. The AP configured with IEEE 802.11n is more energy efficient that AP configured with IEEE 802.11g.

iv) When the AP reaches the saturation point, the maximum throughput and the power consumption remains constant. The throughput results are shown in Fig. 4.16b and Fig. 4.17b. The saturation point in terms of capacity for the AP acting as a transmitter is around 90 Mb/s for IEEE 802.11n and 20 Mb/s for IEEE 802.11g while the AP acting as a receiver is around 45 Mb/s for IEEE 802.11n and 23 Mb/s for IEEE 802.11g. It is important to note that there is a bigger difference in terms of capacity between IEEE 802.11n and IEEE 802.11g technologies, as we expected.

v) When the indoor AP is acting as a transmitter or receiver, the datagram loss is different for both the cases. The results of datagram loss are shown in Fig. 4.16c and Fig. 4.17c. We can observe a marked difference in terms of datagram loss between both technologies, especially when the indoor AP is acting as a transmitter. Because, when the AP is configured with IEEE 802.11n the datagrams are not dropped due to the saturation of the physical interface. The purpose of IEEE 802.11n standards is to improve network throughput over the two previous standards, 802.11a and 802.11g, with a significant increase in the maximum bitrate from 54 Mb/s to 600 Mb/s (theoretically, using MIMO technologies).

In order to compare the impact of the datagram size on the power consumption of the AP working under IEEE 802.11g and IEEE 802.11n technologies, Fig. 4.18a and Fig. 4.19a report the comparison of the average power consumption at the IEEE 802.11g AP and IEEE 802.11n AP as a function of the datagram size for a constant traffic generation rate of 20 Mb/s. As it can be seen, the datagram size has a considerable impact on power consumption when the AP is acting as a transmitter as well as receiver. We can observe that:

i) When the datagram size becomes extremely low, the AP configured with IEEE 802.11n is more energy efficient than the AP configured with IEEE 802.11g. The results of average power consumption are shown in Fig. 4.18a

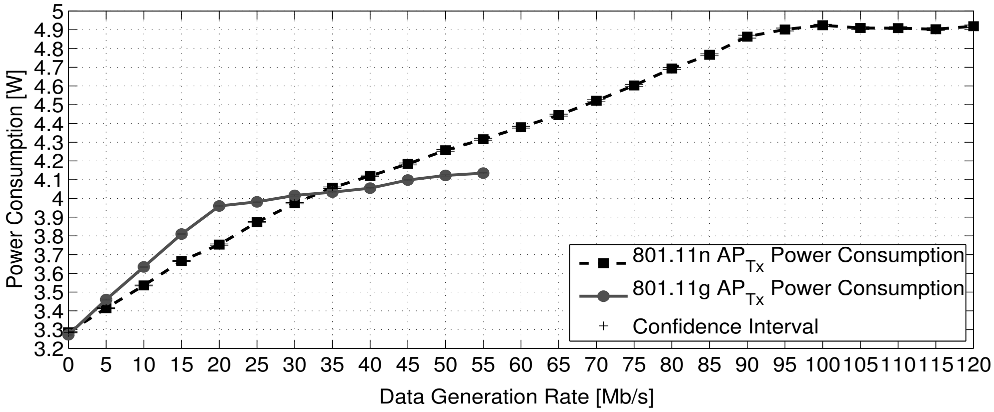

(a) Average Power Consumption (AP in Tx)

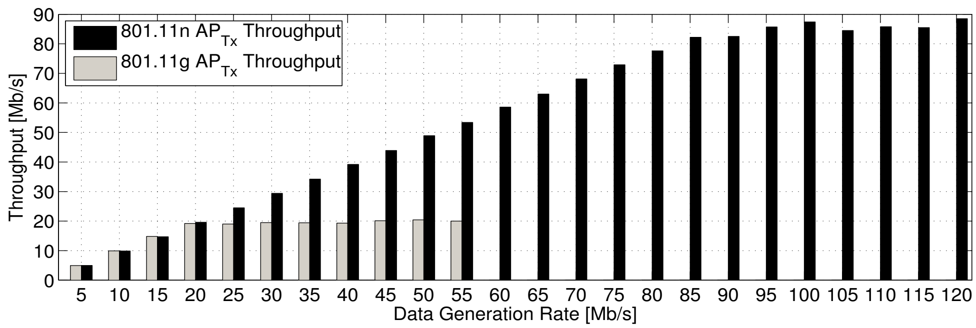

(b) Throughput (AP in Tx)

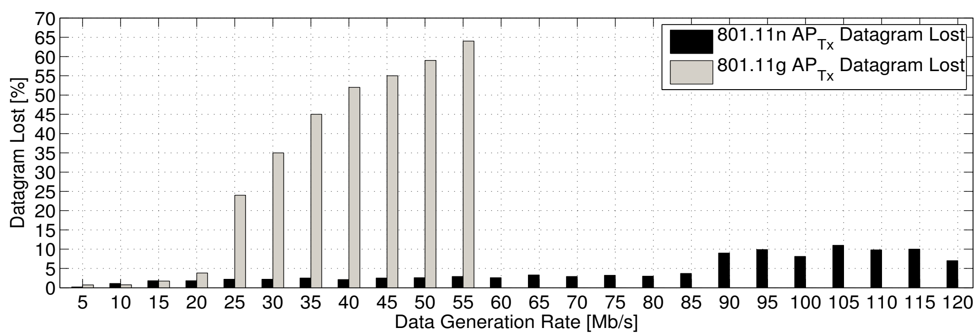

(c) Datagram loss (AP in Tx)

Figure 4.16: **WiFi IEEE 802.11g/n Indoor WADs:** Comparison of the average power consumption and network performance for the IEEE 802.11g AP and IEEE 802.11n AP as a function of different traffic generation rates for a constant datagram size of 1280 bytes. AP acting as a transmitter

and Fig. 4.19a. However, in this figure the effect of the datagram size on the power consumption is not clear because the real throughput for IEEE 802.11g is lower than the expected throughput as shown in Fig. 4.18b and Fig. 4.19b. Therefore, Fig. 4.20a and Fig. 4.20b show the comparison of the average en-

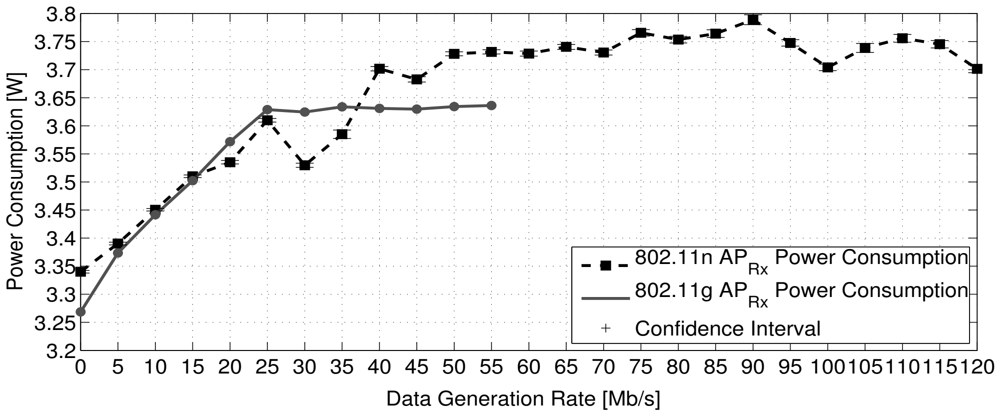

(a) Average Power Consumption (AP in Rx)

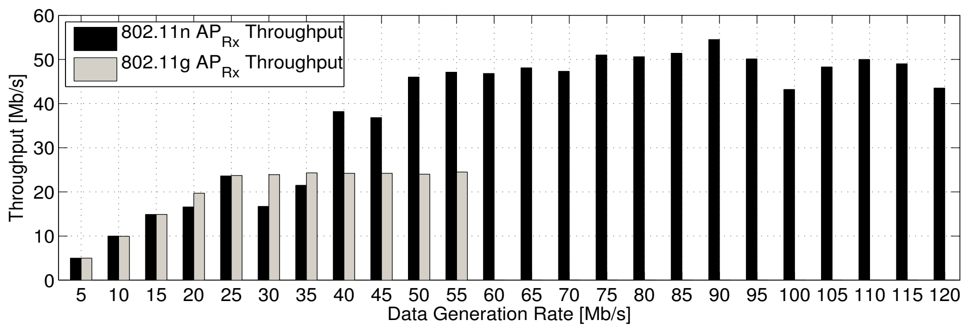

(b) Throughput (AP in Rx)

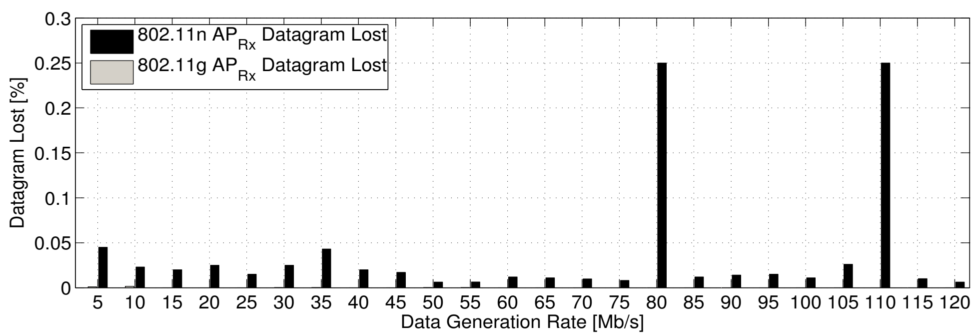

(c) Datagram loss (AP in Rx)

Figure 4.17: **WiFi IEEE 802.11g/n Indoor WADs:** Comparison of the average power consumption and network performance for the IEEE 802.11g AP and IEEE 802.11n AP as a function of different traffic generation rates for a constant datagram size of 1280 bytes. AP .

ergy per bit at the IEEE 802.11g AP and IEEE 802.11n AP as a function of the datagram size for a constant traffic generation rate of 20 Mb/s.

ii) When the packet size is closer and lower of the MTU, the AP configured with IEEE 802.11n is more energy efficient than the AP configured with IEEE

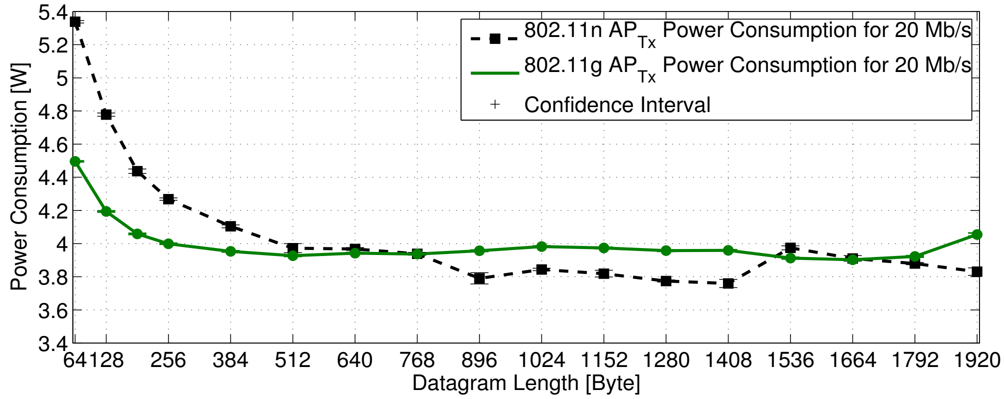

(a) Average Power Consumption (AP in Tx)

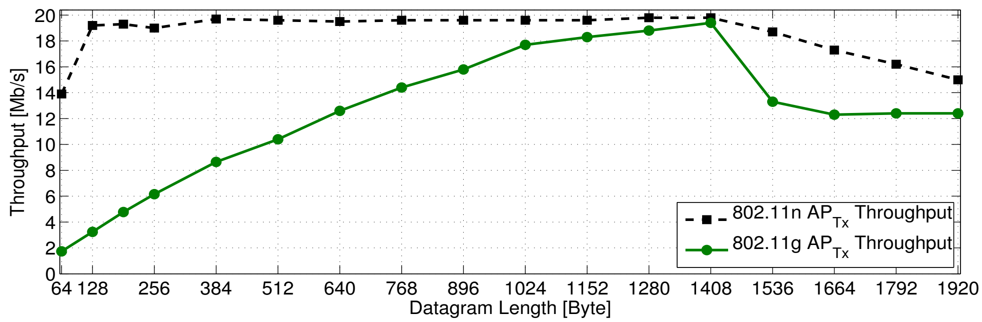

(b) Throughput (AP in Tx)

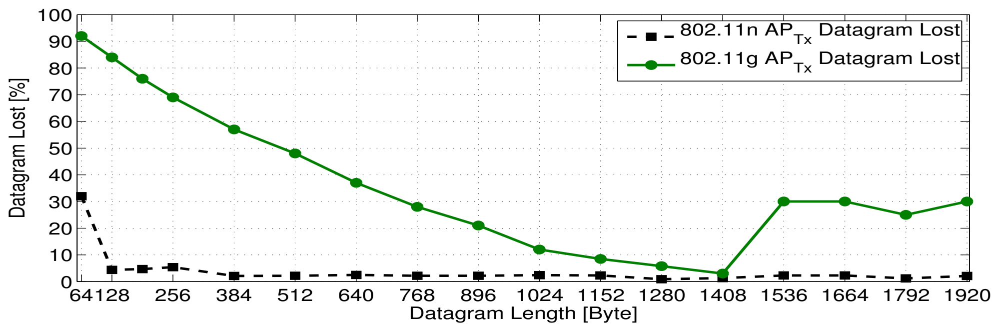

(c) Datagram loss (AP in Tx)

Figure 4.18: **WiFi IEEE 802.11g/n Indoor WADs:** Comparison of the average power consumption and network performance at the IEEE 802.11g AP and IEEE 802.11n AP as a function of the datagram size for a constant traffic generation rate of 20 Mb/s. AP acting as a transmitter.

802.11g. For those samples the network performance is also similar as shown in Fig. 4.18a and Fig. 4.19a for datagram size of 1280 and 1408 bytes. As it can be seen in these figures the IEEE 802.11n is more energy efficient than IEEE 802.11g for any datagram size.

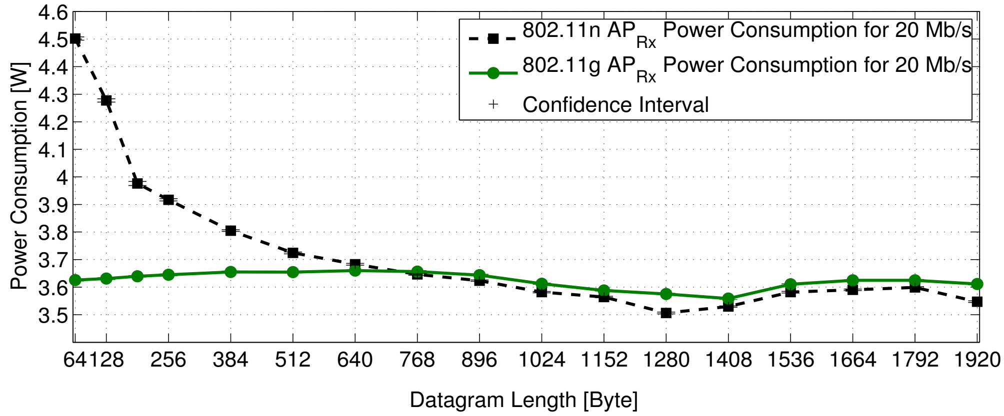

(a) Average Power Consumption (AP in Rx)

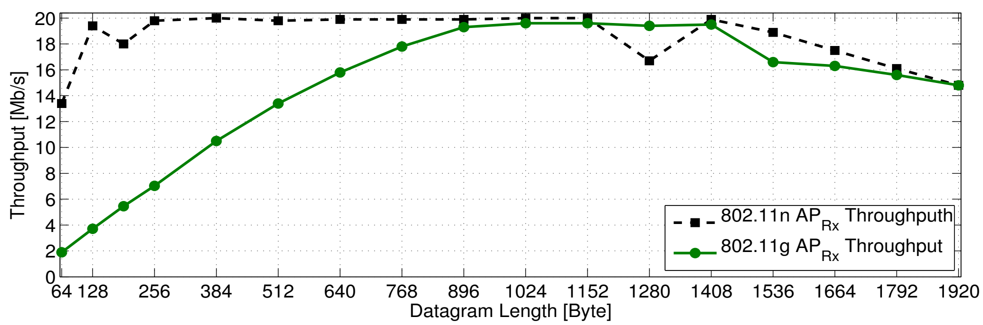

(b) Throughput (AP in Rx)

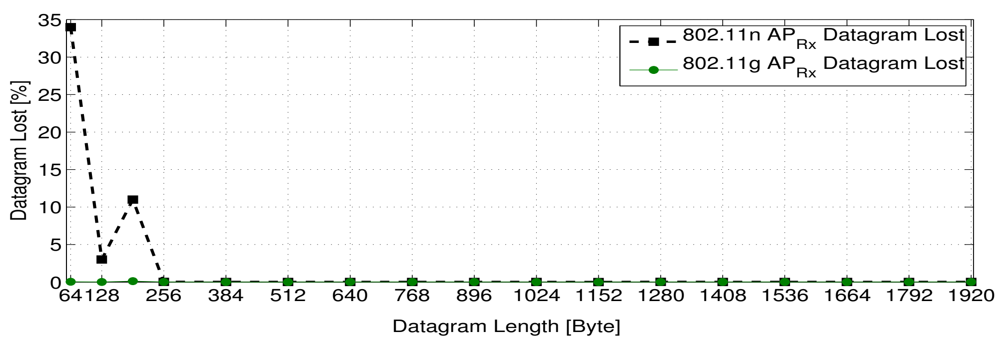

(c) Datagram loss (AP in Rx)

Figure 4.19: **WiFi IEEE 802.11g/n Indoor WADs:** Comparison of the average power consumption and network performance at the IEEE 802.11g AP and IEEE 802.11n AP as a function of the datagram size for a constant traffic generation rate of 20 Mb/s. AP .

iii) When the datagram size becomes extremely large, fragmentation takes place, the throughput utilization decreases as shown in Fig. 4.18b and Fig. 4.19b. The AP configured with IEEE 802.11n is more energy efficient than the AP configured with IEEE 802.11g.

iv) The impact of the small datagram size on the throughput is shown in Fig. 4.18b and Fig. 4.19b. The throughput also decreases for the small datagram size in both cases when the AP is configured with IEEE 802.11g and IEEE 802.11n. However, this effect is more evident on IEEE 802.11g, it occurs for datagram size from 64 until 1204 bytes while for IEEE 802.11n, it occurs for datagram size from 64 bytes until 128 bytes. When the AP is configured with IEEE 802.11n is more throughput efficient than with IEEE 802.11g for all the different datagram sizes.

v) The impact of the datagram size on the datagram loss is shown in Fig. 4.18c when the AP is acting as a transmitter, the results show that the datagram loss increases for the large datagram only when AP is configured with IEEE 802.11g. The datagram loss also increases for the small datagram size in both cases when the AP is configured with IEEE 802.11g and IEEE 802.11n. However, this effect is more evident on IEEE 802.11g, it occurs for datagram size from 64 until 1024 bytes while for IEEE 802.11n, it occurs for datagram size from 64 bytes until 128 bytes.

vi) The impact of the datagram size on the datagram loss is shown in Fig. 4.19c when the AP is , the results show that the datagram loss increases for the small datagram only when AP is configured with IEEE 802.11g. This behavior is related to the memory resources of the device and it was already explained previously.

4.4 WiMAX Outdoor WADs: Power Consumption Behavior of IEEE 802.16 Wireless Access Devices

Here, we will describe the network setups and the methodology used in order to evaluate the power efficiency of an outdoor WiMAX network deployed in a rural area. The network setups exploited in the WiMAX scenario are sketched in Fig. 4.21.

4.4.1 Network settings

The WiMAX network is composed of a BS deployed on the rooftop of a building and a single static Subscriber Station (SS) deployed on the rooftop of another building. The testbed is deployed across the Orange Labs Campus in Lannion, France. The BS and the SS are about 800 meters away from each other and are operating under line of sight conditions. The WiMAX equipment is compliant with the IEEE 802.16–2004 version of the standard and implements the TDD duplexing scheme. The devices operate between 5.47 and 5.725 GHz using omni–directional antennas with a gain of 8 dB. With regard to QoS, the devices support the Best Effort (BE), the Real–time Polling Service (rtPS), the Non–real–time Polling Service (nrtPS), and the Unsolicited Grant Service (UGS) traffic classes. The BE class has been used throughout the entire measurements campaign reported in this work. It is important

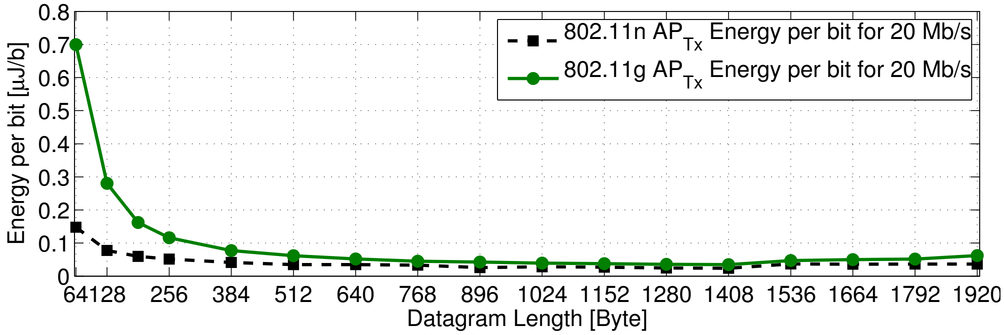

(a) Average energy per bit (AP in Tx)

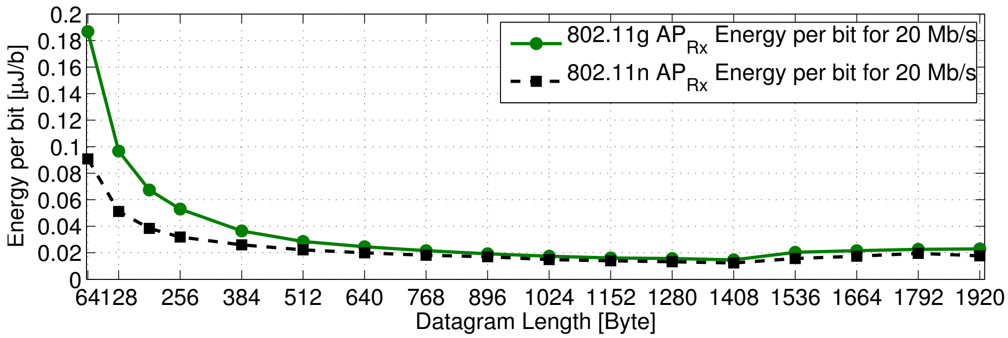

(b) Average energy per bit (AP in Rx)

Figure 4.20: **WiFi IEEE 802.11g/n Indoor WADs:** Comparison of the average energy per bit at the IEEE 802.11g AP and IEEE 802.11n AP as a function of the datagram size for a constant traffic generation rate of 20 Mb/s

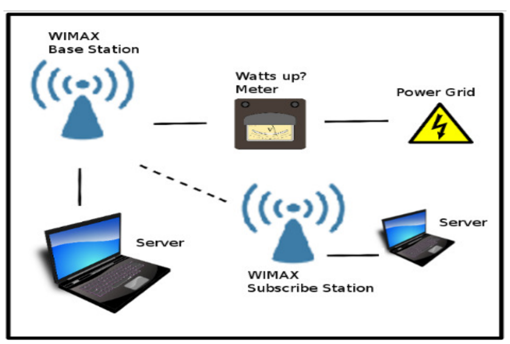

(a) WiMAX Testing Scenario

(b) Outdoor Base Station

Figure 4.21: **WiMAX Outdoor WADs:** Network scenario used for the measurement campaign.

to note that, unless otherwise specified, the rate adaptation algorithm has been set to *auto–modulation* and the transmission power has been left to its default value equal to 18 dBm (≈63.1 mW).

4.4.2 Testing Methodology

4.4.2.1 Traffic Generation and Power Consumption Monitoring

Traffic is generated using the Iperf traffic generator[ipe] and is injected into the network trough either the *Server* or the *client*. In the former case, we aimed at measuring the power consumed by the BS when it is acting as a transmitter, while in the latter case we aimed at measuring the power consumed by the BS when it is . In both cases the power consumption figures reported in this work refer to the BS.

The power consumption is measured using the *Watts Up?*[wat] power meter. *Watts Up?* is a "plug load" meter that measures the amount of electricity used by whatever electrical appliance is plugged into it. The meter incorporates digital electronics to perform accurate power consumption measurements. Such measurements are then logged into the device's internal memory with a granularity of 0.1 Watts and a sampling period of 1 second.

The *Watts Up?* meter is interconnected through its USB interface to the *Server* where a custom data logging software is used in order to extract the power consumption samples. It is important to remark that the power consumption is monitored for the whole device. Therefore, the results reported in this section account for both the power consumed by the processing board for handling the incoming and outgoing traffic (i.e. for segmentation and reassembling, protocol overheads, computing checksums, etc.) as well as for the power consumed to deliver the actual frame over the wireless link (i.e. power amplifiers, modulator/demodulator, etc.).
NOTE: We were not able to use *energino* power meter in this experiments since *energino* was in a early phase when we obtained the permission for using WiMAX testbed.

4.4.2.2 Experimental Details

Synthetic traffic is modeled as single UDP flows. Results reported in this section are the average of 4 runs. The results are reported in terms of a 95% confidence interval. Each run was performed for 500 seconds. The following scenarios have been considered:

- **Variable Traffic Generation Rate, Fixed Packet Length**. In this test, the datagram size is kept constant at 1280 bytes, while the traffic generation rate is progressively increased from 0.1 Mb/s from 0.1 Mb/s up to 30 Mb/s.

- **Constant Traffic Generation Rate, Variable Packet Length**. In this test, the traffic generation rate is kept constant while the datagram size is progressively increased from 32 to 2816 bytes in steps of 256 bytes. Two different settings have been considered for the traffic generation rate resulting in application throughput of 1 Mb/s and 5 Mb/s.

- **Variable Traffic Generation Rate, Mixed Transmission Power**. In this test, the datagram size is kept constant at 1280 bytes while the traffic

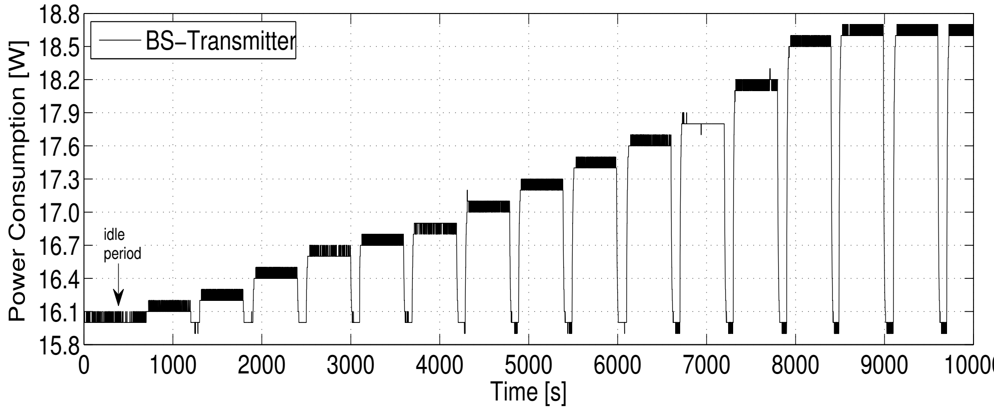

Figure 4.22: **WiMAX Outdoor WADs:** Power consumption when synthetic traffic is injected at an increasing rate at the BS.

generation rate is progressively increased. This test has been repeated using 10 dBm (≈10 mW) and 26 dBm (≈398 mW) transmission power levels.

- **Variable Traffic Generation Rate, Fixed Modulation Type**. In this test, the datagram size is kept constant at 1280 bytes while the message generation rate is progressively increased. The rate control algorithm is disabled and the transmission rate is set manually using the command line interface. The experiment is repeated for each of the transmission rates supported by the wireless adapter (see Table 4.1).

4.4.3 Experimental Measurements and Analysis for IEEE 802.16 Wireless Access Devices

In this Section, we present the results from the measurements campaign using WiMAX test environments. We use the following notation for the figures throughout the section (a) BS–Receiver is when BS is and (b) BS–Transmitter when BS is acting as a transmitter.

4.4.3.1 Traffic Effect on Power Consumption of Wireless Access Devices

In order to study the relationship between traffic load and power consumption, we performed a set of measurements aimed at characterizing the power consumption of the WiMAX networks when synthetic traffic is injected at an increasing rate. The outcomes of this set of measurements are reported in Fig. 4.22. Each step in the power consumption corresponds to an increase in the traffic rate, starting from no traffic up to 30 Mb/s. As it can be seen, the power consumption of the BS in idle mode is ≈ 16.05 W and monotonically increases with the traffic until a saturation point is reached.

The average power consumption of the BS as a function of different traffic generation rates is shown in Fig. 4.23a, for a fixed datagram size of 1280 bytes. The power consumption when the BS is acting as a transmitter increases according to the increase in traffic. The power consumption when the BS is remains unchanged, as expected. We can observe in Fig. 4.23b that when the BS reaches saturation, the maximum throughput value remains constant. The datagram loss starts to increase when the BS reaches saturation, these results are shown in Fig. 4.23c. It is important to remark that the power consumption of BS acting as a transmitter follows the same behavior of the outdoor IEEE 802.11g AP and indoor IEEE 802.11n AP.

4.4.3.2 Datagram Size Effect on Power Consumption of Wireless Access Devices

In Fig. 4.24a, the average power consumption level at the BS as a function of the datagram size for a constant throughput is presented. This gives us certain insights in order to understand "how" the datagram size impacts power consumption. Results are plotted for the BS acting as a transmitter or receiver, respectively. As it can be seen, the power consumption behavior for this experiment is similar to the behavior observed for both outdoor IEEE 802.11g AP and indoor IEEE 802.11n AP (see Fig. 4.3 and Fig. 4.13). The datagram size has a considerable impact on power consumption when the BS is acting as a transmitter. However, when the BS is , there is no impact on power consumption for any datagram size. Instead, for the WiFi cases analyzed in previous subsections, when the AP is , the impact on power consumption for any datagram size follows similar behavior of the AP when acting as a transmitter but with a lower power consumption. Such differences in power consumption while the BS/AP is in receiving mode can be attributed to the manner in which the MAC receives and processes the packets in the case of the two access technologies.

Finally, we can observe that (i) for small datagram sizes, the BS power is wasted because the BS consumes significantly more power than for the large datagram sizes under the same traffic conditions, and (ii) when the datagram size becomes extremely large, fragmentation takes place and consequently, the throughput utilization decreases. This effect is shown in Fig. 4.24b, the results show the throughput for the experiments performed by 5 Mb/s. Therefore, the optimal datagram length in terms of power consumption and network performance for a static client is 1280 bytes. The datagram loss for these set of experiments was lower than 1%.

4.4.3.3 Transmission Power Level Effect on the Power Consumption of Wireless Access Devices

In the next set of measurements, we report only the power consumption statistics relative to the case in which the BS is acting as a transmitter. The power consumption when the BS is remains always unchanged as we have explained before. We considered two different transmission power levels, i.e., 10 dBm and 26 dBm. The results are reported in Fig. 4.25a. The Fig. 4.25a shows the average power consumption at the BS as a function of different traffic generation rates for transmission power of 10 dBm and 26 dBm with Datagram size is equal to 1280 bytes.

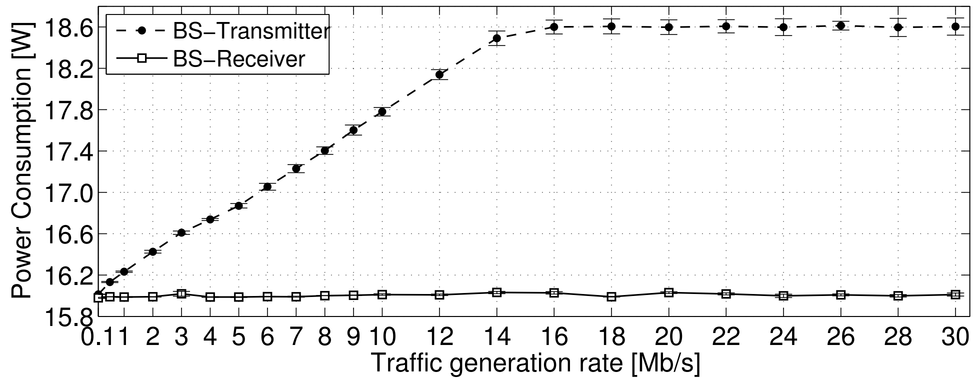

(a) Power Consumption (BS in Tx and Rx)

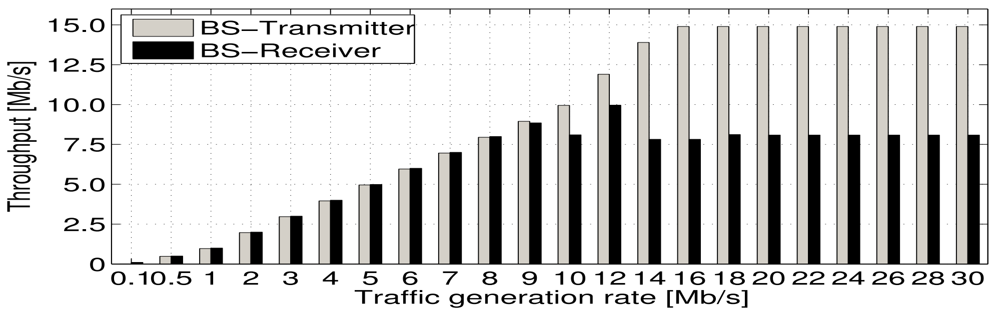

(b) Throughput (BS in Tx and Rx)

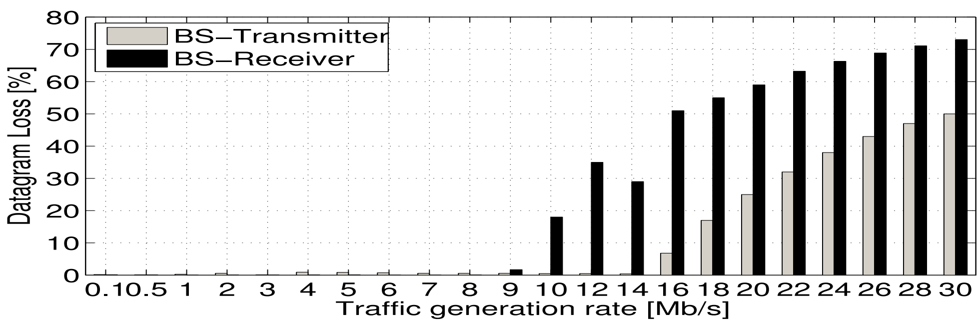

(c) Datagram loss (BS in Tx and Rx)

Figure 4.23: **WiMAX Outdoor WADs:** Average power consumption and network performance as a function of different traffic generation rates for a constant datagram size of 1280 bytes.

Results show that two different transmitter power levels are characterized by the same power consumption in saturation. The reason for this behavior is that the contribution of the power amplifier to the overall consumption is below the sampling capability of the meter used in our measurements (i.e. lower than 0.1 W). On the other hand what came as a surprise is the fact that, when using the high transmission power level (26 dBm), the saturation is reached for slower data rates than when using

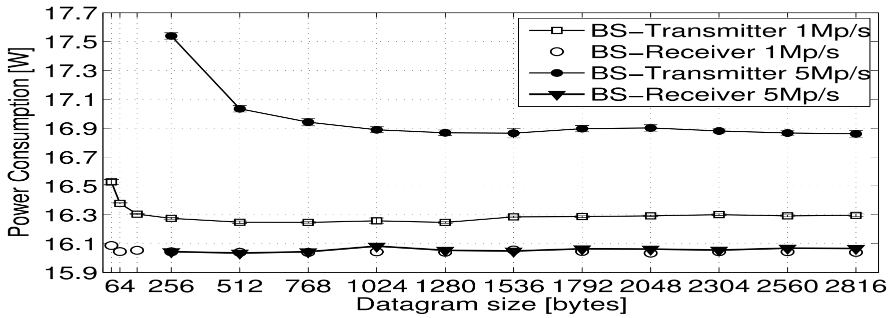

(a) Power Consumption (BS in Tx and Rx)

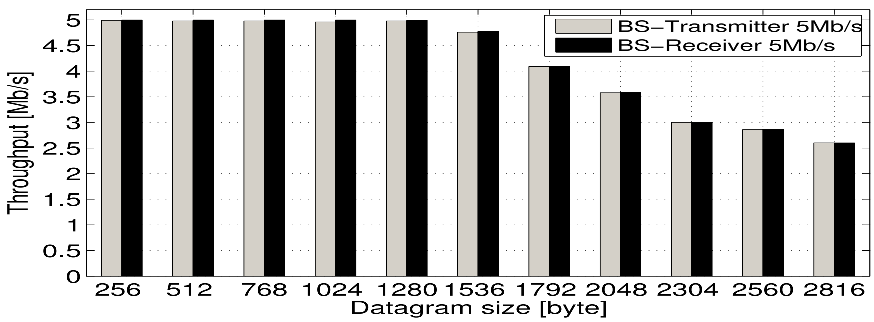

(b) Throughput for the experiment with 5 Mb/s (BS in Tx and Rx)

Figure 4.24: **WiMAX Outdoor WADs:** Average power consumption and throughput at either the BS as a function of the datagram size for a constant traffic generation rate (1 and 5 Mb/s). Datagram loss was less than 1% during all measurements.

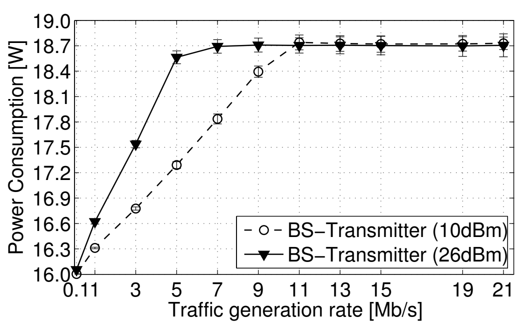

(a) Power Consumption (BS in Tx)

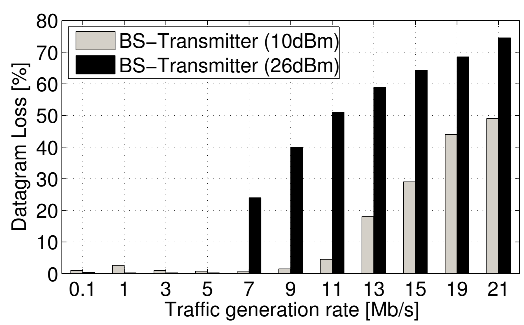

(b) Datagram loss (BS in Tx)

Figure 4.25: **WiMAX Outdoor WADs:** Average power consumption at the BS and datagram loss as a function of different traffic generation rates for different transmission power levels. Datagram size is equal to 1280 bytes.

the low transmission power level (10 dBm). Moreover, increasing the transmitter power results in an increased datagram loss, while one would expected that a better

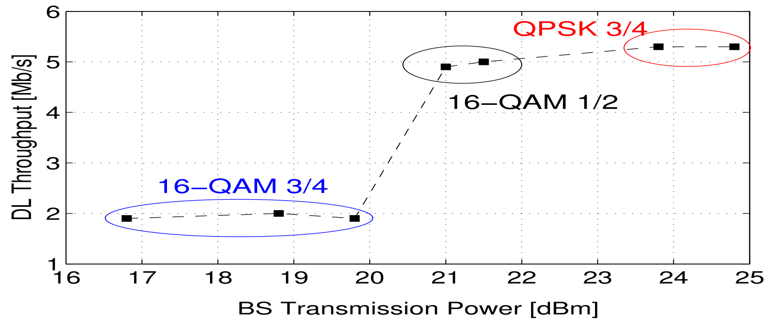

Figure 4.26: **WiMAX Outdoor WADs:** Goodput between BS and SS using different transmission power levels. The results refer to a saturated TCP connection.

SINR would give better performance in terms of packet loss.

In order to investigate this phenomenon, we carried out additional measurements by generating a saturated TCP connection from the BS to the SS. The test was repeated using different transmission power levels. The outcomes are reported in Fig 4.26. As it can be seen, for low transmission power levels, the BS uses high rate modulation and coding schemes (16–QAM 3/4), while when the transmission power level increases the BS switches to less efficient modulation and coding schemes (16–QAM 1/2 and QPSK 3/4). This choice results in less airtime–efficient modulation and coding schemes being used when the transmitter power is set to 26 dBm which in time causes the system to reach the saturation point for lower data–rates (see Fig. 4.25a). Likewise, high datagram loss is experienced by the system when the traffic generation rate increases in that less efficient modulation and coding schemes result is a low bitrate wireless link which in time causes datagrams to be dropped at the wireless interface.

4.4.3.4 Modulation and Coding Schemes on Power Consumption of Wireless Access Devices

Lastly, we study the impact of modulation and coding schemes on power consumption patterns. We forced the modulation and coding schemes to be used by wireless interfaces and measured the power consumption as a function of the traffic generation rate. The results are the following:

- **BPSK 1/2 and QPSK 3/4 modulations:** Fig. 4.27a reports the average power consumption at the BS when acting as a transmitter, as a function of different traffic generation rates for BPSK 1/2 and QPSK 3/4 modulations. Datagram size is equal to 1280 bytes. Fig. 4.27b reports the datagram loss.

- **QPSK 1/2 and 16-QAM 1/2 modulations:** Fig. 4.27c reports the average power consumption at the BS when acting as a transmitter, as a function of different traffic generation rates for QPSK 1/2 and 16-QAM 1/2 modulations. Datagram size is equal to 1280 bytes. Fig. 4.27d reports the datagram loss.

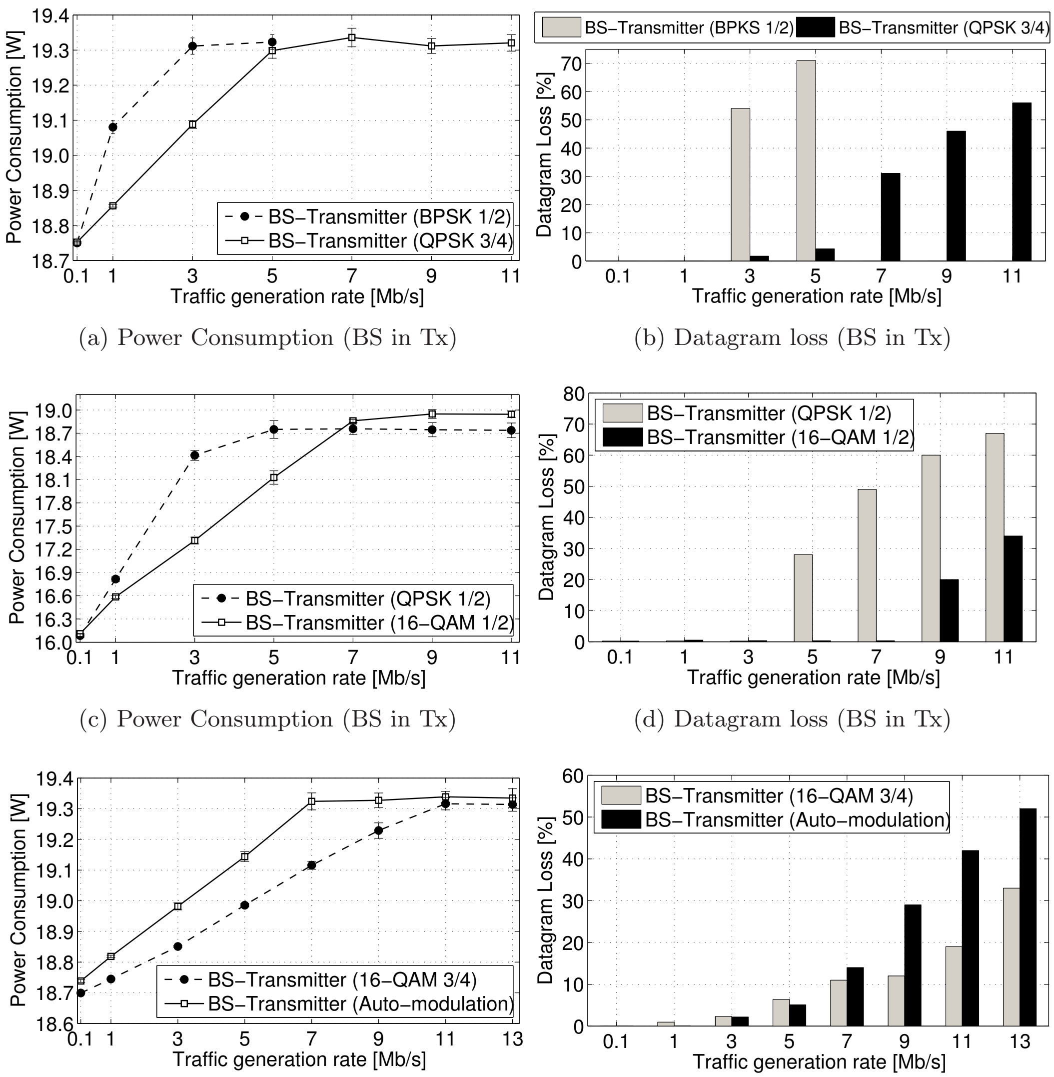

(a) Power Consumption (BS in Tx) (b) Datagram loss (BS in Tx)

(c) Power Consumption (BS in Tx) (d) Datagram loss (BS in Tx)

(e) Power Consumption (BS in Tx) (f) Datagram loss (BS in Tx)

Figure 4.27: **WiMAX Outdoor WADs:** Average of power consumption at the BS (Transmitter) and datagram loss as a function of different traffic generation rate for different modulation types. Datagram size is equal to 1280 bytes.

- **16–QAM 3/4 modulation and Auto–rate:** Fig. 4.27e reports the average power consumption at the BS when acting as a transmitter, as a function of different traffic generation rates for 16-QAM 3/4 modulation and Auto-modulation. Datagram size is equal to 1280 bytes. Fig. 4.27f reports the datagram loss.

The figures shows that for the (i) QPSK 3/4 modulation is better than BPSK modulation 1/2 and (ii) 16-QAM 1/2 modulation is better than QPSK 1/2 modulation in terms of power consumption and network performance for a static client.

Therefore higher modulation rates are more power efficient. This is understood to be due to the fact that higher modulation and coding schemes keep the transmitter RF interface in the "on" state for a shorter amount of time. Of course this holds in a situation in which the channel condition is good. Finally, we can see also that the 16-QAM 3/4 modulation is better than *auto–modulation* in terms of power consumption and network performance for a static client. This is because the rate control algorithms are based in parameters related with the channel, such as, RSSI and transition success probabilities. However, the rate control algorithm cannot quickly adapt to the channel variations and it chooses a lower modulation scheme even when the channel conditions allow the use of a higher modulation scheme.

4.5 Conclusions

In this Chapter, we proposed a measurement–based methodology for characterizing the power consumption behavior of networked WADs. In particular, we focused our attention on indoor–outdoor WiFi and WiMAX WAD and we derived their power consumption figures as a function of (i) the traffic load, (ii) the modulation and coding schemes, (ii) the size of the datagrams used and (iv) different transmission power levels. The main observations of this Chapter are:

- The power consumption of the WAD depends on several factors, such as the amount of traffic, packet size, transmission power level, modulation and coding schemes and channel conditions.
- Large packets use energy more efficiently than small ones as well as high modulation and coding schemes are more energy efficient. Additionally, the transmit power levels have very little effect on the power consumed by the WADs.
- The power consumption of WAD follows a linear behavior until the WAD reaches a saturation point in terms of throughput. The same behavior was observed for all WADs used in our investigation such as (i) IEEE 802.11g and IEEE 802.11n indoor WADs, (ii) IEEE 802.11g Outdoor WADs and (iii) WiMAX WADs.
- A significant fraction of the power consumed by these devices is not traffic dependent in both the WiFi and WiMAX cases. More specifically, we found that injecting traffic in the network until the saturation point results in only a $\approx$20% increase in power consumption with regards to the power consumption in idle mode, i.e. when there is no traffic in the network besides the regular signaling.

As it can be seen from the results, the challenges in wireless networking in terms of energy efficiency are (i) improving the energy efficiency of the WADs when it is transmitting data as well as when it is in idle mode and (ii) introduce novel indicator of energy efficiency as part of the standard of each wireless technologies.

This page is intentionally left blank

Chapter 5

Energy and Power Consumption Metrics and Models for Wireless Access Devices

Contents

5.1 Introduction

A proper power consumption model represents a foundation for developing and evaluating power management schemes and energy efficient protocols in the wireless access networks. We argue that the fundamental power consumption behavior of real WADs is critically important to be properly modelled before optimizing or developing energy–aware design even at higher communication layers. The main goal of this Chapter is to propose specific power consumption models and metrics for application level estimation of energy consumption for designing energy–aware wireless network. In particular, we utilize the measured power consumption performance of the WAD presented in Chapter 4 in order to implement realistic power consumption models for WADs, which reflects the power consumption in various functioning states and during transitions between states of the WAD. By applying the power consumption models, we are able to evaluate and analyze the energy efficiency of various WADs. Experimental measurements with real WADs validated the proposed metrics and models.

In this Chapter, we propose a simple, accurate and general model based on decomposition of the power consumption components that can be monitored and evaluated separately. The proposed model is based on monitoring measurable parameters and computing specific efficiency metrics. The main contributions are the following:

(i) We present several metrics for estimating (a) the optimal message size to be used by the WADs, in terms of power consumption, in order to save energy and (b) the average amount of energy spent by the WAD in order to transmit one bit.

(ii) We propose a simple and accurate power consumption model for the WADs which is validated by experimental measurements with real WADs using different setting parameters;

Based on this power consumption model and the associated metrics, we intend to propose and build a energy monitoring and control framework for power–aware protocols that will be presented in Chapter 6.

5.2 Energy Consumption Metrics

In this Section we focus on the definition of several energy efficiency metrics to be used for designing energy–aware wireless network. Here, we use the results of the experiments explained in the Chapter 4 for calculating the following metrics.

5.2.1 Optimal Message Size

Firstly, we present the optimal message size to be used by the WADs, in terms of power consumption, in order to save energy. Here, we used the results presented in Fig. 4.3, 4.13 and 4.24 for modeling this metric. We assume that the pattern of message error in these figures follows a Bernoulli process (i.e., errors are independent and identically distributed). Therefore, the average *energy efficiency* of the i–th experimental run (expressed in J/b) can be written as:

$$\boxed{\eta_\mathbf{i} = \frac{\mathbf{P_i}}{\mathbf{T_i} \cdot (\mathbf{1} - \varepsilon_\mathbf{i})}} \tag{5.1}$$

Where,

- $\cdot_i$ is a variable referenced to the i–th experiment;
- T_i is the traffic generation rate (expressed in b/s);
- P_i is the power measured during the i–th experimental run;

Table 5.1: Optimal message size to saving energy

WADs Type	T_i **[Mb/s]**	L^* **[bytes]**
Outdoor IEEE 802.11g see Fig. 4.3	10	1280
Indoor IEEE 802.11n see Fig. 4.13	20	1280
Indoor IEEE 802.11g see Fig. 4.18	20	1280
WiMAX see Fig. 4.24a	1 and 5	1280

- ε_i is the probability that a message is not correctly received by the intended destination during the i–th experimental run[1];

This metric can be used to study the impact of various parameters on the overall "energy awareness" figure of the system. As an example, we could consider running a set of measurements keeping a constant traffic generation rate and varying the message size, as presented in Chapter 4 specifically in Fig. 4.3. In this way, we could experimentally identify, for a given traffic load, the optimal message size. This could be, in turn, used to define optimal message fragmentation strategies at Layer 3.

Using the notation above, for $T_i = \hat{T}\ \ \forall i$, we define the optimal message size as:

$$\boxed{\mathbf{L}^*(\hat{\mathbf{T}}) = \arg\min_{\mathbf{i}} \eta_{\mathbf{i}}|_{\mathbf{T_i}=\hat{\mathbf{T}}}} \tag{5.2}$$

Where,

- η_i is the energy efficiency of the WAD;
- L^* is the optimal message size (expressed in bits);
- $\hat{T}$ is a specific traffic generation rate (expressed in b/s);

From the experimental measurements reported in Fig. 4.3, it turns out that in our experimental settings, considering $T_i = \hat{T} = 10$ Mb/s, the optimal message size is $L^*(10Mb/s) = 1280$ bytes, which resulted in an energy efficiency value $\eta^* = 3\ \mu J/bit$. The same result is obtained using the Fig. 4.13, Fig. 4.18 and Fig. 4.24a (see Table 5.1).

5.2.2 Average Energy Cost per Bit

Here, the average amount of energy spent by the WAD in order to transmit one bit is calculated. Given a set of experiments Ψ characterized by a set of traffic generation rates and message sizes $\{T_i, L_i\}_{i=1,\dots,N}$, we can define the average energy cost per bit (E_b) as :

[1] It is relevant to remark that the message loss probability ε_i depends on a number of factors, including channel conditions, which may change over time.

Table 5.2: **WiFi Outdoor WAD:** Energy cost per bit for Outdoor IEEE 802.11g WAD

Modulation	Auto	BPSK 3/4	QPSK 3/4	16–QAM 3/4	64–QAM 3/4
$\mathbf{E_b(Tx)}$ [μ**J/b**]	0.130	0.870	0.590	0.250	0.102
$\mathbf{E_b(Rx)}$ [μ**J/b**]	0.049	0.062	0.055	0.051	0.047

$$\boxed{\mathbf{E_b^{\Psi}} = \sum_{\mathbf{i=1}}^{\mathbf{N}} \frac{\mathbf{P_i - P_b}}{\mathbf{T_i \cdot N}}} \tag{5.3}$$

Where,

- P_b is the power measured during the experimental run when the traffic generation rate is equal to zero;
- N is the number of i–th experimental run performed with lower packet loss (It is recommended to choose the experiments with packet loss lower than 10%);

Such a value can be used as a benchmark to assess the energy efficiency of WADs, given a well defined test suite Ψ, i.e., a set of representative experiments. As an example, in Fig. 4.2a the setting $L_i = 1280$ bytes and $T_i = \{5, 10, 15, 20, 25, 30, 35\}$ Mb/s, the average energy cost per bit of the WAD used in our measurements campaign resulted in $0.13\mu J/bit$ (see Fig. 4.2). In Table 5.2) the average energy cost per bit for Outdoor IEEE 802.11g WAD working under different configuration is shown.

5.3 Power Consumption Modeling

In this Section, we aim at introducing a simple, yet accurate model for estimating the power consumption of WADs as a function of the traffic rate and of the datagram size. Throughout the Section, we use the following notation:

- x is the amount of traffic transmitted or received by the WAD (expressed in Mb/s).
- s is the datagram size (expressed in bytes).
- $R_{Tx/Rx}(x)$ is the model for power consumption at the WAD as a function of traffic load.
- $S_{Tx/Rx}(s)$ is the model for power consumption at the WAD as a function of datagram size.

Notice that the notation $\cdot_{Tx/Rx}$ refer to the scenario when the WAD is acting as transmitter or receiver, respectively.

5.3.1 Measurements–Based Modeling of Power Consumption as a function of Traffic

We used a curve fitting approach in order to construct a model able to match well the power consumption measurements vs traffic presented in the Chapter 4. Different types of functions were tested, including polynomials up to the 4^{th} order, mixes of sum of sinusoid functions and piecewise linear functions. The metric used to assess goodness of the fit was the standard root-mean-square error (RMSE).

The RMSE is a numerical indicator of the differences between values predicted by a model and the values actually observed The RMSE is given by

$$RMSE = \frac{1}{N}\sum_{i=1}^{N}(y_i - \hat{y}_i)^2, \tag{5.4}$$

Where,

- $\cdot_i$ is a variable referenced to the i−th real value;
- y_i is the measured value;
- $\hat{y}_i$ is the modeled value;
- N is the total number of real values used for modeling the curve;

We first focus on the power consumption model as a function of the traffic generation rate. In the next set of Figures we report the model for the power consumption at the BS/AP Vs. different traffic generation rates for a constant datagram size of 1280 bytes. The model parameters have been optimized using Matlab in order to minimize the RMSE.

5.3.1.1 Polynomial Fitted Curve

Fig. 5.1 show the polynomial fitted curve of the power consumption at the AP with a datagram size equal to 1280 bytes.
1) The *Quadratic Fitting Curve* is given by (see *fit 1* in Fig. 5.1):

$$f(x) = p1 \cdot x^2 + p2 \cdot x + p3 \tag{5.5}$$

Where the coefficients with 95% confidence bounds are:

- p1 = -0.001506 (-0.002507, -0.0005047)
- p2 = 0.1989 (0.1418, 0.2561)
- p3 = 10.45 (9.776, 11.13)

Goodness of fit are: SSE: 1.47, R–square: 0.9715, Adjusted R–square: 0.9651, RMSE: 0.4042

2) The *Cubic Fitting Curve* is given by (see *fit 2* in Fig. 5.1):

$$f(x) = p1 \cdot x^3 + p2 \cdot x^2 + p3 \cdot x + p4 \tag{5.6}$$

Where the coefficients with 95% confidence bounds :

- p1 = -7.652e-05 (-0.0001154, -3.769e-05)
- p2 = 0.004807 (0.001553, 0.008061)
- p3 = 0.06597 (-0.008985, 0.1409)
- p4 = 10.93 (10.47, 11.38)

Goodness of fit: SSE: 0.4106, R–square: 0.992, Adjusted R–square: 0.989, RMSE: 0.2265

3) The *4th Degree Fitting Curve* is given by (see *fit 3* in Fig. 5.1):

$$f(x) = p1 \cdot x^4 + p2 \cdot x^3 + p3 \cdot x^2 + p4 \cdot x + p5 \tag{5.7}$$

Where the coefficients with 95% confidence bounds are:

- p1 = 3.989e-07 (-2.566e-06, 3.364e-06)
- p2 = -0.0001204 (-0.0004493, 0.0002085)
- p3 = 0.006318 (-0.005462, 0.0181)
- p4 = 0.0492 (-0.09976, 0.1982)
- p5 = 10.95 (10.42, 11.49)

Goodness of fit: SSE: 0.4047, R–square: 0.9921, Adjusted R–square: 0.9877, RMSE: 0.2405

5.3.1.2 Sum of Sinusoid Fitted Curve

Fig. 5.2 shown sum of sinusoid fitted curve of the power consumption at the AP with a datagram size equal to 1280 bytes.
1) The *Sum of Sinusoid-1 Fitting Curve* is given by (see *fit 1* in Fig. 5.2):

$$f(x) = a1 \cdot sin(b1 \cdot x + c1) + a2 \cdot sin(b2 \cdot x + c2) \tag{5.8}$$

Where the coefficients with 95% confidence bounds are:

- a1 = 745.1 (-1.549e+08, 1.549e+08)
- b1 = 0.03648 (-37.99, 38.06)

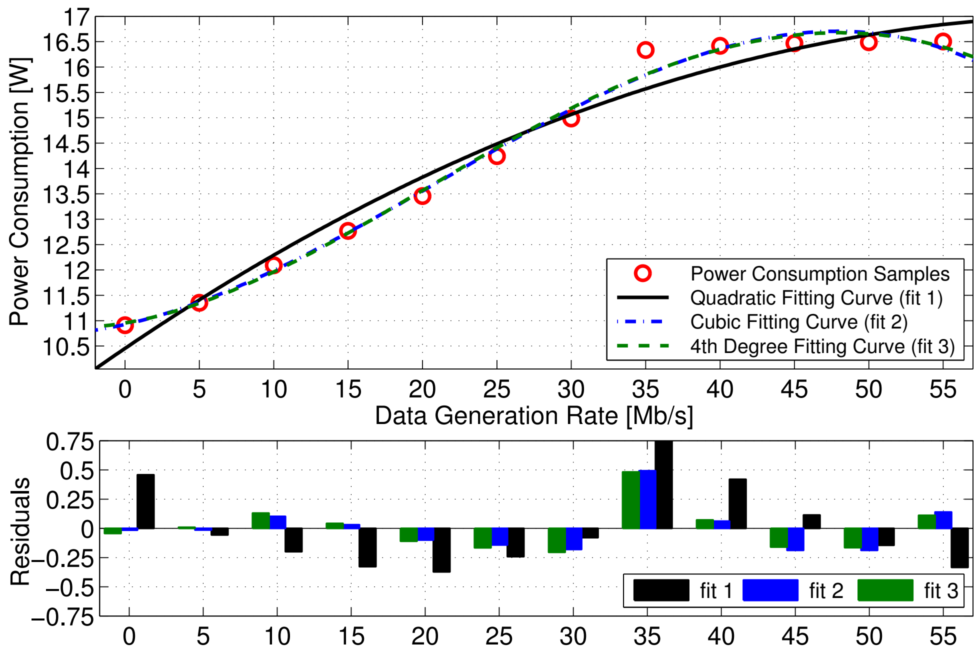

Figure 5.1: **WiFi Outdoor WADs:** Polynomial fitted curve of the power consumption at the AP with a datagram size equal to 1280 bytes.

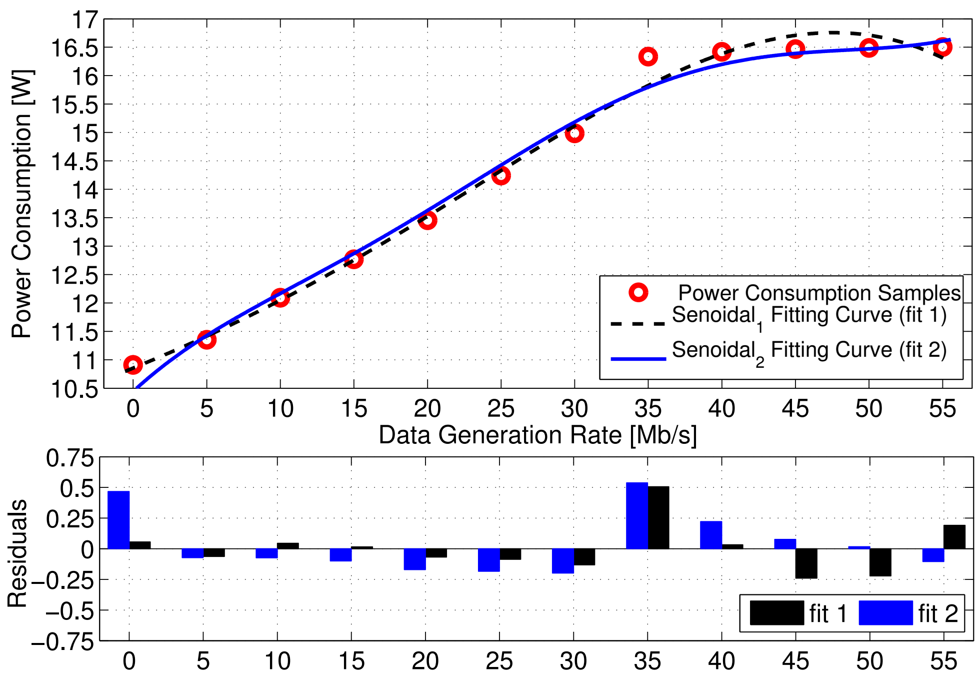

Figure 5.2: **WiFi Outdoor WADs:** Sum of sinusoid fitted curve of the power consumption at the AP with a datagram size equal to 1280 bytes.

- c1 = 0.9826 (-20.87, 22.83)
- a2 = 732.2 (-1.549e+08, 1.549e+08)
- b2 = 0.03684 (-38.48, 38.55)
- c2 = 4.124 (-32.34, 40.59)

Goodness of fit: SSE: 0.4416, R–square: 0.9914, Adjusted R–square: 0.9843, RMSE: 0.2713

2) The *Sum of Sinusoid-2 Fitting Curve* is given by (see *fit 2* in Fig. 5.2):

$$f(x) = a1 \cdot sin(b1 \cdot x + c1) + a2 \cdot sin(b2 \cdot x + c2) + a3 \cdot sin(b3 \cdot x + c3) \tag{5.9}$$

The coefficients with 95% confidence bounds are:

- a1 = 31.71 (-2.197e+06, 2.197e+06)
- b1 = 0.0299 (-742, 742.1)
- c1 = -0.05582 (-3.293e+04, 3.293e+04)
- a2 = 16.84 (-2.035e+06, 2.035e+06)
- b2 = 0.05314 (-1944, 1944)
- c2 = 2.164 (-7.024e+04, 7.024e+04)
- a3 = 2.752 (-1.528e+05, 1.528e+05)
- b3 = 0.09784 (-621.1, 621.3)
- c3 = 3.831 (-1.928e+04, 1.929e+04)

Goodness of fit: SSE: 0.6976, R–square: 0.9865, Adjusted R–square: 0.9504, RMSE: 0.4822

5.3.1.3 Piecewise Linear Fitted Curve

Fig. 5.3 shown the piecewise linear fitted curve of the power consumption at the AP with a datagram size equal to 1280 bytes when AP is acting ans transmitter and receiver.
1) The *Piecewise Linear Fitting Curve* is given by (see *fit 1* in Fig. 5.3a and Fig. 5.3b for AP in Tx and Rx respectively):

$$f_{Tx/Rx}(x) = p1 \cdot x + p2 \tag{5.10}$$

Where the coefficients with 95% confidence bounds are:

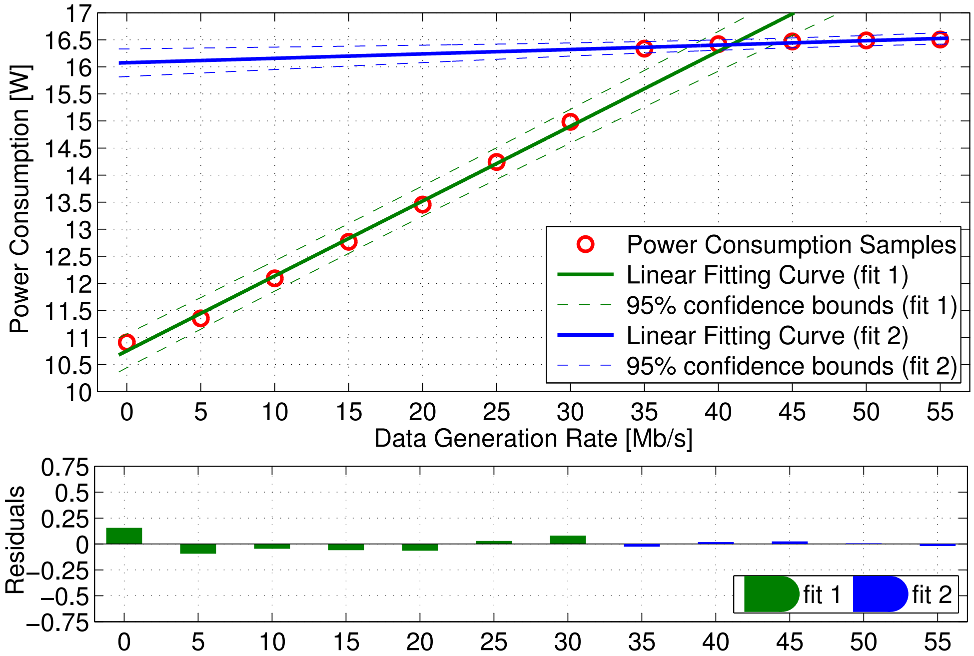

(a) **802.11g Outdoor WAD:** AP in Tx

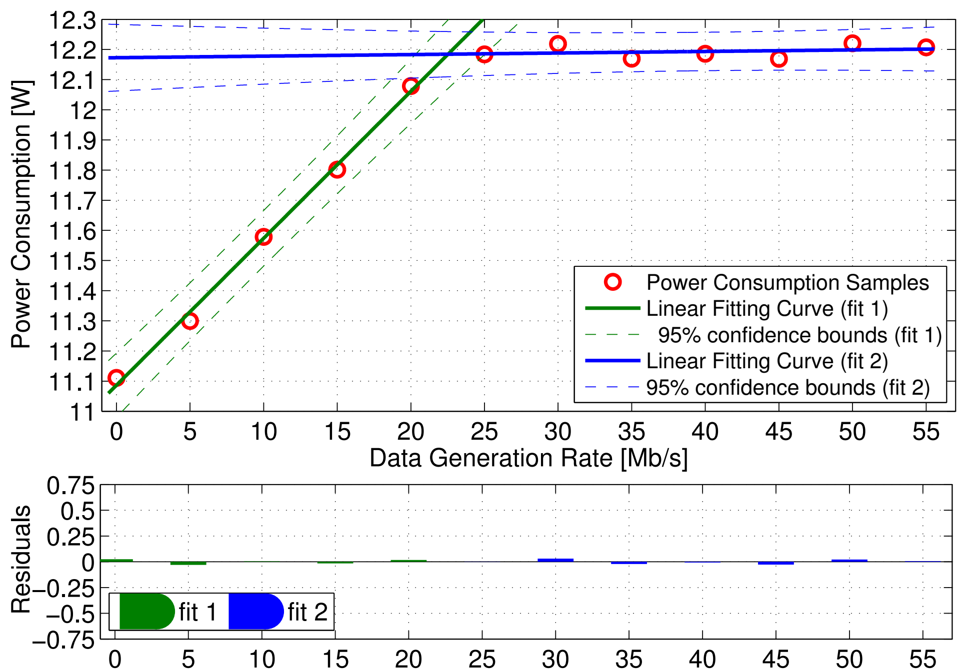

(b) **802.11g Outdoor WAD:** AP in Rx

Figure 5.3: **WiFi Outdoor WADs:** Piecewise linear fitted curve of the power consumption at the AP with a datagram size equal to 1280 bytes.

Table 5.3: **WiFi Outdoor WAD:** Goodness of the different fit used by modeling the power consumption as a function of traffic

Metric	Quadratic	Cubic	4th Degree	Sinusoid-1	Sinusoid-2	Piecewise Linear
RMSE	0.4042	0.2265	0.2405	0.2713	0.4822	0.06326

- p1 = 0.1383 (0.1286, 0.1481)/ 0.3854 (0.3433, 0.4275)
- p2 = 10.75 (10.58, 10.93)/11.57 (11.54, 11.61)

Goodness of fit are: SSE: 0.05019/0.002097, R–square: 0.9963/0.9965, Adjusted R–square: 0.9955/0.9953, RMSE: 0.1002/0.02644

2) The *Piecewise Linear Fitting Curve* is given by (see *fit 2* in Fig. 5.3a and Fig. 5.3b for AP in Tx and Rx respectively):

$$f_{Tx/Rx}(x) = p3 \tag{5.11}$$

Where the coefficients with 95% confidence bounds are:

- p3 = 16.44 (16.41, 16.48)/ 12.17 (12.08, 12.27)

Goodness of fit are: SSE: 0.002078/0.002691, R–square: 0.8889/0.06539, Adjusted R–square: 0.8518/-0.1215, RMSE: 0.02632/0.0232

It is important to note that the curve fitting approach was used for modeling the power consumption measurements for all the experiments performed in the Chapter 4. For all cases considered WiFi and WiMAX WADs (indoor/outdoor and 802.11gn/802.16), the best fit was given a simple model, *Piecewise Linear Fitting Curve*, in which the power consumption was linear as a function of the traffic rate until a given threshold was reached (see Table 5.5). After such a threshold, the power consumption was constant regardless of the traffic rate. The slope of the curve and the threshold value depend on a number of factors, including technology considered, transmission power level and the modulation scheme in use.

Additionally, the parameters used to modeling the power consumption with the *Piecewise Linear Fitting Curve* have a physical meaning, and those parameters explained very well the power consumption behavior of the WAD (see Subsection 5.3.1.4). Additionally, those parameters are easily obtainable as showed in Subsection 5.3.1.5. Aversely, if we use *Quadratic, Cubic, 4th Degree, Sinusoid-1 and Sinusoid-2 Fitting Curve* the parameters used for modeling the power consumption of WADs do not have a physical meaning and it is required to collect several measurements for modeling the power behavior.

5.3.1.4 R–Model: Power Consumption Model as a Function of Traffic

More formally, the power consumption model as a function of the traffic rate is described in the following:

$$\boxed{\mathbf{R_{Tx/Rx}(x)} = \begin{cases} \alpha(s) \cdot x + \beta & \text{if } 0 \leq x \leq h(s) \ \text{ Mb/s,} \\ \gamma & \text{if } x > h(s) \ \text{ Mb/s,} \end{cases}} \tag{5.12}$$

The parameters have the following physical meaning:

- $\alpha(\mathbf{s})$ $[\mu J/b]$ is the amount or energy spent by the WAD in order to transmit or receive 1 bit from the session layer with a datagram size of s bytes;
- β $[W]$ is the amount of power consumed by the WAD in idle mode;
- γ $[W]$ is the maximum amount of power consumed by the WAD and represents the saturation power consumption;

It is worth remarking that the power consumption model for the dependency on x has parameters that in turn depend on s.

5.3.1.5 R–Model Build

In order to use our model to estimate the power consumption of a WAD as a function of the transmission rate, three parameters are required (see Fig. 5.4):

(i) The amount of power consumed by the WAD in idle mode (β). This value is easily obtained by measuring the power consumption of the WAD without traffic.

(ii) The amount of power consumed by the WAD in saturation regime (γ). This value is obtained by measuring the power consumption of the WAD when an high amount of traffic is injected into the network. The rule of the thumb is to generate a traffic that is equal or higher than the wireless link's nominal data rate.

(iii) The amount of power consumed by the WAD below the saturation regime (α). This value is obtained by measuring the power consumption of the WAD when injecting an amount of traffic such that the packet loss over the wireless link is negligible (i.e. lower than 1%).

5.3.1.6 R–Model Validation

We first focus on the power consumption model as a function of the traffic generation rate. In Fig. 5.5 we report the model for the power consumption at the BS/AP vs. different traffic generation rates for a constant datagram size of 1280 bytes. It

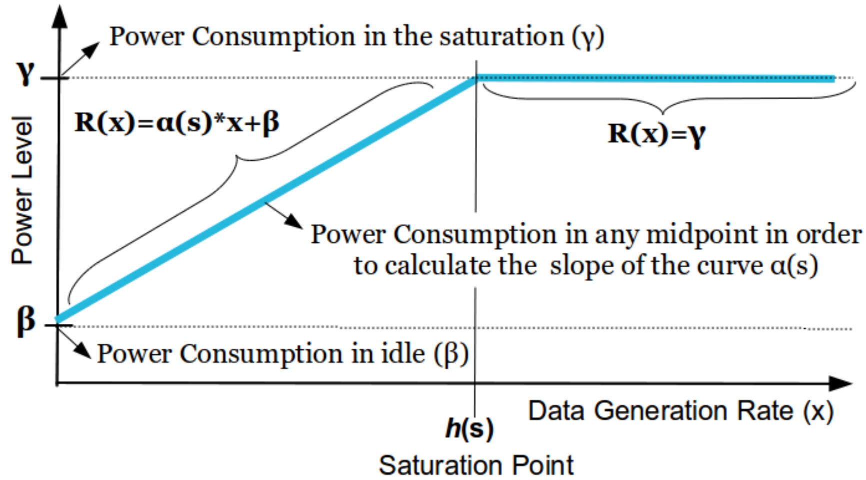

Figure 5.4: **R–Model:** Estimating the power consumption of a WAD as a function of the transmission rate.

is worth noticing that these values are obtained using only three data–points from Fig. 5.5. Such data points have been chosen according to the above guidelines. As it can be seen from Fig. 5.5a, Fig. 5.5b, Fig. 5.5c and Fig.5.5d, where empirical energy consumption data–points are plotted together with the values predicted using our model, the match is very good.

Table 5.4 reports the modeled parameters for R–Model obtained for a datagram size $s = 1280$ bytes for a WiFi Outdoor WAD working under different settings. The RMSE figures obtained are small for all the cases, which confirm the ability of our model to estimate the actual power consumption in a variety of settings.

5.3.2 Measurements–Based Modeling of Power Consumption as a Function of Datagram Size

Here, we focus on the power consumption model as a function of the datagram size. We also used a curve fitting approach in order to construct a model able to match well the power consumption measurements vs traffic presented in the Chapter 4. Different types of functions were tested, including polynomials up to the 4^{th} order, exponential and piecewise log–linear functions. The metric used to assess goodness of the fit was the standard RMSE as before. In the next set of figures we report the model for the power consumption at the BS/AP vs. different datagram size for a constant traffic generation rates.

It is worth noticing that, in order to fit all the model we used data–points corresponding to datagram lengths greater than 128 bytes. The reason behind such choice is that due to MAC protocol overheads it is not possible to inject traffic at 10 Mb/s using payloads smaller than 128 bytes. As a matter of fact injecting traffic at 10 Mb/s using a payload length of 32 bytes would require a packet injection rate of $\approx$ 39000 pkts/s, on the other hand the actual packet injection rate in a WiFi

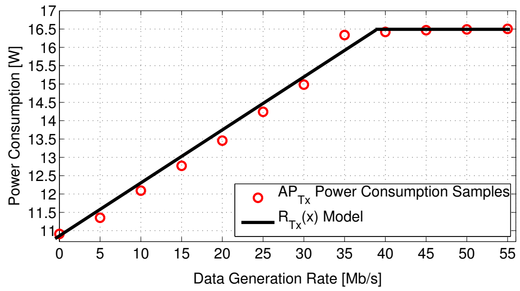

(a) **802.11g Outdoor WAD:** AP in Tx

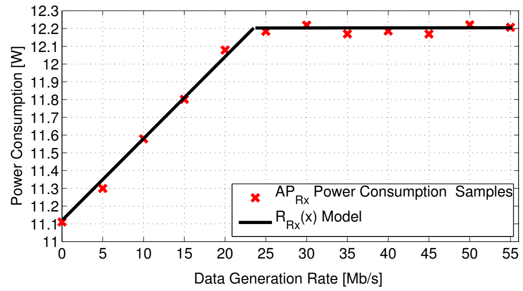

(b) **802.11g Outdoor WAD:** AP in Rx

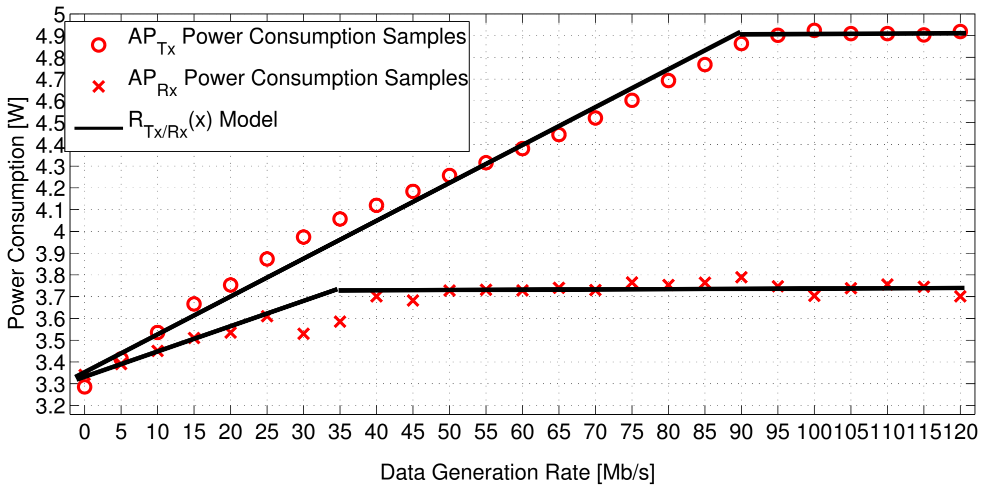

(c) **802.11n Indoor WAD:** AP in Tx/Rx

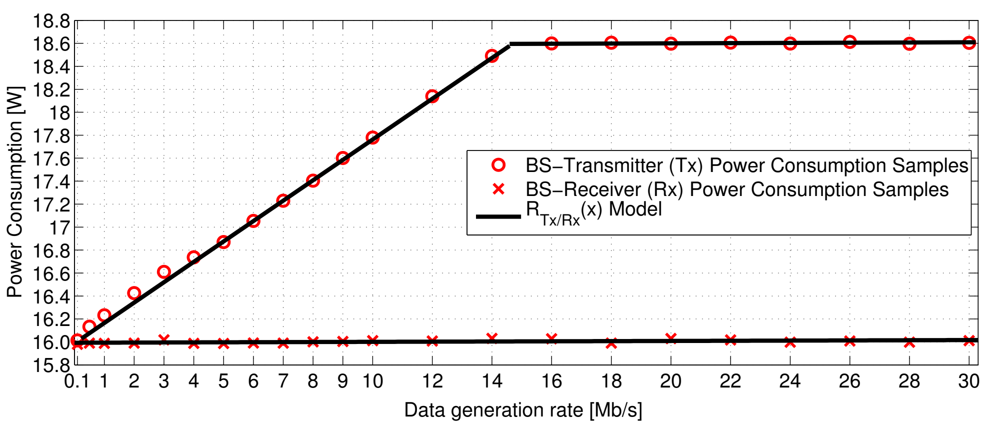

(d) **802.16 WAD:** BS in Tx/Rx

Figure 5.5: **R–Model:** Real and modeled power consumption of a WAD as a function of the transmission rate.

network has an upper bound mandated by the IEEE 802.11 Distributed Coordination Function (DCF) [iee 2007]. In particular it is easy to derive [Gast 2003] that,

Table 5.4: **WiFi Outdoor WAD:** Linear R–Model parameters ($s = 1280$ bytes).

	Model	$\beta(\mathbf{s})$ [**W**]	$\alpha(\mathbf{s})$ [μ**J/b**]	γ [**W**]	**h(s)** [**Mb/s**]	**RMSE**
Auto–modulation	$R_{Tx}(s)$	10.90	0.13	16.43	32	0.06326
	$R_{Rx}(s)$	10.90	0.049	12.20	22	0.02644
BPSK 3/4	$R_{Tx}(s)$	10.90	0.87	19.76	6	0.03356
	$R_{Rx}(s)$	10.90	0.062	11.00	5	0.01115
QPSK 3/4	$R_{Tx}(s)$	10.90	0.59	19.30	15	0.04325
	$R_{Rx}(s)$	10.90	0.055	11.50	13	0.02961
16–QAM 3/4	$R_{Tx}(s)$	10.80	0.25	18.00	24	0.06677
	$R_{Rx}(s)$	10.90	0.051	10.90	25	0.05544
64–QAM 3/4	$R_{Tx}(s)$	10.80	0.102	15.7	30	0.05543
	$R_{Rx}(s)$	10.90	0.047	10.20	28	0.02666

using UDP packets that are 32 bytes long, the maximum number of packet transmission rate that can be sustained by an IEEE 802.11g interface using the highest modulation rate (54 Mb/s) is about 9800 pkts/s.

The model parameters have been optimized using Matlab in order to minimize the RMSE.

5.3.2.1 Polynomial Fitted Curve

Fig. 5.6 show the polynomial fitted curve of the power consumption at the AP with different datagram size.

1) The *Quadratic Fitting Curve* is given by (see *fit 1* in Fig. 5.6):

$$f(x) = p1 \cdot x^2 + p2 \cdot x + p3 \tag{5.13}$$

Where the coefficients with 95% confidence bounds are:

- p1 = 1.308e-06 (7.478e-07, 1.868e-06)
- p2 = -0.003428 (-0.004576, -0.002281)
- p3 = 14.28 (13.8, 14.76)

Goodness of fit are: SSE: 1.47, R–square: 0.8406, Adjusted R–square: 0.816, RMSE: 0.2875

2) The *Cubic Fitting Curve* is given by (see *fit 2* in Fig. 5.6):

$$f(x) = p1 \cdot x^3 + p2 \cdot x^2 + p3 \cdot x + p4 \tag{5.14}$$

Where the coefficients with 95% confidence bounds:

- p1 = -1.67e-09 (-2.388e-09, -9.522e-10)
- p2 = 6.386e-06 (4.178e-06, 8.594e-06)
- p3 = -0.007634 (-0.009566, -0.005703)
- p4 = 15.06 (14.62, 15.5)

Goodness of fit: SSE: 0.3422, R–square: 0.9492, Adjusted R–square: 0.9366, RMSE: 0.1689
3) The *4th Degree Fitting Curve* is given by (see *fit 3* in Fig. 5.6):

$$f(x) = p1 \cdot x^4 + p2 \cdot x^3 + p3 \cdot x^2 + p4 \cdot x + p5 \tag{5.15}$$

Where the coefficients with 95% confidence bounds are:

- p1 = 1.669e-12 (4.361e-13, 2.901e-12)
- p2 = -8.498e-09 (-1.357e-08, -3.423e-09)
- p3 = 1.557e-05 (8.567e-06, 2.256e-05)
- p4 = -0.01212 (-0.01577, -0.008477)
- p5 = 15.64 (15.09, 16.19)

Goodness of fit: SSE: 0.1894, R–square: 0.9719, Adjusted R–square: 0.9617, RMSE: 0.1312

5.3.2.2 Exponential Fitted Curve

Fig. 5.7 shown exponential fitted curve of the power consumption at the AP with different datagram size.
1) The *Exponential Fitting Curve* is given by (see *fit 1* in Fig. 5.7):

$$f(x) = a \cdot exp(b \cdot x) + c \cdot exp(d \cdot x) \tag{5.16}$$

Where the coefficients with 95% confidence bounds are:

- a = 3.223 (2.357, 4.09)
- b = -0.003065 (-0.005031, -0.0011)
- c = 11.82 (10.77, 12.88)
- d = 2.009e-05 (-3.32e-05, 7.338e-05)

Goodness of fit: SSE: 0.4505, R–square: 0.9501, Adjusted R–square: 0.9386, RMSE: 0.1862

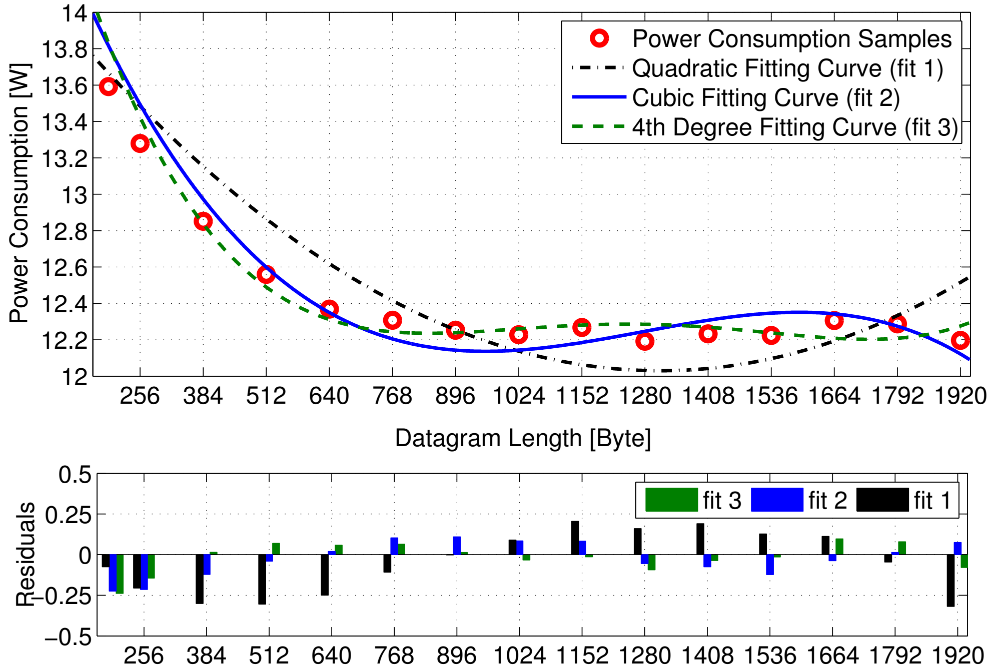

Figure 5.6: **WiFi Outdoor WADs:** Polynomial fitted curve of the power consumption at the AP with different datagram size.

5.3.2.3 Piecewise Log–Linear Fitted Curve

Here, we investigate the average power consumption at the AP as a function of the datagram size for a constant traffic generation rate of 10 Mb/s plotted using a semi–logarithmic scale (see Fig. 5.8). As it can be see in the figure, the linearity of the plot is observed using semi–logarithmic scale.

Fig. 5.9 shown the piecewise log–linear fitted curve of the power consumption at the AP with different datagram size.

1) The *Piecewise Log–Linear Fitting Curve* is given by (see *fit 1* in Fig. 5.9a and Fig. 5.9b for AP in Tx and Rx respectively):

$$f(Tx/Rx) = a \cdot log(x) + c \tag{5.17}$$

Where the coefficients with 95% confidence bounds are:

- a = -0.9588 (-1.094, -0.824)/ -0.8269 (-0.9074, -0.7464)
- c = 18.59 (17.78, 19.41)/ 17.29 (16.78, 17.79)

Goodness of fit are: SSE: 0.01362/0.003643, R–square: 0.9898/0.9939, Adjusted R–square: 0.9873/0.9951, RMSE: 0.05835/0.03018

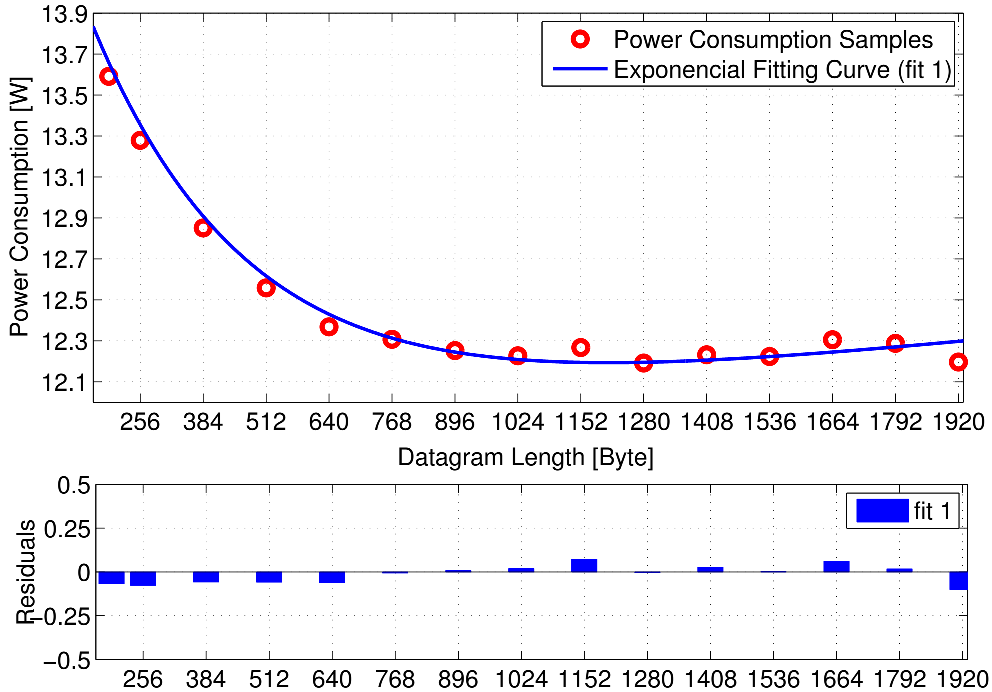

Figure 5.7: **WiFi Outdoor WADs:** Exponential fitted curve of the power consumption at the AP with different datagram size.

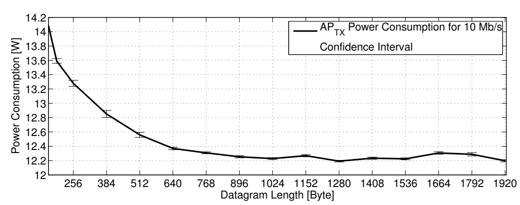

(a) AP acting as transmitter.

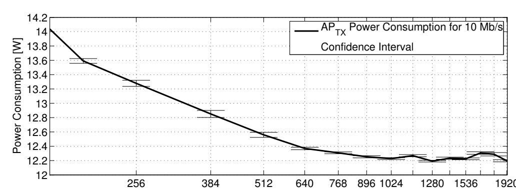

(b) AP acting as transmitter semi–logarithmic scale.

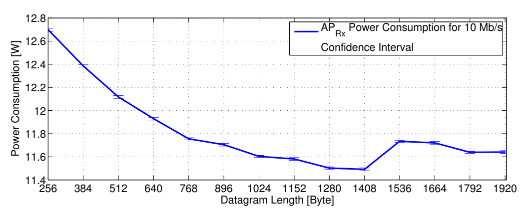

(c) AP acting as receiver.

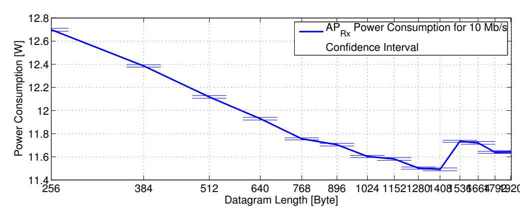

(d) AP acting as receiver semi–logarithmic scale.

Figure 5.8: Average power consumption at the AP as a function of the datagram size for a constant traffic generation rate of 10 Mb/s plotted using a semi–logarithmic scale.

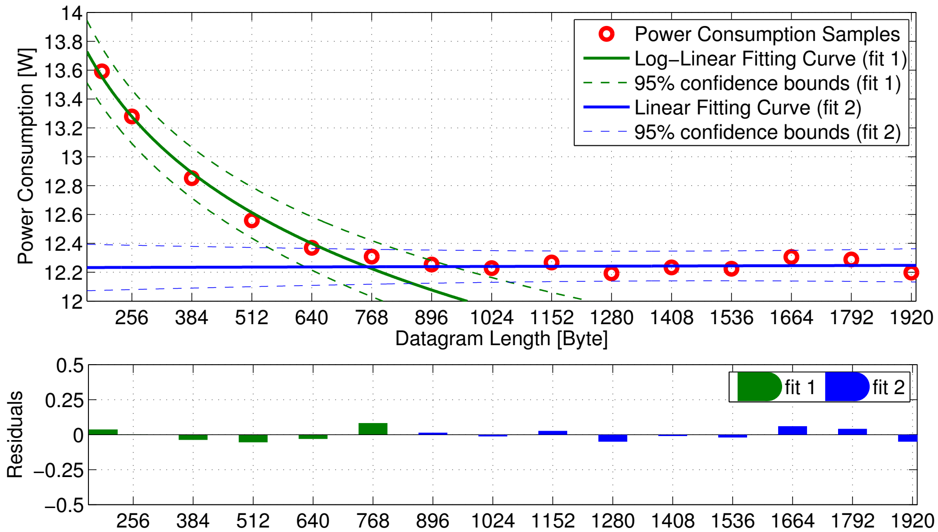

(a) **802.11g Outdoor WAD:** AP in Tx

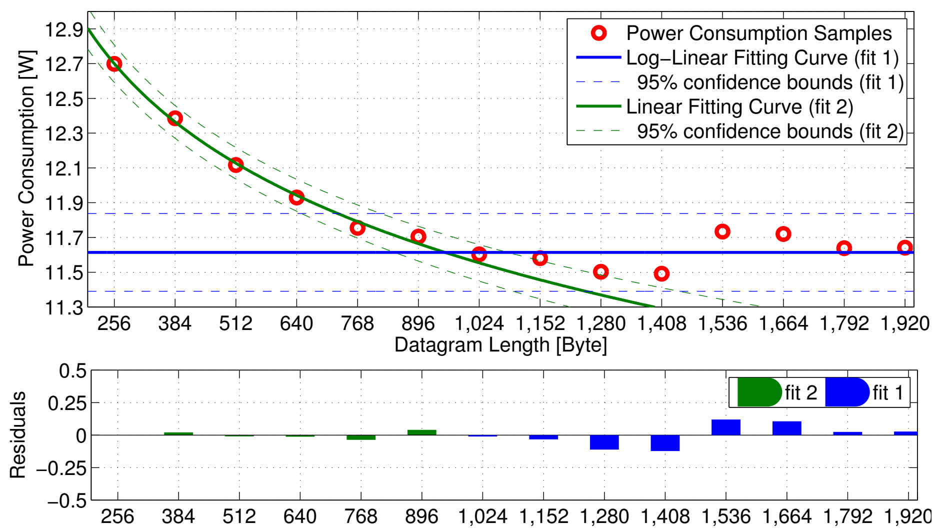

(b) **802.11g Outdoor WAD:** AP in Rx

Figure 5.9: **WiFi Outdoor WADs:** Piecewise log–linear fitted curve of the power consumption at the AP with different datagram size.

2) The *Piecewise Log–Linear Fitting Curve* is given by (see *fit 2* in Fig. 5.9a and Fig. 5.9b for AP in Tx and Rx respectively):

$$f_{Tx/Rx}(x) = d \tag{5.18}$$

Where the coefficients with 95% confidence bounds are:

- d = 12.23 (12.09, 12.37)/ 11.61 (11.54, 11.69)

Goodness of fit are: SSE: 0.01197/0.05571, R–square: 0.005974/2.22e-16, Adjusted

Table 5.5: **WiFi Outdoor WAD:** Goodness of the different fit used by modeling the power consumption as a function of datagram size

Metric	Quadratic	Cubic	4th Degree	Exponential	Piecewise Log–Linear
RMSE	0.2875	0.1689	0.1312	0.1862	0.049855

R–square: -0.136/2.22e-16, RMSE: 0.04136/0.08921

It is important to note that the curve fitting approach was used for modeling the power consumption measurements for all the experiments performed in the Chapter 4. For all cases considered WiFi and WiMAX WADs (indoor/outdoor and 802.11gn/802.16), the best fit was given a simple model, *Piecewise Log–Linear Fitting Curve*, in which the power consumption was decreasing linear in logarithmic scale as a function of the datagram size until a given threshold was reached (see Table 5.5). After such a threshold, the power consumption was constant regardless of the datagram size. The slope of the curve and the threshold value depend on a number of factors, including technology considered, transmission power level, the modulation scheme in use and traffic load.

Additionally, the parameters used for modeling the power consumption with the *Piecewise Log–Linear Fitting Curve* have a physical meaning, and those parameters explained very well the power consumption behavior of the WAD (see Subsection 5.3.1.4). Additionally, those parameters are easily obtainable as shown in Subsection 5.3.2.5.

5.3.2.4 S–Model: Power Consumption Model as a function of Datagram Size

More formally, the power consumption model as a function of the datagram size is described in the following:

$$\boxed{\mathbf{S_{Rx/Tx}(s)} = \begin{cases} -\delta(x)\cdot log(s) + \varepsilon(x) & \text{if } p \leq s \leq q \text{ byte,} \\ \eta(x) & \text{if } s > q \text{ byte,} \end{cases}} \tag{5.19}$$

The parameters have the following physical meaning:

- $\delta(\mathbf{x})$ $[\mu W/bytes]$ is the amount of power consumed by WAD in order to transmit or receive 1 byte from the session layer arriving at a rate of x Mb/s;
- $\varepsilon(\mathbf{x})$ $[W]$ is the maximum power consumed by the WAD, transmitting at x Mb/s, using extremely small packets;
- $\eta(\mathbf{x})$ $[W]$ is the minimum power consumed by the WAD to transmit traffic at a rate of x Mb/s;

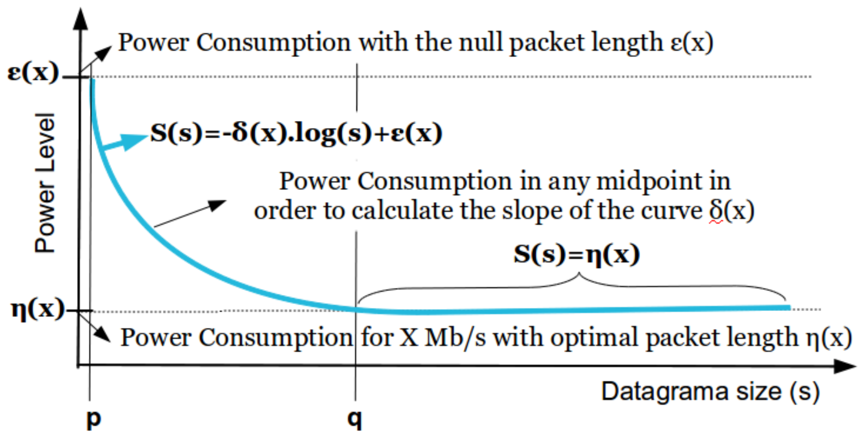

Figure 5.10: **S–Model:** Estimating the power consumption of a WAD as a function of the datagram size.

It is worth remarking that the power consumption model for the dependency on x has parameters that in turn depend on s and vice versa.

5.3.2.5 S-Model Build

In order to use our model to estimate the power consumption of a WAD as a function of the datagram size, we need three parameters (see Fig. 5.10):

(i) The amount of power consumed by the WAD while transmitting/receiving at x Mb/s using the optimal datagram length ($\varepsilon(x)$). This value is obtained by measuring the power consumption of the WAD using as the datagram size the MTU.

(ii) The amount of power consumed by the WAD while transmitting/receiving at x Mb/s using a datagram length such that the packet loss over the wireless link is below 1% ($\eta(x)$).

(iii) The amount of power consumed by the WAD while transmitting/receiving at x Mb/s using the null datagram length, i.e. no payload ($\eta(x)$).

5.3.2.6 S-Model Validation

Here, we focus on the power consumption model as a function of the datagram size. In Fig. 5.11 we report the model for the power consumption at the BS/AP vs. different datagram size. It is worth noticing that these values are obtained using only three data–points from Fig. 5.5. Such data points have been chosen according to the above guidelines. As it can be seen from Fig. 5.11a, Fig. 5.11b, Fig. 5.11c and Fig.5.11d, where empirical energy consumption data–points are plotted together

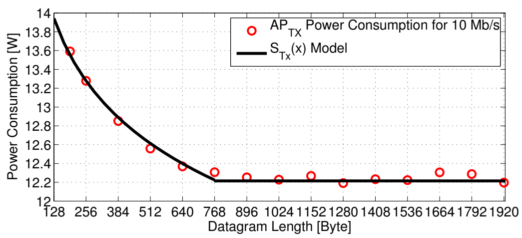

(a) **802.11g Outdoor WAD:** AP in Tx

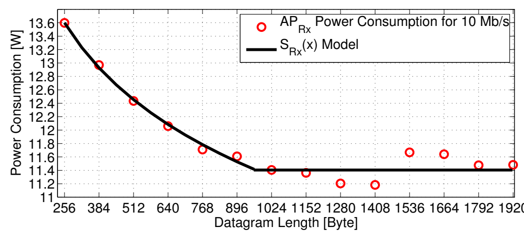

(b) **802.11g Outdoor WAD:** AP in Rx

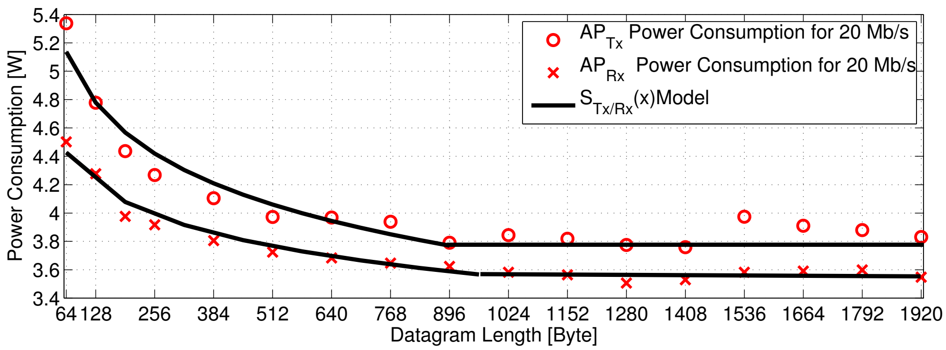

(c) **802.11n Indoor WAD:** AP in Tx/Rx

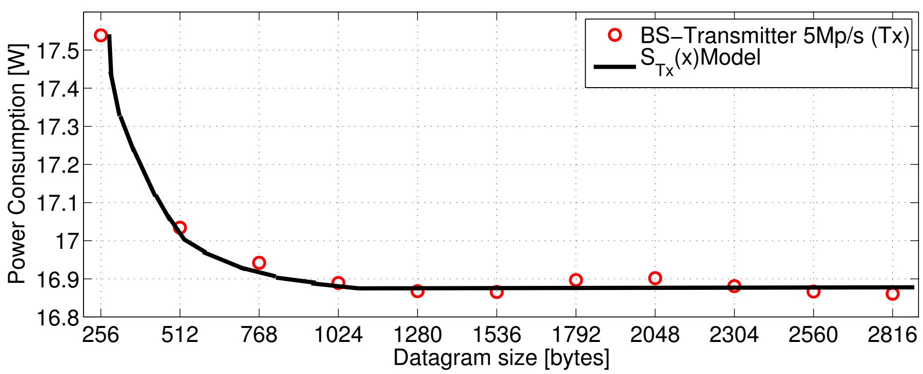

(d) **802.16 WAD:** BS in Tx/Rx

Figure 5.11: **S–Model:** Real and modeled power consumption of a WAD as a function of the datagram size.

with the values predicted using our model, the values predicted by our model to match very well with the empirical data points.

Table 5.6 reports the modeled parameters for the S–Model obtained for a rate $x = 10$ Mb/s.

Table 5.6: **WiFi Outdoor WAD:** Log–Linear S–Model parameters ($x = 10$ Mb/s).

	$\delta(x)$ $[\mu W/b]$	$\varepsilon(x)$ $[W]$	$\eta(x)$ $[W]$	q q	RMSE $[W]$
$S_{Tx}(s)$	-0.9588	18.59	12.23	768	0.056
$S_{Rx}(s)$	-0.8269	17.29	11.61	990	0.059695

5.4 Conclusions

A simple and accurate power consumption model, which can be easily plugged into typical network simulations tools such as ns3 or Omnet++, is essential to drive the design and development of energy aware network protocols and algorithms. Such an approach will pave the way to an *energy proportional networking* paradigm, where wireless networks are designed in order to provide coverage and capacity only when and where needed. The main observations of this Chapter includes:

- The power consumption of WAD is divided into two parts (i) the first part is related to the power consumption of the circuit plus the basic operation of the WAD and (ii) the second one depends on the technology considered (WiFi/WiMAX) and the settings, including the transmission power level, the datagram size, the modulation and coding schemes and specially the traffic load.

- The first part of power consumption varies significantly according with technology considered (WiFi/WiMAX) and type of WAD, indoor and outdoor, and it remains constant during the time.

- The second part of power consumption is variable in time and it is strongly influenced by the setting parameters, including the transmission power level, the datagram size, the modulation and coding schemes and specially the traffic load.

- The power consumption of WAD as a function of traffic load follows a linear behavior until the WAD reaches a saturation point. The *saturation* means the data generation rate is higher than the physical link data–rate. The slope of the line and the saturation value depend on a number of factors, including transmission power levels, technology considered (WiFi/WiMAX) and the modulation scheme in use.

- For estimating the power consumption of a WAD as a function of the transmission rate, only three easily measurable parameters are required: 1) power consumption in idle mode, 2) power consumption in any midpoint in order to compute the slope of the curve and 3) power consumption in the saturation.

- For estimating the power consumption of a WAD as a function of the datagram size, only three easily measurable parameters are required: 1) power consumption with the null packet length, i.e. no payload, 2) power consumption in any midpoint, i.e. smaller packet length, in order to compute the slope of the curve and 3) power consumption for X Mb/s with optimal packet length.

Finally, in this Chapter we show that the power consumption of WAD depends not only on the application characteristics, i.e. length of sending data, transmission power levels, but also device features, including technology considered (WiFi/WiMAX) and indoor/ outdoor type of WAD. Therefore, the proposed power consumption models and metrics can be used to guide the choices in many different sides of the design space, i.e. application system design, hardware design, WAD simulator design, upper layer protocol design and evaluation.

This page is intentionally left blank

Chapter 6

Energy–Saving Solutions for Wireless Access Networks

Contents

6.1 Introduction

The smart–phone and tablet revolution continue their fast seizure of our daily lives as they become smaller, smarter, more powerful and faster. Consequently, the number of WiFi hotspots deployed is increasing exponentially. The trend may be strengthened as WiFi offload technology (which automatically redirects the traffic generated by smart–phones and mobile devices from 3G to WiFi networks) gets deployed at scale. Typically, WiFi access points are operated at full power, given that network operators are generally reluctant to shut–down portions of their networks in order to preserve full availability. However, "always available" does not need to mean "always fully powered". Our work starts from the firm belief that there is significant space for improving the energy efficiency of wireless access infrastructures, while at the same time preserving the quality of service delivered to end users.

In Chapter 4, Chapter 5 and [Gomez 2011, Gomez 2012a, Gomez 2012b], we analyzed and experimentally measured the power consumption of several WADs, including WiFi and WiMAX. In all cases, it turned out that a significant fraction of the energy consumed by these devices is not traffic–dependent. More specifically, we found that injecting traffic in the network until the saturation point results in only a $\approx 20\%$ increase in power consumption with respect to the power consumed when there is no traffic in the network besides the regular signaling. In order to achieve significant energy savings, it is imperative to find the means for reducing the power consumed when little or no traffic is present.

In this Chapter, we propose and experimentally validate a monitoring and control framework that can support different energy–saving strategies in heterogeneous wireless networks. The energy–saving strategies are implemented based on the switching of the operating modes of wireless access devices (i.e., whether they need to remain on, or they can be turned off, or switched to a low–power mode etc.). To make appropriate energy–saving decisions, the framework takes into account the network traffic and usage scenarios, and also by accounting for the cost of switching of the operating modes. The main contributions of this Chapter are as follows:

- A practical energy–saving decision algorithm, which exploits an energy monitoring and control framework.
- A measurement–based evaluation of proposed algorithm in a WiFi testbed deployed at Telekom Innovation Laboratories in Berlin, Germany.

The proposed algorithm adapts the energy consumption of a wireless infrastructure to the network conditions in terms of both current user density *and* traffic patterns. The implementation and operation of the proposed algorithm on the real testbed confirms that our framework is flexible enough to support practical use–cases. The experimented results show that the proposed algorithm considerably lowers the energy footprint of the network with very limited performance penalty for end users.

6.2 Energy–Saving Architectures, Techniques and Algorithms for Wireless Access Networks

Wireless networks easily become over–dimensioned during periods of low traffic demands, which directly depends on the deployment area and the network usage guided by human mobility and traffic requirements. For instance, these periods are common at night time and the weekend for enterprise or universities deployments. In order to adapt the network capacity and topology to the actual traffic demands of the users, it is mandatory to design energy–saving algorithms and techniques for wireless infrastructure networks.

In this section, we present an energy–saving architecture composed by an energy monitoring and control framework to be implemented in order to support energy–saving algorithms and techniques. In the proposed energy monitoring and control framework, the WADs can be in different operation modes, with varying levels of energy consumption. We describe these modes, and then propose an algorithm for adapting the operation mode of WADs under different traffic and coverage conditions.

6.2.1 Energy–Saving Architectures: Energy Monitoring and Control Framework

Commonly, the typical parameters considered on WAD design are the radio coverage, peak capacity and other service requirements while the power consumption is not considered at all. Consequently, the WADs are not hardware and software designed for taking into account the power consumed on its operations. In [Riggio], we presented a preliminary framework and hardware–software prototype for monitoring the power consumed for the WAD and enabling the implementation of energy saving approaches. In this chapter, we extended that work to a more complete and practical energy monitoring and control framework, the architecture is depicted in Fig. 6.1, to support energy–saving algorithms. The energy monitoring and control framework required minor upgrades in the current wireless networks deployments in terms of (i) external hardware solutions for energy monitoring and switching off/on WAD and (ii) software installation for monitoring users, traffic load and network performance statistics. The main components of our energy monitoring and control framework are:

- **The Context Manager (CoMa)** is responsible for gathering relevant information, such as network and power utilization statistics, from the WADs, energy monitoring devices, mobile devices as well as external databases (see [Göndör 2011] for details). The statistics are collected using a Context Collecting Agent (CCA) installed in each WAD and stored in the CoMa database. These statistics mainly include the WAD configurations and locations, the number of connected users, amount and type of traffic for each wireless interface, power consumption of the WAD and other network performance indicators.

- **The Energy Decisions (ED)** unit makes the necessary decisions to choose operation modes and schedules these actions to be executed by the Energy Controller. The ED can be considered as a repository of energy–efficient algorithms.

- **The Energy Controller (EC)** contains the logic for monitoring the energy consumption of the WADs and writing these statistics to CoMa database. The EC also triggers the actions scheduled by the ED. For example, the ED schedules turning off the WADs when there are no users in the network. The

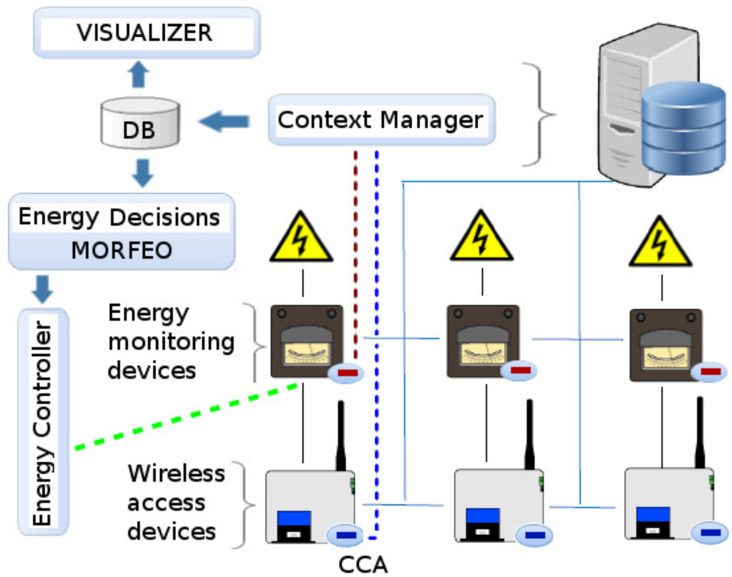

Figure 6.1: Schematic of the energy monitoring and control framework supporting implementation of energy–saving solutions

components required for implementing the EC can be either a commercial platform [EPC] or based on an open–source platform [Gomez 2012b]. The actions supported by EC are (i) switching On/Off the device, (ii) switching On/Off the wireless interfaces and (iii) changing the transmission power of each wireless interface.

- **The Visualizer (VS)** displays a graphical interface of the actions scheduled by the ED and the network statistics about power consumption, users and traffic load collected from the CoMa database (see [Uzun 2012] for details).

WADs and user terminals also play an important role in this framework. User terminals can be static, nomadic or mobile and they are associated to the WADs via a single wireless hop. They need to send feedback about the network performance to the WADs to be able to make energy efficiency decisions without compromising service quality. A special applications software (APP) is installed in the user terminal for sending statistics to CoMa.

6.2.2 Energy–Saving Techniques: Operation Modes for Wireless Access Devices

Using the energy monitoring and control framework and based on our measurements presented on Chapter 5, we identify four modes of operation for WADs based on their energy consumption:

- **Full–Power Mode (FPM):** The WAD and its interfaces are switched on and are operating with highest transmission power level. This mode provides full coverage and capacity.

- **Active Mode (AM):** The WAD and its interfaces are always on and operating with the default transmission power level, which is lower than the highest transmission power level.

- **Partial or Sector Sleep Mode (PSM or SSM):** The WAD is powered on but one or more sectors or interfaces are switched off. Note that similar power–saving modes are already implemented for client–side devices. Here, we introduce this mode for WADs. In this mode, if there are no associated users, sectors or interfaces can be turned off for energy savings. When there are associated users but no traffic, a configurable duty–cycle can be used to periodically turn off the sectors or interfaces. However, the duty–cycle should be automatically and immediately deactivated, when traffic is detected.

- **Off Mode (OM):** The WAD is turned off and only the energy monitoring device is powered. The energy consumed for the energy monitoring device should be always smaller than the power consumed by the WAD in Active Mode. The Off Mode takes advantage of the network over–dimensioning and overlapping coverage provided by different WADs. The goal is to use Off Mode for keeping a minimal set of devices in Active Mode in order to provide full coverage and required capacity with minimal energy consumption. It is important to remark that the energy consumed for the energy monitoring device maintained on only for switching ON the WAD again should be always smaller than the power consumed by the WADs in Active Mode.

The proposed method can represented as a finite state machine (FSM), which is shown in Fig. 6.2. It is important to note that the complete or partial FSM can be used to design both algorithms and sequential logic techniques for saving energy. The decision to switch from one operation mode to another can be taking based on the transition conditions of each WAD. The different conditions considered are:

- **Active Condition (AC):** The WAD has associated clients sending or receiving traffic.

- **Idle Condition (IC):** The WAD has associated clients but its clients are not sending or receiving traffic.

- **Zero condition (ZC):** The WAD has no associated clients.

- **Head Condition (HC):** The WAD can take over the load of other WADs that are switching to Off Mode.

In the FSM, the Full–Power Mode increases the transmission power of the devices under Active Mode when they satisfy *Head Condition*. This increases the coverage area and hence, makes it possible to put WADs which satisfy the *Zero Condition* under Off Mode. The WADs in Partial/Sector Sleep Mode switch to Active Mode,

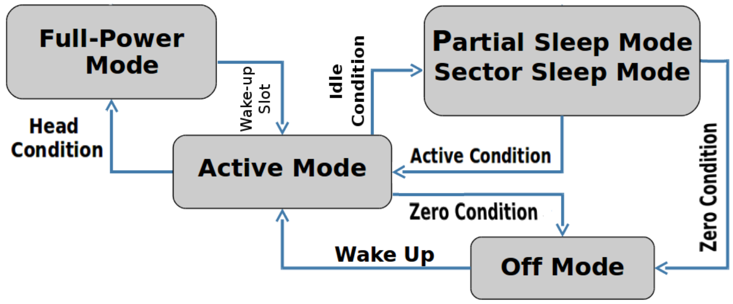

Figure 6.2: The finite state machine for the different operation modes supported by the proposed framework.

Table 6.1: State transition table for Operation Modes Switching

Operation Modes	FPM	AM	PSM or SSM	OM
Active Condition	–	–	AM	–
Idle Condition	–	PSM or SSM	–	–
Zero condition	–	OM	OM	–
Head Condition	–	FPM	–	–
Wake Up	AM	–	–	AM

when they satisfy *Active Condition*, to provide additional capacity and coverage to their users. Finally, WADs in Off Mode switch to Active Mode when a *wake up* decision is taken, this decision can be taken according with the design chose i.e. if it is required to have all the WADs in the network in Active Mode due to high traffic. Thus, the FSM allows adapting the network capacity and save energy (see also Table 6.1).

6.2.3 Energy–Saving Algorithms: MORFEO Energy–Saving Decision Algorithm

In this section, we present *morfeo* an algorithm for energy–saving decisions in a wireless infrastructure network that uses the (i) the energy monitoring and control framework and (ii) the different operation modes supported by the WADs in order to adapt the network capacity and topology to the actual traffic demands. The proposed algorithm *morfeo* operates in three steps: *Initialisation*, *Reactive updates*, and *Correction*.

1) In the Initialisation step, *morfeo* takes decisions about the most appropriate role for each WAD in a *proactive manner* based on the network deployment and context information.

2) Then, during *Reactive updates*, the statistics about the current network conditions, such as the number of users and the amount of traffic, are collected from

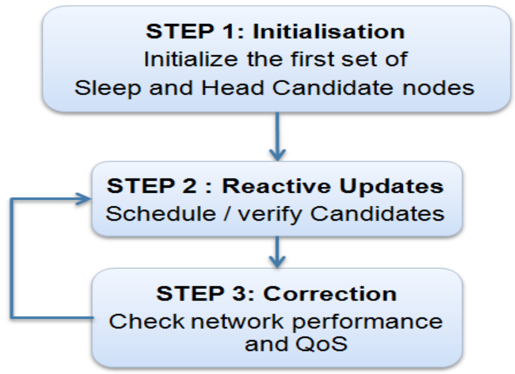

Figure 6.3: Flow diagrams of the *morfeo*'s cycle

CoMa and analyzed. Based on this analysis, *morfeo* decides the most appropriate operation mode for each WAD. To this end, *morfeo* divides time into decision slots to ensure there is enough time for the CoMa to collect statistics, and also for the EC to switch the WADs to the different operation modes based on the energy-saving decisions by *morfeo*. The minimum time slot duration is calculated as the time required for pushing and collecting statistics to/from the CoMa.

3) Finally, *morfeo* switches to the *Correction* step, which takes place after one time-slot duration. Here, if the network performance suffers degradations and the QoS cannot be guaranteed for the current traffic load, the *Correction* algorithm reverts to decisions taken in *Reactive updates*. Also, if there is a possibility to save more energy, *Reactive updates* may be called to update the topology to put more nodes in low-power operation modes. Hence, after its first run, *morfeo* stays in *Correction* and uses *Reactive updates* as needed and thus, adapts the operation modes, and hence, the energy consumption to user demand.

The flow diagrams of the *morfeo*'s cycle is shown in Fig. 6.3. In the following, we present each of the three steps in more detail.

6.2.3.1 *Step 1:* Initialisation

In this step, *morfeo* groups nodes into three different groups: *sleep candidates*, *head candidates*, and *special candidates*.

- **Sleep Candidates:** If the energy consumption can be reduced by switching certain WADs into a low power mode, i.e., Off or, Partial or sector sleep mode, these nodes are marked as *sleep candidates*.

- **Head Candidates:** The WADs, which can take over the load of other WADs

Algorithm 1 *Step 1: Initialisation*

```
for all WADs ∈ Network do
    if ∃ WAD with Sleep Characteristics then
        WAD is Sleep Candidate
    else if ∃ WAD with Head Characteristics then
        WAD is Head Candidate
    else if ∃ WAD with Unpredictable Traffic then
        WAD is Special WAD
    end if
end for
```

are identified (i.e., due to overlapping coverage) and these nodes are marked as *head candidates*.

- **Special Candidates:** Based on the context, under special conditions, a set of nodes may need to be always in Active mode. These conditions mainly appear in scenarios where high amount of traffic is expected but the actual behavior of the expected traffic may not be predicted (i.e., a stadium, where the traffic load is expected only on special events such as concert or soccer matches). In this case, such nodes are marked as *special candidates*.

The proposed algorithm *morfeo* uses the Algorithm 1 to classify each WAD in different groups (i.e., sleep candidates and head candidates). To make these decisions, *morfeo* uses different types of information, such as deployment information, which includes the network topology, coverage and network access technologies. Also, the energy cost analysis of the different operating modes of the WADs and the limitations in switching and sojourn times in different operating modes based on the deployed hardware plays an important role in these decisions. In addition, *morfeo* takes into account the context information, which includes the application scenario, predicted traffic load, and QoS constraints.

6.2.3.2 *Step 2:* Reactive Updates

In this step, *morfeo* evaluates several conditions for each WAD based on network traffic and topology and decides on the operation modes. To make these decisions, *morfeo* evaluates several conditions for each WAD based on network traffic and topology. Based on these conditions (see Subsection 6.2.2), *morfeo* uses the Algorithm 2 to assign operation modes to each WAD in different groups (i.e., sleep candidates and head candidates).

Specifically, the current traffic situation of the sleep candidates is analyzed and the WAD is switched to Off Mode if it is under *Zero Condition*. If the WAD is under *Idle Condition*, it is switched to Partial/Sector Sleep Mode. Otherwise, if the WAD is under *Active Condition*, the procedure for balancing the network load is applied. Here, the users are handed over to the head candidates if it is possible. The WAD

Algorithm 2 *Step 2: Reactive updates*

```
1: for all Sleep Candidates ≠ Off Mode do
2:   if WAD in Zero Condition then
3:     WAD → Off Mode
4:   else if WAD in Idle Condition then
5:     WAD → Partial/Sector Sleep Mode
6:   else if WAD in Active Condition then
7:     if ∃ Head Candidate and low traffic then
8:       handover users to Head Candidate
9:       Head Candidate ← Head Condition
10:      WAD → Sleep Candidates
11:    end if
12:  end if
13: end for
14: for all Head Candidates do
15:  if WAD in Head Condition and coverage adaptation needed then
16:    WAD → Full-Power Mode
17:    Tilt or Power Adaptation
18:  end if
19: end for
```

is added back to the set of sleep candidates to check the possibility of switching to Partial/Sector Sleep or Off Modes (line 10, Algorithm 2). Finally, all the WADs in the *Head Condition* are switched to Full–power mode only if coverage adaptations are needed. According to the type of technology, tilting optimization or increasing the transmission power may also be used to extend and improve the coverage area.

6.2.3.3 *Step 3:* Correction

After reactive updates, and one time-slot duration, *morfeo* transitions to *Correction*, which is detailed in Algorithm 3. Here, *morfeo* evaluates the network performance and if the QoS constraints are not satisfied, the WADs that are in low power modes are switched to Active Mode. Otherwise, *morfeo* calls *Reactive updates* in order to discover if more WADs could be put to low power modes this means Off Mode or Partial Sleep Mode.

Finally, we consider that it might be possible to allow partial coverage rather than full coverage, i.e., in an enterprise deployment, APs might be turned off to provide reduced coverage at night when very low traffic load is expected. In this case, in order to give a chance (i) to the incoming users for connectivity and (ii) to the network to reconfigure the operation modes of the WADs, a wake up slot is introduced. During this time-slot, all the WADs are switched to Active Mode to check whether the operating conditions have changed. The wake–up slot is also executed during *Correction* (line 1–5 in Algorithm 3).

Algorithm 3 *Step 3: Correction*

```
while MORFEO is active do
  Sleep(Time–slot)
  if Wake up–slot and partial–coverage profile then
    for all WADs do
      WAD → Active Mode
    end for
  else
    if Network performance OK and traffic not increasing then
      → Reactive updates (Step 2)
    else
      if ∃ WAD ∈ Off Mode then
        WAD → Active Mode
      else if ∃ WAD ∈ Partial/Sector Sleep Mode then
        WAD → Active Mode
      else if ∃ WAD ∈ Full–Power Mode then
        WAD → Active Mode
      end if
    end if
  end if
end while
```

After the first run, *morfeo* stays in *Correction* and analyses network performance and current conditions based on the statistics collected from CoMa. If the analysis indicates further energy savings, *Reactive updates* evaluate changes in operation modes and goes back to *Correction*, and *morfeo* continues in this cycle as shown in Algorithm 4.

Algorithm 4 *MORFEO*: Cycle of *morfeo* for saving energy in the network while maintaining QoS

```
Step 1: Initialisation Phase
while 1 do
  if ∃ Sleep and Head Candidates ∈ Network then
    Step 2: Reactive phase
  end if
  Sleep(Time–slot)
  Step 3: Correction Phase
end while
```

The flow diagrams of the *morfeo* procedures is depicted in Fig. 6.4

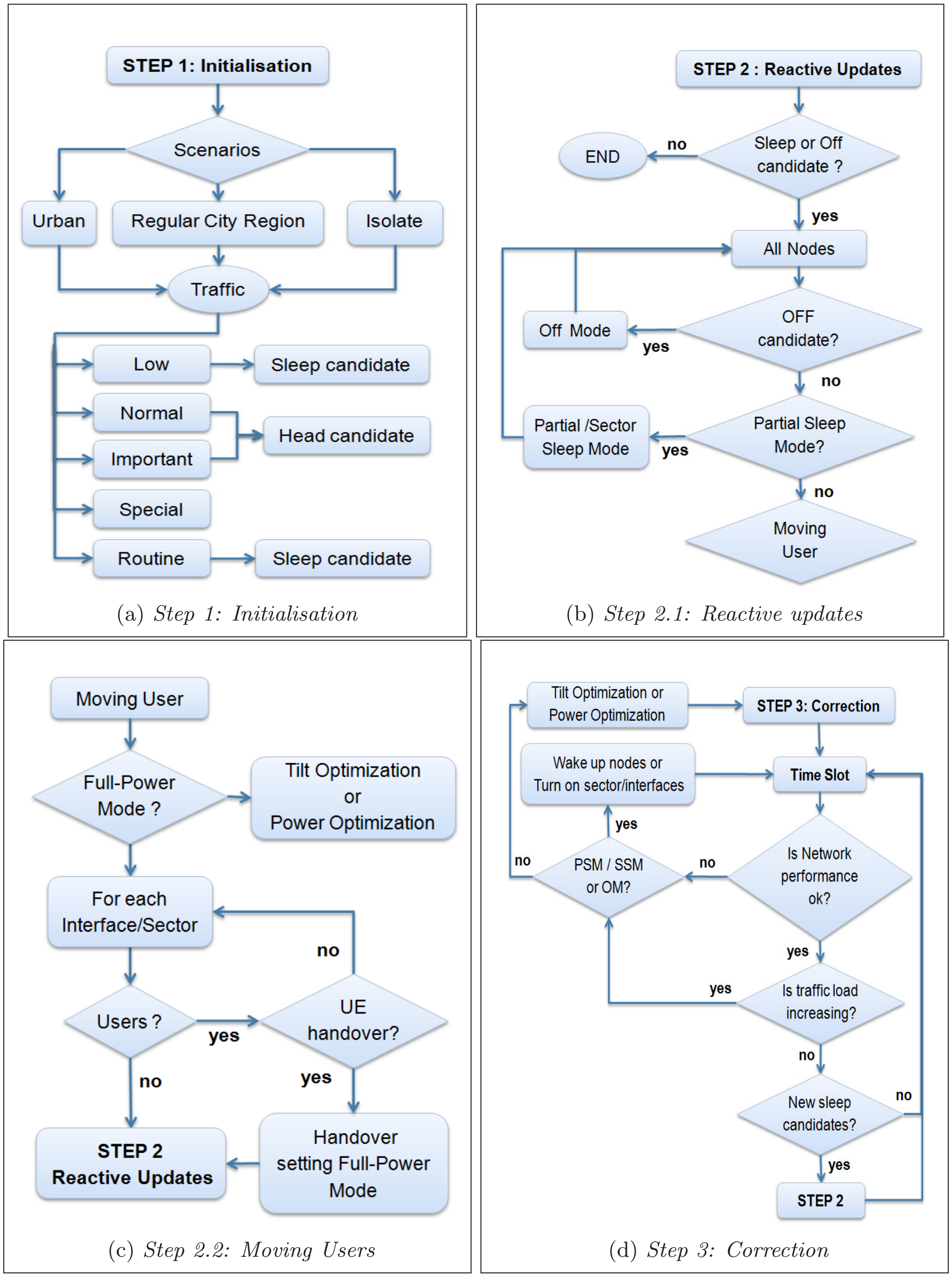

(a) *Step 1: Initialisation*

(b) *Step 2.1: Reactive updates*

(c) *Step 2.2: Moving Users*

(d) *Step 3: Correction*

Figure 6.4: Flow diagrams of the *morfeo* procedures for partial coverage

6.3 Switching Times Impact Analysis

In this section, we analyze the impact of switching operation modes on the energy efficiency of *morfeo* decisions. It can be experimentally measured, indeed, that

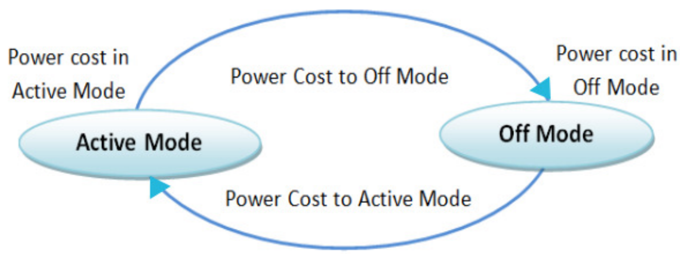

Figure 6.5: Cycle and power cost required for switching between Active/Off Mode

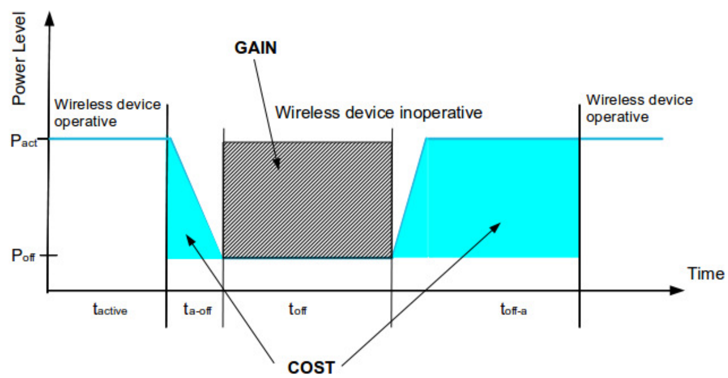

Figure 6.6: Graphical representation of the energy saved and of that wasted due to switching time.

switching between different modes bears a cost. We also describe the parameters that *morfeo* needs as input in order to make the right decisions for allowing energy–saving in any wireless network. Here, we focus on WiFi network as a proof of concept. However the same analysis can apply to any wireless devices such as base stations, eNodeB or femtocells.

6.3.1 Impact of Active–Off Mode Switching Times

As switching times can be very large (i.e., waking up a WiFi access point from idle mode can easily take 100 seconds), the cost is non–negligible. This implies that it is not convenient to put a device in low power modes for short time intervals.

Let us first consider the situation in which only two modes (Active and Off Mode) are supported. Fig. 6.5 shows the cycle and power cost required for switching from Active to Off Mode and vice–versa. It is actually possible to define a minimum off–time for which the energy gains (in terms of energy saved with respect to keeping the device in Active Mode) compensates the energy waste (related to the energy spent in switching from Active Mode to Off Mode, from Off Mode back again to Active Mode and Off Mode).

The situation is graphically depicted in Fig. 6.6. During switching, the device spends additional energy $E_{a-off} + E_{off-a}$, which we refer to as cost. In our model, we represent the total energy consumed by the system in Active Mode as:

$$E_{active}(t) = P_{active} \cdot t \tag{6.1}$$

Where:

- P_{active} is the power consumed by the system in Active Mode, without traffic (expressed in W);
- t (s) is the time spent in this mode;

Similarly, the total energy consumed by the WAD in Off Mode is:

$$E_{off}(t) = P_{off} \cdot t \tag{6.2}$$

Where:

- P_{off} is the power consumed in Off Mode;

We also take into account the total energy consumed for switching from Active to Off Mode:

$$E_{a-off} = P_{a-off} \cdot t_{a-off} \tag{6.3}$$

Where:

- P_{a-off} is the *average* power consumed in order to totally turn off the WAD (expressed in W);
- t_{a-off} is the time required for this switching;

Similarly, the total energy consumed for switching from Off to Active Mode is:

$$E_{off-a} = P_{off-a} \cdot t_{off-a} \tag{6.4}$$

Where:

- P_{off-a} is the power consumed by the system in order to turn on the WAD (expressed in W);
- t_{off-a} is the time required by the WAD to be completely operational again;

To be able to save energy by switching the device to Off Mode, for a given time period t, the following condition must be satisfied:

$$E_{active} > E_{a-off} + E_{off} + E_{off-a} \tag{6.5}$$

Rewriting the equations in terms of power and time, we get:

$$P_{active} \cdot t^* \quad > \quad P_{off} \cdot (t^* - t_{a-off} - t_{off-a}) + E_{a-off} + E_{off-a}$$

- E_{off} the energy consumption in the Off Mode is calculated as the remaining time after deducting the times spent for switching between the two modes;

- t^* is the minimum time the WAD needs to be in Off Mode in order to save energy;

By reorganising the terms, we get:

$$\boxed{t^* > \frac{E_{a-off} + E_{off-a} - P_{off} \cdot (t_{a-off} + t_{off-a})}{P_{active} - P_{off}}} \tag{6.6}$$

We can further simplify Equation 6.6, when we take into account the power cost of each device in the system in different modes. We denote with:

- P_{wd} the power consumed by the WAD in Active Mode (expressed in W);

- P_{pm} the power consumed by the energy monitoring device (expressed in W), for *energino* [Gomez 2012b] or EPC [EPC] power meters;

- $P_{wd(a-off)}$ is the average power consumed by the WAD to be totally turned off (expressed in W);

- $P_{wd(off-a)}$ is the average power consumed by the WAD to be totally turned on (expressed in W), both excluding the energy consumption of the monitoring device;

Hence, we can rewrite the power consumption of each mode as:

$$\begin{cases} P_{active} = P_{wd} + P_{pm} \\ P_{off} = P_{pm} \\ P_{a-off} = P_{wd(a-off)} + P_{pm} \\ P_{off-a} = P_{wd(off-a)} + P_{pm} \end{cases} \tag{6.7}$$

By plugging these into the Equation 6.6, we get:

$$\boxed{t^* > \frac{P_{wd(a-off)} \cdot t_{a-off} + P_{wd(a-off)} \cdot t_{off-a}}{P_{wd}}} \tag{6.8}$$

In terms of current consumption, if the potential difference denoted with $V(t)$ is constant in time, we get:

$$\boxed{t^* > \frac{I_{wd(a-off)} \cdot t_{a-off} + I_{wd(a-off)} \cdot t_{off-a}}{I_{wd}}} \tag{6.9}$$

In Fig. 6.7a, the measurement results from a sample WAD_1 are reported. The WAD used is a commercial available *Saxnet Meshnodes III*, which are specialized for outdoor usage under extreme environmental conditions. It is part of a

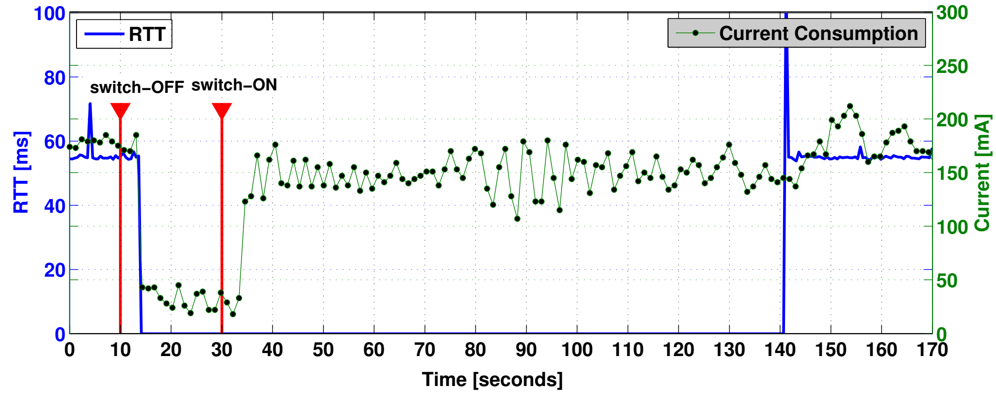

(a) Measurements for a sample WAD_1

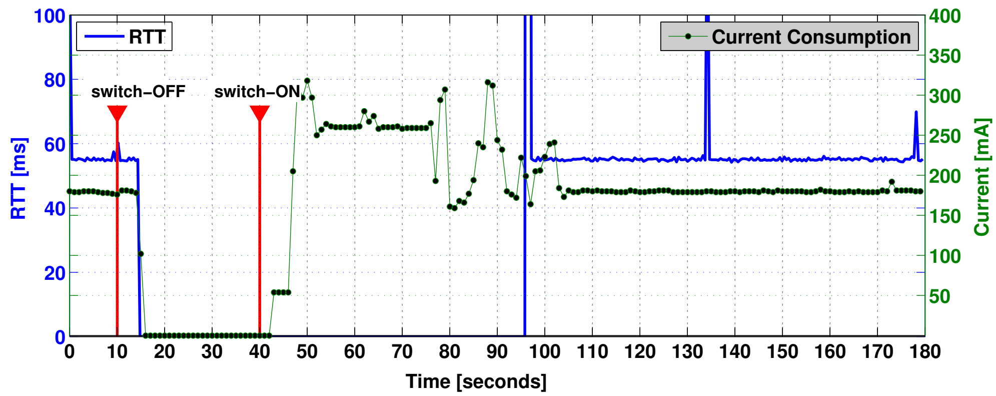

(b) Measurements for a sample WAD_2

Figure 6.7: Switching time: measurements for Wireless Access Devices

testbed [Uzun 2012] deployed at Deutsche Telekom Laboratories in Berlin, Germany, see additional details in Section 6.4.2. The WAD_1 takes (i) $\approx$ 6 seconds in order to turn off completely and (ii) $\approx$ 113 seconds in order to be on and completely operational again. Since for this WAD_1, the Active Mode and switching mode powers are almost the same, based on the Equation 6.9, $t^* \approx 0$. Once the WAD is put in Off Mode, *morfeo* does not evaluate the conditions that can lead to its wake–up before $t^* + t_{a-off} + t_{off-a}$, which is approximately 120 seconds, for WAD_1.

The Fig. 6.7b reports an additional example from WAD_2. The WAD used is a commercially available *Saxnet* for indoor usage. The WAD_2 takes (i) $\approx$ 5 seconds in order to turn off completely and (ii) $\approx$ 60 seconds in order to be on and completely operational again. Since for this indoor WAD_2, the Active Mode and switching mode powers are different, based on the Equation 6.9, t^* is $\approx$ 15 seconds. Therefore, once the WAD_2 is put in Off Mode, *morfeo* does not evaluate the conditions that can lead to its wake–up before approximately $\approx$ 80 seconds, for this indoor WAD_2. As a conclusion, we can note that the cost to put WAD_2 on is higher than the cost of the device in Active Mode.

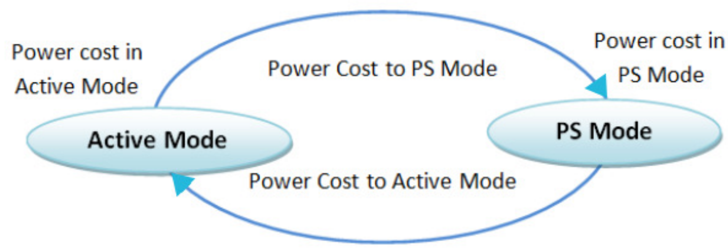

Figure 6.8: Cycle and power cost required for switching between Active/Partial Sleep Mode

6.3.2 Impact of Active–Partial Sleep Mode Switching Times

A similar reasoning applies to the case in which also a Partial Sleep Mode is supported. Also in this case it is possible to define a minimum time the device has to spend in Partial Sleep Mode to amortize the cost of switching. Fig. 6.8 shows the cycle and power cost required for switching from Active to Partial Sleep Mode and vice–versa

In Equation 6.6, we replace the energy consumption E_{off} with the energy consumption of Partial Sleep Mode, E_{psm}. The switching costs are E_{a-psm} and E_{psm-a}, which capture the cost of switching from Active Mode to Partial Sleep Mode and vice–versa, respectively.

$$E_{active} > E_{a-psm} + E_{psm} + E_{psm-a} \tag{6.10}$$

Using similar simplifications, it can be shown that: t^+, the minimum time that amortises the cost of switching from Active Mode to Partial/Sector Sleep Mode, is derived as:

$$\boxed{t^+ > \frac{P_{wi(a-psm)} \cdot t_{a-psm} + P_{wi(a-psm)} \cdot t_{psm-a}}{P_{wd}}} \tag{6.11}$$

Where:

- t_{a-psm} (s) and t_{off-a} (s) are the times required for the wireless interface to be totally turned off/on, respectively;
- $P_{wi(a-psm)}$ (expressed in W) and $P_{wi(psm-a)}$ (expressed in W) are the average power consumed by the WAD to turn off/on the wireless interface, respectively;

We experiment with different configurations for Partial Sleep Mode with a WAD with two wireless interfaces. The results are shown in Fig. 6.9. First, we configure the WAD in full Partial Sleep Mode by switching off all the wireless interfaces and measure the power consumed as ≈ 10.38 W. Then, we configure the WAD such that one wireless interface is up and the other is down, and measure the power consumed

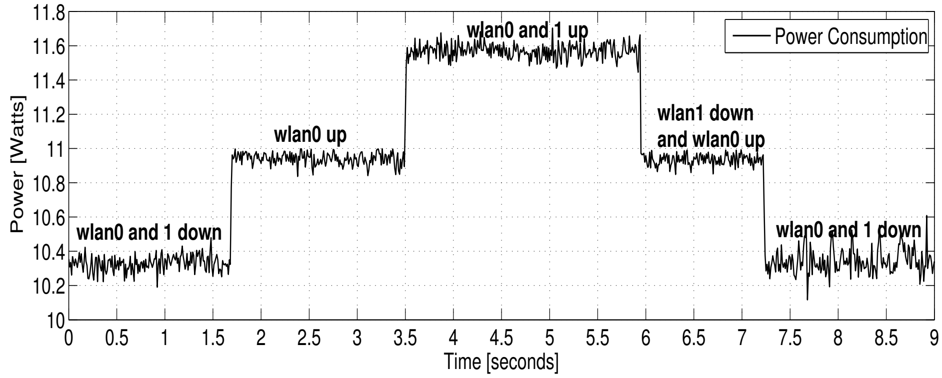

(a) Power consumed versus time

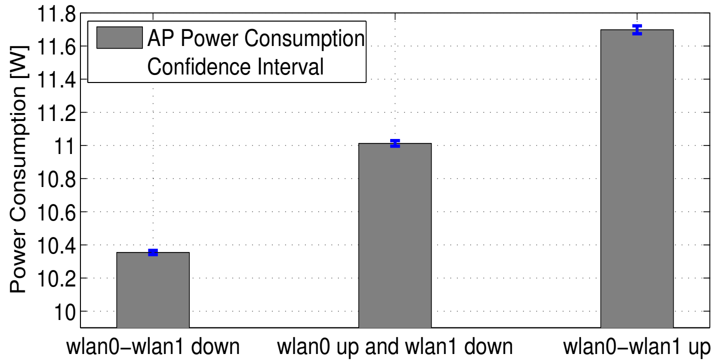

(b) Average power consumed

Figure 6.9: Average power consumed for Partial Sleep Mode

as ≈ 11 W . Finally, we configure the WAD in Active Mode by switching on all the wireless interfaces of the WAD. The power consumed for Active Mode is 11.63 W. Therefore, the energy cost of each wireless interface is constant and approximately equal to 0.62 W. We repeated the experiment in the reverse sequence (i.e., from two interfaces up to only one interface up and both interfaces down) and observed similar results. The switching times were less than 10 ms[1]. Based on these experiments, we concluded that the power cost for switching between Active and Partial Sleep Modes were negligible and no noticeable service disruptions happen.

This trivially requires that in our system, in order to have any energy gain, the energy spent in Active Mode should be greater than the energy spent in Partial Sleep Mode. As this always holds true, the minimum time required for saving energy to switch a WAD to Partial Sleep Mode is $t^+ = 0$, i.e., there is no condition on the minimum time to spend in Partial Sleep Mode.

The minimal amounts of time to be spent in Off and Partial Sleep Modes defines a limit on the dynamics of *morfeo*, i.e., on its ability to track variation in context and traffic. Yet, the values we experimentally measured for WiFi-based WADs are much

[1]10 ms is the time granularity of our measurement framework.

shorter than what can be found in cellular network technology where, i.e. switching Partial Sector Mode–Active Mode or Off Mode–Active Mode may be necessary every tens of minutes or even hours.

6.4 Performance Evaluation

We implemented *morfeo* in python and installed the energy monitoring and control framework in a 8-node testbed deployed at Deutsche Telekom Laboratories in Berlin, Germany [Uzun 2012] . In this section, we present the experimental evaluation of *morfeo* under several practical scenarios. To this end, we first describe our experimented methodology, and conclude with energy measurement results and network traffic performance. The goal of our evaluation is to show that *morfeo* can save energy under different conditions without degrading service quality.

6.4.1 Network Settings

The testbed is composed of 8 custom IEEE 802.11a/b/g Access Point (AP) and 13 clients. Fig. 6.10 shows the network topology. The testbed covers an area of approx. 9600 m^2, which is divided into four separate courtyards. The APs are commercial available Saxnet meshnode III equipped with multiple wireless interfaces. They are also connected via Ethernet to a wired backbone network. The WiFi antennas are sector type and the operating frequency was set to 5.18GHz for wireless backbone links and 2.24GHz for wireless access links. The rate adaptation algorithm has been set to the default auto, and the transmission power has also been left as the default value of 17dBm (≈50.12 mW) for all experiments.

6.4.2 Testing Methodology

6.4.2.1 Traffic Generation and Power Consumption Monitoring

Traffic is generated using the Iperf traffic generator and is injected into the network from APs to clients. The power consumption is measured using the EPC [EPC] power meter. The EPC is a commercial solution for real–time monitoring of power consumption. The power consumption statistics are logged by EPC with a granularity of 0.1 W and a sampling period of 1 second.

6.4.2.2 Experimental Details

To test the network under different traffic conditions, we generate synthetic traffic in the form of single UDP or TCP flows with a duration of 300 seconds. During this time, we collect power consumption measurements and network performance statistics from each AP. We considered the following network profiles:

i) **Normal Profile:** The network is working in its default setting with all nodes in Active mode, and *morfeo* is not activated.

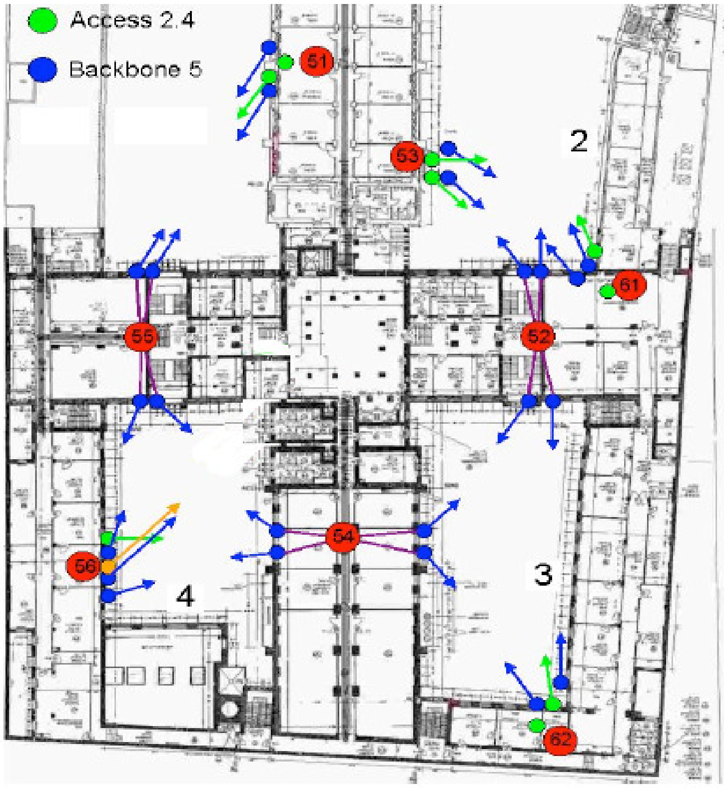

Figure 6.10: Network topology for testing scenarios. The red dots represent the WiFi APs used in our experiments. The green and blue dots and arrows show the antenna directions for access and backbone interfaces, respectively.

ii) **Isolated Profile:** Partial coverage is allowed and the APs work in an isolated manner without any overlapping coverage with neighboring APs.

iii) **Partial–coverage Profile:** Partial coverage is allowed and the network coverage is achieved with 2 head candidates.

iv) **Full–coverage Profile:** Full coverage is required and the network coverage is again achieved with 2 head candidates. It is important to note that in the Full–coverage profiles, the head candidates are able to entirely cover the coverage area of the sleep candidates and hence, operate with higher transmission powers.

In our experiments, we activated *morfeo* during 15 slots. We calculated the minimum time–slot, based on how long CoMa takes collecting measurements and how fast the operation modes can be switched by EC. We measured this time $\approx$ 40 seconds. We also set the slot 4 as the wake–up slot for the partial–coverage scenarios.

For the *Initialisation* step, for the Partial–coverage and Full–coverage profiles, we set 3 APs as a sleep candidate (52, 61, 62), 2 APs as head candidates (54, 55),

Table 6.2: Netowrk scenario description

AP Identifier	Number of Interfaces	Number of Users	Profile Isolated	Profile Partial and Full
52	3	2	Sleep candidate	Sleep candidate
51	3	0	Special Candidates	Special Candidates
53	1	1	Sleep candidate	Isolated
54	4	4	Sleep candidate	Head candidates
55	3	3	Sleep candidate	Head candidates
56	3	0	Special Candidates	Special Candidates
61	2	1	Sleep candidate	Sleep candidate
62	2	2	Sleep candidate	Sleep candidate

2 APs with a special candidates (51, 56). For the Isolated profiles, 6 APs were set as sleep candidates and 2 APs as special candidates (51,56). The situation of node 53 is special, as it is isolated from the other APs, and hence, even if it is a sleep candidate, it needs to stay in Active Mode if a user associates as it is not able to handover its users to a head node (see Table 6.2).

Each experiment duration is set for 700 seconds and we run each experiment 3 times. The following experiments were performed for each profile:

i) *Scenario*$_1$*–No users:* The network is working without users.

ii) *Scenario*$_2$*–No traffic:* There are users associated to the network, but they do not generate traffic.

iii) *Scenario*$_3$*–UDP traffic:* There are users in the network generating UDP traffic. Each user generates a flow of 2Mbps.

iv) *Scenario*$_4$*–TCP traffic:* There are users in the network generating TCP traffic.

6.4.3 Results Analysis

Based on the measurement results, we first look at the average power consumption of each AP under the four different scenarios and profiles. Table 6.2 shows the number of interfaces and the user distribution per AP.

- **Scenario**$_1$**:** In Fig. 6.11 the average power consumption of each AP in the network working under scenarios$_1$ where the network is working without users is presented. The Fig. 6.11 show that the average power consumed in the normal profile is in most cases higher than the power consumed by the APs with *morfeo* in the other profiles. The results show that while sleep candidates 52, 61 and 62 can significantly save energy, the head candidates 54 and 55 are able to save energy in this scenario, with no users. Here, if partial–coverage is allowed, the sleep candidate nodes are able to save significant energy.

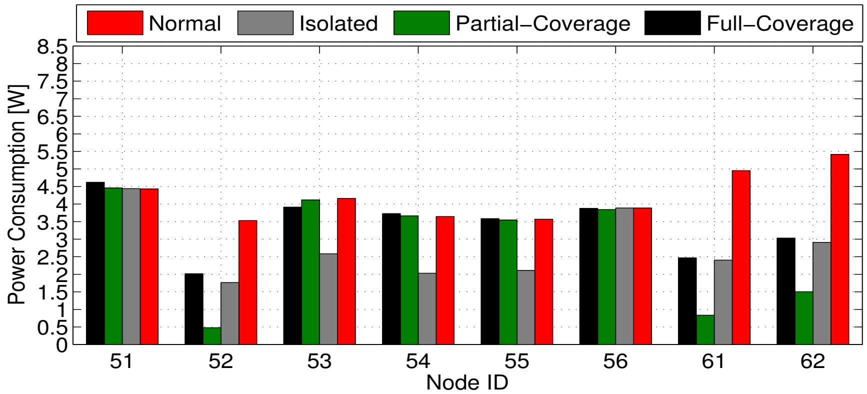

Figure 6.11: Average power consumption of each AP in the network working under different scenarios_1 where the network is working without users.

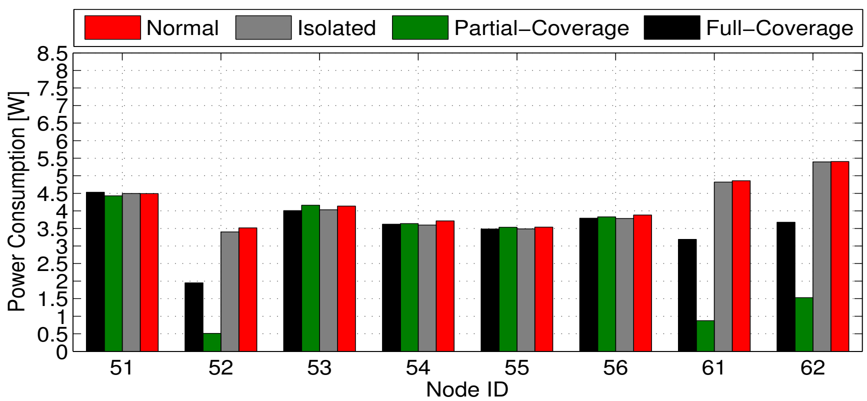

Figure 6.12: Average power consumption of each AP in the network working under different scenarios_2 where the network is working with users without traffic.

- **Scenario_2:** In Fig. 6.12 the average power consumption of each AP in the network working under scenarios_2 where the network is working with users without traffic is presented. The Fig. 6.12 shows that the average power consumed in the normal profile is in most cases higher than the power consumed by the APs with *morfeo* in the other profiles as observed in scenario_1. Here, sleep and head candidates are able to save significant energy in Full and Partial profile. However, in Isolated profile we assume that the network topology does not allow the presence of head candidates and hence the APs can be only switching to Partial Sleep Mode. In this scenario only a limited amount of energy is saved (see gray bar in Fig. 6.12).

- **Scenario_3:** In Fig. 6.13 the average power consumption of each AP in the network working under scenarios_3 where the network is working with users and UDP traffic is presented. In this scenario, the observations are similar

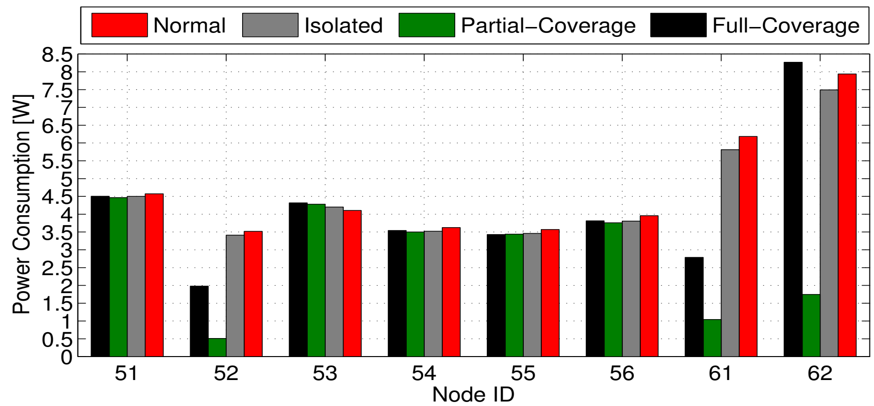

Figure 6.13: Average power consumption of each AP in the network working under different scenarios_3 where the network is working with users and UDP traffic.

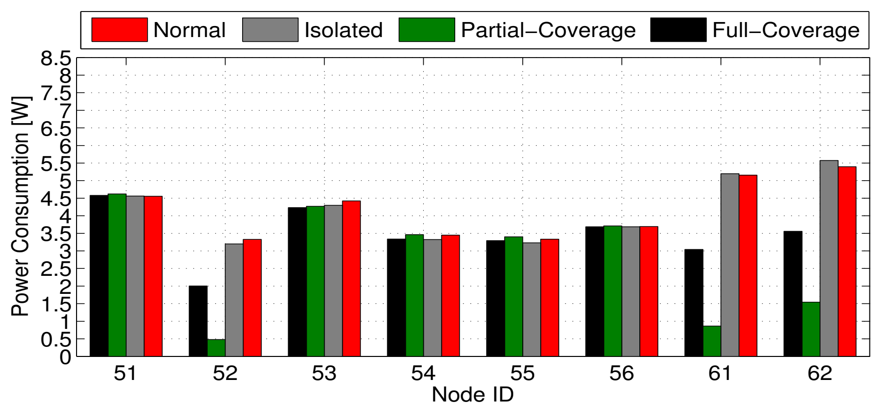

Figure 6.14: Average power consumption of each AP in the network working under different scenarios_4 where the network is working with users and TCP traffic.

to scenarios_1 and scenarios_2. Since, partial–coverage is allowed, the sleep candidate nodes are able to save significant energy while the head candidates take of the traffic in the network.

- **Scenario_4:** In Fig. 6.14 the average power consumption of each AP in the network working under the last scenarios_4 where the network is working with users and TCP traffic is presented. In this scenario, the sleep candidate nodes are able to save significant energy while the head candidates guarantee the QoS required by TCP traffic.

In Fig. 6.15, normalized values of the average network power consumption for the different testing scenarios are presented. We calculated the normalized network power consumption by considering the power consumption in the normal profile as the reference index for the scenarios. The Fig. 6.11, 6.12, 6.13, 6.14 and Fig. 6.15 show that the energy savings with *morfeo* vary from 3–45% of the total of power

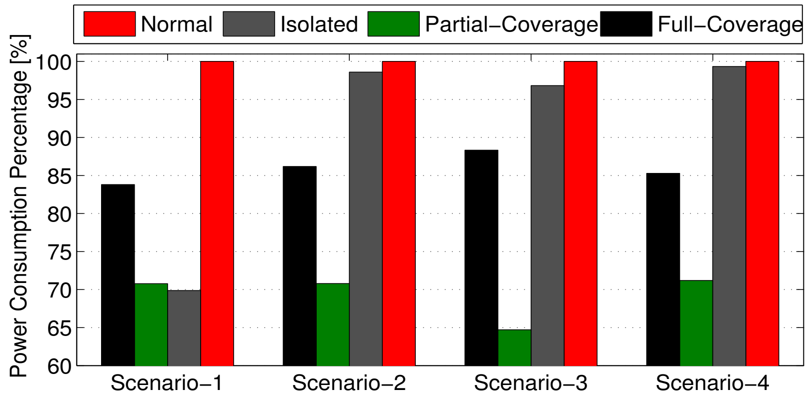

Figure 6.15: Normalized Network Power Consumption for the different testing scenarios.

consumed in the normal profile, even if the only a number of nodes could be sleep candidates. As expected, the best opportunity for energy savings occurs when the network has no associated users. In this case, *morfeo* can save between 15-30%. When there are users associated to the network, the Isolated profile experiences the worst case in terms of energy saving due to the fact that the network topology does not allow the presence of head candidates. Hence, *morfeo* can only opt for Partial or Sector Sleep Mode for the APs. Instead, in the Partial–coverage and Full–coverage profiles, the presence of the 25% of head candidates allows the network to save energy while maintaining the coverage and capacity.

The results also show that:

- The Partial–coverage profile saves the highest energy since this profile allows some coverage holes in the network for short periods. This is because, in the Partial–coverage profile, the head candidates are not sharing completely the coverage area of the sleep candidates and hence the wake–up slot is activated. Here, the APs are put in Off Mode even if they are not sharing the same coverage area with the head candidates.

- This limitation holds true for all the experiments even when the network is operating without users (see Fig. 6.12). However, note that, in the Partial–coverage profile, the wake–up slot is activated every 4^{th} slot in order for the incoming users to associate to the network. Therefore, in this profile, there is a cycle between periods of full and partial–coverage.

- It is important to note that lower number of wake–up slots enables more energy savings, but with the consequence of fewer full–coverage periods. Therefore, wake–up slot frequency must be carefully chosen and should represent the network dynamics in terms of both users and traffic.

- In the Full–coverage profile, the head candidates are sharing completely the

Table 6.3: Network performance for each AP working under $Scenario_3$ and $Scenario_4$

AP Identifier	**Number of Interfaces**	**Number of Users**	**UDP [Mb/s]**	**Packet Loss [%]**	**TCP [MBytes]**
52	3	2	4	0.01	246
53	1	1	2	0.02	322
54	4	4	8	0.00	1324
55	3	3	6	0.00	756
61	2	1	2	0.00	322
62	2	2	4	0.01	419

coverage area of the sleep candidates, and hence the wake-up slot is not activated. Here, the APs are put in Off Mode only if they are sharing the coverage area with head candidates. Clearly, this condition limits the amount of energy that can be saved compared to Partial–coverage, where the APs are put in Off Mode even if they are not sharing the same coverage area with the head candidates.

- Finally, we observe that the most effective way to save energy is by putting the AP in Off Mode as much as possible. Therefore, an accurate network coverage map will allow more effective planning in terms of head and sleep candidates, which will eventually lead to higher energy savings.

Finally, the Table 6.3 reports the iperf outputs for each AP under different profiles. In the case of UDP traffic, the packet loss was less than 1% in all the experiments. In the case of TCP traffic, we observed the same performance for both scenarios. Therefore, the network performance does not suffer any degradation when *morfeo* is operating. It is important to note the UDP and TCP results are presented in a single column since the obtained results are the same across all the profiles.

6.5 Conclusions

In this Chapter, we presented energy–saving solutions for improving the energy efficiency of wireless access networks. The *morfeo* algorithm, together with the energy monitoring and control framework, allows appropriate energy saving decisions to adapt the energy consumption of a wireless infrastructure to the actual network conditions in terms of both user distribution and traffic patterns. The experimental evaluation of *morfeo* in a real network deployment confirmed that the proposed solution can provide significant energy savings with minimal network performance degradation. We have designed *morfeo* to take advantage of context and measurement–based network information, and adapts network operation in any wireless network. The main observations of this Chapter include:

- The results show that the average power consumed in the normal profile is in most cases higher than the power consumed by the APs with *morfeo* in the other profiles.

- The results show that the energy savings with *morfeo* vary from 3–45% of the total of power consumed in the normal profile, even if the only a number of nodes could be sleep candidates.

- The Partial–coverage profile saves the highest energy since this profile allows some coverage holes in the network for short periods. Here, the wake–up slot is activated every n slot in order for the incoming users to associate to the network. Therefore, in this profile, there is a cycle between periods of full and partial–coverage.

- It is important to note that a lower number of wake–up slots enables more energy savings, but with the consequence of fewer full–coverage periods. Therefore, wake–up slot frequency must be carefully chosen and should represent the network dynamics in terms of both users and traffic.

- We observe that the most effective way to save energy is by putting the AP in **Off Mode** as much as possible. Therefore, an accurate network coverage map will allow more effective planning in terms of head and sleep candidates, which will eventually lead to higher energy savings.

This page is intentionally left blank

Chapter 7

Conclusions

Contents

7.1 Achievements and Contributions

In this Thesis, we followed an experimental methodology for understanding *how*, *where* and *when* power is consumed in WADs. The approaches, methodologies, and solutions proposed in this Thesis can be easily reused for analyzing and understanding the power consumption of other network devices. We quantified the power consumption of WADs taking into account the most influential parameters that affect it.

We introduced *energino*, an affordable solution for real–time energy consumption monitoring in wireless networks. The hardware schematics and the software architecture were discussed in order to encourage the research community to use and extend *energino*. Using *energino* power meter, we proposed a measurement–based methodology for characterizing the power consumption behavior of networked WADs. In particular, we focused our attention on indoor–outdoor WiFi and WiMAX WAD and we derived their power consumption figures as a function of (i) the traffic load, (ii) the modulation and coding schemes, (ii) the size of the datagrams used and (iv) different transmission power levels.

An accurate power consumption model, which can be easily plugged into typical network simulations tools such as ns3 or Omnet++, is essential to drive the design and development of energy aware network protocols and algorithms. Therefore, we proposed a simple, accurate and general model based on decomposition of the power consumption components that can be monitored and evaluated separately. The proposed model is based on monitoring measurable parameters and computing specific efficiency metrics.

Finally, we designed, implemented and tested energy–saving solutions for improving the energy efficiency of wireless access networks. The proposed algorithm, together with the energy monitoring and control framework, allows appropriate energy saving decisions to adapt the energy consumption of a wireless infrastructure to the actual network conditions in terms of both user distribution and traffic patterns. The experimental evaluation of the proposed algorithm in a real network

deployment confirmed that the proposed solution can provide significant energy savings with minimal degradation of network performance. We have designed the proposed algorithm to take advantage of context and measurement–based network information, and to adapt network operation in any wireless network.
The main observations of this Thesis can be summarized as following:

- The power consumption of the WAD depends on several factors, such as the amount of traffic, packet size, transmission power level, modulation and coding schemes and channel conditions.

- Large packets use energy more efficiently than small ones as well as high modulation and coding schemes are more energy efficient. Additionally, the transmit power levels have very little effect on the power consumed by the WADs.

- The power consumption of WAD follows a linear behavior until the WAD reaches a saturation point. The same behavior was observed for all WADs used in our investigation such as (i) IEEE 802.11g and IEEE 802.11n indoor WADs, (ii) IEEE 802.11g Outdoor WADs and (iii) WiMAX WADs.

- A significant fraction of the power consumed by these devices is not traffic dependent in both the WiFi and WiMAX cases. More specifically, we found that injecting traffic in the network until the saturation point results in only a $\approx$20% increase in power consumption with respect to the power consumption in idle mode, i.e. when there is no traffic in the network besides the regular signaling.

- The power consumption of WAD can be divided into two parts. The first part is that is related to the power consumption of the circuit plus the basic operation of the WAD. While the second one is related to the technology considered (WiFi/WiMAX) and the setting parameters, including the transmission power level, the datagram size, the modulation and coding schemes and specially the traffic load. The first part of power consumption varies significantly according with technology considered (WiFi/WiMAX) and type of WAD, indoor and outdoor, and it remains constant during the time. While the second part of power consumption is variable in the time and it is strongly influenced by the setting parameters, including the transmission power level, the datagram size, the modulation and coding schemes and specially the traffic load.

- The power consumption of WAD as a function of traffic load follows a linear behavior until the WAD reaches a saturation point. The slope of the line and the saturation value depend on a number of factors, including transmission power levels, technology considered (WiFi/WiMAX) and the modulation scheme in use.

- For estimating the power consumption of a WAD as a function of the transmission rate, only three easily measurable parameters are required: 1) power consumption in idle, 2) power consumption in any midpoint in order to compute the slope of the curve, i.e. smaller packet loss, and 3) power consumption in the saturation.

- For estimating the power consumption of a WAD as a function of the datagram size, only three easily measurable parameters are required: 1) power consumption with the null packet length, i.e. no payload, 2) power consumption in any midpoint, i.e. smaller packet length, in order to compute the slope of the curve and 3) power consumption for X Mb/s with optimal packet length.

- The results presented in this thesis shown that the energy savings with the proposed algorithm vary from 3–45% of the total of power consumed for the WAD.

- We observe that the most effective way to save energy is by putting the AP in **Off Mode** as much as possible. Therefore, an accurate network coverage map will allow more effective planning in terms of head and sleep candidates, which will eventually lead to higher energy savings.

7.2 Final Remarks and Future Directions

As it can be seen from the results presented in this Thesis, the power consumption of WAD depends on not only the application characteristics, i.e. length of sending data, transmission power levels, but also on device–level features, including technology considered (WiFi/WiMAX) and indoor/ outdoor type of WAD. Therefore, the proposed power consumption models and metrics can be used to guide the choices in many different sides of the design space, i.e. application system design, hardware design, WAD simulator design, upper layer protocol design and evaluation. Therefore, the challenges in wireless networking in terms of energy efficiency are (i) improving the energy efficiency of the WADs when it is transmitting data as well as when it is in idle mode and (ii) introduce novel indicator of energy efficiency as part of the standard of each wireless technologies

The results presented on this Thesis will be used as based for extending the investigated topics. We are currently analyzing the effects of traffic on power consumption in multi–hop wireless networks with multiple clients considering real application scenarios and traffic classes. We are planning to generalize our power consumption models as a function of two variables; the traffic load and the size of the session level data units in order to propose a more accurate model capable of predicting the power consumed by a WAD when it is transmitting or receiving different types of traffic.

Additionally, as future work, we plan to enhance *energino* by updating its hardware and software for monitoring the power consumption of battery–powered devices, such as mobile phones and mobile gateways. This research topic will be injected in the European FP7 ABSOLUTE project[1], which investigates the design and demonstration of a reliable Hybrid Terrestrial–Aerial Architecture which supports flexible and rapid deployment of a low delay and high capacity wireless network. Here, *energino* and the proposed experimentally–driven approach will be used in order to model the power consumption of the ABSOLUTE new devices (mainly focusing on the land mobile gateway and the LTE based aerial platform). Further, having a good power consumption model for the hybrid system could be useful to estimate the battery duration of the various subsystems under different scenarios.

Finally, since we have designed *morfeo* to take advantage of context and measurement based network information, and adapt network operation in any wireless network. We are also planning to extend the evaluation of *morfeo* to other access network infrastructures, and in particular heterogeneous network deployments. We believe *morfeo* can enable even higher energy savings taking into account the energy–performance–coverage trade–offs of different technologies. The same methodologies and procedures used for running *morfeo* in WLANs will be apply for running *morfeo* in cellular networks.

[1]ABSOLUTE (Aerial Base Stations with Opportunistic Links for Unexpected and Temporary Events), http://www.absolute-project.eu/, EU FP7 Integrated Project.

This page is intentionally left blank

Appendix A

Appendix

A.1 List of Publications

Patents:

- **K. Gomez**, T. Rasheed and L. Reynaud, A Flexibility Management Entity (FME) for Heterogeneous LTE Networks. Referred number: FR1256916, Date: January 2012, Depositor : FRANCE TELECOM.
- **K. Gomez**, T. Rasheed and L. Reynaud, Energy Efficient Routing and Forwarding for Hybrid Aerial Terrestrial Networks Communication. Referred number: FR1350780, Date: January 2013, Depositor: FRANCE TELECOM.

Journals:

- **K. Gomez**, D. Boru, R. Riggio, D. Miorandi and F. Granelli, Measurement–based Modelling of Power Consumption at Wireless Access Network Gateways, Published at Elsevier Computer Networks 2012, COMNET Special Issue on Green Communication Networks.

Conference Papers:

- T. Rasheed, **K. Gomez**, and R. Riggio, On the Support of Multimedia Applications over IEEE 802.11–based Wireless Mesh Networks. 16th International Conference on Telecommunications, Marrakech-Morocco, 25-27 May 2009
- R. Riggio, **K. Gomez**, and D. Miorandi, Mice over Mesh: HTTP Measurements over a WiFi–based Wireless Mesh Network. The 5th International workshop on Wireless Network Measurements, June 26- 2009 Seoul Korea.
- D. Lowe, D. Miorandi, and **K. Gomez**, Activation–inhibition–based data high–ways for wireless sensor networks, in Proc. of ICST Bionetics, December 2009.
- **K. Gomez**, T. Rasheed, R. Riggio, D. Miorandi, I. Chlamtac and F. Granelli, Analysing the Energy Consumption Behaviour of WiFi Networks, in Proc. of IEEE GreenCom'11, Online Conference.
- **K. Gomez**, T. Rasheed, R. Riggio and I. Chlamtac, On Efficient Airtime-based Fair Link Scheduling in IEEE 802.11-based Wireless Networks, in Proc. of IEEE PIMRC 2011.

- S. Kandeepan, **K. Gomez**, T. Rasheed, and L. Reynaud, Energy Efficient Cooperative Strategies in Hybrid Aerial–Terrestrial Networks for Emergencies, in Proc. of IEEE PIMRC 2011.
- R. Fedrizzi, **K. Gomez**, S. Kandeepan, T. Rasheed and C. V. Saradhi, Energy Aware Routing in Heterogeneous Multi–Hop Wireless Networks. in Proc. of IEEE ICC Greenets Workshop 2012.
- R. Riggio, **K. Gomez**, T. Rasheed, D. Miorandi and F. Granelli, Energino: an Hardware and Software solution for Energy consumption monitoring, In Proc. of IEEE Winmee 2012.
- A.Valcarce, T. Rasheed, **K. Gomez**, S. Kandeepan, L. Reynaud4, R. Hermenier, A. Munari, M. Mohorcic, M. Smolnikar and I. Bucaille, Airborne Base Stations for Emergency and Temporary Events. Accepted in 5th International Conference on Personal Satellite Services. Toulouse, France-June 2013.
- **K. Gomez**, C. Sengul, N. Bayer, R. Riggio, T. Rasheed and D. Miorandi. MORFEO: Saving Energy in Wireless Access Infrastructures. Accepted in 14th IEEE International Symposium on a World of Wireless, Mobile and Multimedia Networks (IEEE WoWMoM 2013). Madrid–Spain, Jun 2013.
- S. Kandeepan, **K. Gomez**, T. Rasheed, and L. Reynaud, Adaptive Energy Efficient Communications for Hybrid Aerial-Terrestrial Systems. Accepted in IEEE ICC E2Nets Workshop 2013.

Demo Presentations:

- R. Riggio, **K. Gomez**, T. Rasheed, M. Gerola and D. Miorandi, Mesh your Senses: Multimedia Applications over WiFi-based Wireless Mesh Networks. 6th Annual IEEE Communications Society Conference on Sensor, Mesh and Ad Hoc Communications and Networks (SECON 2009), Rome, Italy, June 23rd, 2009.
- **K. Gomez**, R. Riggio, D. Miorandi, I. Chlamtac and F. Granelli, TUNE-Green: A Distributed Energy Consumption Monitor for Wireless Networks, in Proc. of WoWMoM 2011.
- R. Riggio, C. Sedgul, **K. Gomez** and T. Rasheed. Energino: Energy Saving Tips for Your Wireless Network, in Proc. of SIGCOMM 2012.

Book Chapters:

- **K. Gomez**, D. Lowe and D. Miorandi, Data Highways: An Activator–Inhibitor–Based Approach for Autonomic Data Dissemination in Ad Hoc Wireless Networks. In Biologically Inspired Networking and Sensing: Algorithms and Architectures, ed. Pietro Lio and Dinesh Verma, 223-241 (2012), accessed March 29, 2012. doi:10.4018/978-1-61350-092-7.ch012.

Bibliography

[Al-Hazmi] Yahya Al-Hazmi, Hermann De Meer, Karin A. Hummel, Harald Meyer, Michela Meo and David Remondo. (Cited on pages 17 and 30.)

[ard] *Arduino*. Material Available at: Availableat:http://arduino.cc/. (Cited on pages 23 and 24.)

[Armour] S. Armour, T. O'Farrell, S. Fletcher, A. Jeffries, D. Lister, S. McLaughlin, J. Thompson and P. Grant. (Cited on page 17.)

[ath] *Ath9k*. Available at: http://linuxwireless.org/. (Cited on page 44.)

[Carroll 2010] Aaron Carroll and Gernot Heiser. *An analysis of power consumption in a smartphone*. In Proceedings of the 2010 USENIX conference on USENIX annual technical conference, USENIXATC'10, pages 21–21, Berkeley, CA, USA, 2010. USENIX Association. (Cited on pages 10 and 11.)

[Deruyck 2010] M. Deruyck, W. Vereecken, E. Tanghe, W. Joseph, M. Pickavet, L. Martens and P. Demeester. *Comparison of Power Consumption of Mobile WiMAX, HSPA and LTE Access Networks*. In Proc. of the Telecommunications Internet and Media Techno Economics (CTTE), pages 1–7, June 2010. (Cited on page 15.)

[Dufkova 2010] K. Dufkova, M. Bjelica, Byongkwon Moon, L. Kencl and J.-Y. Le Boudec. *Energy savings for Cellular Network with Evaluation of Impact on Data Traffic Performance*. In Proc. of IEEE EW, Lucca, Italy, 2010. (Cited on pages 16 and 17.)

[Ebert 2002] Jeanpierre Ebert, Brian Burns and Adam Wolisz. *A Trace–based Approach for Determining the Energy Consumption of a WLAN Network Interface*. In Proc. of the European Wireless Conference, pages 230–236, 2002. (Cited on pages 10, 11, 12 and 14.)

[ec] *Electricity and natural gas price statistics, European Commission*. Available at: http://epp.eurostat.ec.europa.eu/statistics_explained/index.php. (Cited on pages 3 and 4.)

[Elayoubi 2011] S.-E. Elayoubi, L. Saker and T. Chahed. *Optimal Control for Base Station Sleep Mode in Energy Efficient Radio Access Networks*. In INFOCOM, 2011 Proceedings IEEE, pages 106–110, April 2011. (Cited on pages 16 and 17.)

[EPC] *Power Control*. Material Available at: http://www.gude.info/index.php. (Cited on pages 12, 95, 105 and 109.)

[Ergen 2007] M. Ergen and P. Varaiya. *Decomposition of Energy Consumption in IEEE802.11*. In Proc. of IEEE ICC, pages 403–408, Glasgow, Scotland, June 2007. (Cited on pages 13 and 14.)

[EUF] *European Union Funded Projects Information in Green Networks*. Material Available at: http://cordis.europa.eu/fp7/ict/sustainable-growth/. (Cited on page 4.)

[Feeney 2001] Laura Marie Feeney and Martin Nilsson. *Investigating the Energy Consumption of a Wireless Network Interface in an Ad Hoc Networking Environment*. In Proc. of the Twentieth Annual Joint Conference of the IEEE Computer and Communications Societies, Anchorage, USA, April 2001. (Cited on pages 10, 11, 12, 14, 22 and 35.)

[Fehske 2009] Albrecht J. Fehske, Fred Richter and Gerhard P. Fettweis. *Energy Efficiency Improvements through Micro Sites in Cellular Mobile Radio Networks*. In Proc. of the IEEE Global Communications Conference, pages 1–5, 2009. (Cited on page 18.)

[Fischer 2011] T. Fischer, T. Hühn, R. Kuck, R. Merz, J. Schulz-Zander and C. Sengul. *Experiences with BOWL: managing an outdoor WiFi network (or how to keep both internet users and researchers happy?)*. In Proceedings of the 25th international conference on Large Installation System Administration, LISA'11, pages 24–24, Berkeley, CA, USA, 2011. USENIX Association. (Cited on page 44.)

[GAP 2012] *Global Action Plan*, 2012. Available at: http://www.globalactionplan.org.uk/. (Cited on page 4.)

[Garcia-Saavedra 2011] Andres Garcia-Saavedra, Pablo Serrano, Albert Banchs and Matthias Hollick. *Energy–efficient Fair Channel Access for IEEE 802.11 WLANs*. In Proc. of the World of Wireless, Mobile and Multimedia Networks (WoWMoM), 2011 IEEE International Symposium on a, pages 1–9, June 2011. (Cited on page 14.)

[Gast 2003] Matthew Gast. *When Is 54 Not Equal to 54? A Look at 802.11a, b, and g Throughput*, 2003. Material Available at: http://www.oreillynet.com/pub/a/wireless/2003/08/08/wireless_throughp\ut.html. (Cited on page 80.)

[Göndör 2011] S. Göndör, A. Uzun and A. Küpper. *Towards a Dynamic Adaption of Capacity in Mobile Telephony Networks using Context Information*. In Proceedings of the 11th International Conference on ITS Telecommunications, pages 606–612, St. Petersburg, Russia, Aug 2011. IEEE. (Cited on page 94.)

[Gomez 2011] K. Gomez, R. Riggio, T. Rasheed, F. Granelli, Miorandi D. and Chlamtac I. *Analysing the energy consumption behaviour of WiFi networks*.

In Proc. of IEEE GreenCom, September 2011. (Cited on pages 8, 12, 22 and 93.)

[Gomez 2012a] Karina Gomez, Dejene Boru, Roberto Riggio, Tinku Rasheed, Daniele Miorandi and Fabrizio Granelli. *Measurement–based Modelling of Power Consumption at Wireless Access Network Gateways*. Computer Networks, vol. 56, pages 2506–2521, July 2012. (Cited on pages 8, 12, 22 and 93.)

[Gomez 2012b] Karina Gomez, Roberto Riggio, Tinku Rasheed, Daniele Miorandi and Fabrizio Granelli. *Energino: an Hardware and Software solution for Energy consumption monitoring*. volume 56, pages 2506–2521, May 2012. (Cited on pages 7, 32, 93, 95 and 105.)

[Gomez 2013] Karina Mabell Gomez, Cigdem Sengul, Nico Bayer, Roberto Riggio, Tinku Rasheed and Daniele Miorandi. *MORFEO: Saving Energy in Wireless Access Infrastructures*. In 14th IEEE International Symposium on a World of Wireless, Mobile and Multimedia Networks (IEEE WoWMoM 2013), Madrid, Spain, June 2013. (Cited on page 8.)

[gw1] *Warming to evolution: University of California, Berkeley*. Available at: `http://evolution.berkeley.edu/evolibrary/news/060701_warming`. (Cited on page 3.)

[gw2] *Global Warming Fast Facts, National Geographic News*. Available at: `http://environment.nationalgeographic.com/environment/global-warming/`. (Cited on page 3.)

[gw3] *Global Climate Change and Biodiversity University of East Anglia, Summary of papers and discussion*. Available at: `www.jncc.gov.uk/pdf/MJHGlobalclimatechange_14.08.03.pdf`. (Cited on page 3.)

[Halperin 2010] Daniel Halperin, Ben Greenstein, Anmol Sheth and David Wetherall. *Demystifying 802.11n Power Consumption*. In Proc. of the 2010 International Conference on Power Aware Computing and Systems, HotPower'10, pages 1–5, Berkeley, CA, USA, 2010. USENIX Association. (Cited on pages 10, 11, 13 and 14.)

[iee] *Why Are Electricity Prices Increasing?, Edison Electric Institute (IEE)*. Available at: `http://www.eei.org/ourissues/finance/Documents/Brattle_Report.pdf`. (Cited on page 3.)

[iee 2007] *IEEE Standard for Information technology-Telecommunications and information exchange between systems-Local and metropolitan area networks-Specific requirements - Part 11: Wireless LAN Medium Access Control (MAC) and Physical Layer (PHY) Specifications*, Jun. 2007. (Cited on page 80.)

[ipe] *Iperf Traffic Generator*. Available at: http://iperf.sourceforge.net/. (Cited on pages 32 and 59.)

[J.-M. 2010] Kelif J.-M., Coupechoux M. and F. Marache. *Limiting Power Transmission of Green Cellular Networks: Impact on Coverage and Capacity*. Communications (ICC) IEEE International Conference, pages 1–6, May 2010. (Cited on page 18.)

[Jardosh 2009] Amit P. Jardosh, Konstantina Papagiannaki, Elizabeth M. Belding, Kevin C. Almeroth, Gianluca Iannaccone and Bapi Vinnakota. *Green WLANs: On-Demand WLAN Infrastructures*. Mob. Netw. Appl., vol. 14, pages 798–814, December 2009. (Cited on pages 4, 17 and 30.)

[Lochin 2003] Emmanuel Lochin, Anne Fladenmuller, Jean yves Moulin, Serge Fdida and A Manet. *Energy Consumption Models for Ad-Hoc Mobile Terminals*. In In Med-Hoc Net, 2003. (Cited on page 11.)

[Lorincz 2010] Josip Lorincz, Antonio Capone and Massimo Bogarelli. *Energy Savings in Wireless Access Networks through Optimized Network Management*. In Proc. of the 5th IEEE International Conference on Wireless Pervasive Computing, pages 449–454, Mondena, Italy, 2010. IEEE Press. (Cited on pages 17 and 18.)

[Marsan 2009] M.A. Marsan, L. Chiaraviglio, D. Ciullo and M. Meo. *Optimal Energy Savings in Cellular Access Networks*. In Proc. of IEEE ICC, Dresden, Germany, 2009. (Cited on pages 16 and 17.)

[Marsan 2010] Marco Ajmone Marsan and Michela Meo. *Energy Efficient Management of two Cellular Access Networks*. SIGMETRICS Perform. Eval. Rev., vol. 37, pages 69–73, Mar. 2010. (Cited on page 16.)

[Micallef 2010] G. Micallef, P. Mogensen and H. O. Scheck. *Cell Size Breathing and Possibilities to Introduce Cell Sleep Mode*. European Wireless Conference, pages 111–115, April 2010. (Cited on pages 4, 16 and 17.)

[Nedevschi 2008] S. Nedevschi, S. Ratnasamy and J. Padhye. *Hot Data Centers vs. Cool Peers*. In Proceedings of HotPower–Workshop on Power Aware Computing and Systems, December 2008. (Cited on page 17.)

[Pathak 2011] Abhinav Pathak, Y. Charlie Hu and Ming Zhang. *Bootstrapping energy debugging on smartphones: a first look at energy bugs in mobile devices*. In Proceedings of the 10th ACM Workshop on Hot Topics in Networks, HotNets-X, pages 5:1–5:6, New York, NY, USA, 2011. ACM. (Cited on page 11.)

[Pentikousis 2010] K. Pentikousis. *In Search of Energy–Efficient Mobile Networking*. IEEE Communications Magazine, vol. 48, no. 1, pages 95–103, 2010. (Cited on page 16.)

[Perrucci 2008] G.P. Perrucci, F.H.P Fitzek, G. Sasso and M. Katz. *Energy Saving Strategies for Mobile Devices using Wake–up Signals*. In 4th International Mobile Multimedia Communications Conference (MobiMedia 2008), Oulu, Finland, 2008. ICTS/ACM. (Cited on page 16.)

[Rantala 2009] Enrico Rantala, Arto Karppanen, Seppo Granlund and Pasi Sarolahti. *Modeling energy efficiency in wireless internet communication*. In Proceedings of the 1st ACM workshop on Networking, systems, and applications for mobile handhelds, MobiHeld '09, pages 67–68, New York, NY, USA, 2009. ACM. (Cited on page 11.)

[RFG 2008] *Impacts of Information and Communication Technologies on Energy Efficiency*, 2008. Available at: `http://ec.europa.eu/information_society/activities/sustainable_growth/docs/studies/2008/2008_bio_ict4ee-summary_en.pdf`. (Cited on page 4.)

[Rice 2010] Andrew Rice and Simon Hay. *Measuring mobile phone energy consumption for 802.11 wireless networking*. Pervasive Mob. Comput., vol. 6, no. 6, pages 593–606, December 2010. (Cited on pages 10 and 11.)

[Richter 2010] Fred Richter, Albrecht J Fehske, Patrick Marsch and Gerhard P. Fettweis. *Traffic Demand and Energy Efficiency in Heterogeneous Cellular Mobile Radio Networks*. Vehicular Technology Conference, pages 1–6, May 2010. (Cited on page 18.)

[Riggio] Roberto Riggio, Karina Mabell Gomez, Tinku Rasheed and Cigdem Sengul. (Cited on pages 8 and 94.)

[Saker 2009] L. Saker, S.E. Elayoubi and H.O. Scheck. *System Selection and Sleep Mode for Energy Saving in Cooperative 2G/3G Networks*. Vehicular Technology Conference Fall,, pages 1–5, September 2009. (Cited on page 16.)

[sma 2010] *SMART 2020: Enabling the low carbon economy in the information age*, 2010. Available at: `www.smart2020.org/_assets/files/02_Smart2020Report.pdf`. (Cited on page 4.)

[Tauber 2011] M. Tauber, S. N. Bhatti and Y. Yu. *Application Level Energy and Performance Measurements in a Wireless LAN*. In Proc. of the GreenCom2011 - IEEE/ACM 2011 International Conference on Green Computing and Communications, Chengdu, Sichuan, China, August 2011. (Cited on page 14.)

[Uzun 2012] A. Uzun, S. Göndör, N. Bayer, L. Kollecker and A. Küpper. *Visualizing the Effects of Power Management Algorithms for Mobile Networks under Realistic Conditions*. In Proceedings of the Conference on Electronics Goes Green 2012, Berlin, Germany, Sep. 2012. IEEE. (Cited on pages 31, 95, 106 and 109.)

[wat] *Watts Up?* Material Available at: https://www.wattsupmeters.com/. (Cited on pages 12, 21 and 59.)

[Watanabe 2012] Takahiro Watanabe, Koji Minoura, Fumiko Watanabe Nara, Koji Shichi, Kazuho Horiuchi, Takeshi Kakegawa and Takayoshi Kawai. *Last glacial to post glacial climate changes in continental Asia inferred from multi-proxy records from Lake Hovsgol, northwest Mongolia*. Global and Planetary Change, vol. 88-89, no. 0, pages 53 – 63, 2012. (Cited on page 3.)

[Xiao 2010] Yu Xiao, Petri Savolainen, Arto Karppanen, Matti Siekkinen and Antti Ylä-Jääski. *Practical Power Modeling of Data Transmission over 802.11g for Wireless Applications*. In Proc. of the 1st International Conference on Energy-Efficient Computing and Networking, e–Energy'10, pages 75–84, New York, USA, 2010. ACM. (Cited on pages 13 and 14.)

List of Abbreviations

η_i Energy efficiency of the WAD

AP_{Rx} AP is

AP_{Tx} AP is acting as a transmitter

E_b Energy cost per bit

I_{real} Actual converting current consumed

$L^*(\hat{T})$ Optimal message size to saving energy

$R_{Tx/Rx}(x)$ Power Consumption Model as a function of traffic load

$S_{Rx/Tx}(s)$ Power Consumption Model as a function of datagram size

t^* Minimum time the WAD needs to be in Off Mode in order to save energy

t^+ Minimum time the WAD needs to be in Partial/Sector Sleep Mode in order to save energy

V_{real} Actual converting voltage consumed

16–QAM 16–Quadrature Amplitude Modulation

64–QAM 64–Quadrature Amplitude Modulation

AC Active Condition

APP Applications Software

APPs Applications Software

BE Best Effort

BOWL Berlin Open Wireless Lab

BPSK Binary Phase Shift Keying

BS WiMAX Base Station

BS–Receiver BS is

BS–Transmitter BS is acting as a transmitter

CCA Context Collecting Agent

CoMa Context Manager

CTS Clear to Send

DCF Distributed Coordination Function

EC Energy Controller

ED Energy Decisions

EPC Expert Power Controller

EU European Union

FSM finite state machine

HC Head Condition

HSPA High Speed Packet Access

IC Idle Condition

ICT Information and Communication Technology

IDE Integrated Development Environment

INET Intelligent Networks

LTE Long Term Evolution

MAC Medium Access Control

MIMO Multiple–Input/Multiple–Output

MTU Maximum Transmission Unit

NIC Network Interface Card

NIDAM National Instruments 6218 Data Acquisition Module

nrtPS Non–real–time Polling Service

OM Off Mode

PDU Protocol Data Unit

PSM Partial Sleep Mode

QoS Quality of Service

QPSK Quadrature Phase Shift Keying

rtPS Real–time Polling Service

RTS Request To Send

SEAR Resource on–demand Strategy Power on or off Resources

SS Subscriber Station

SSM Sector Sleep Mode

SSR Solid State Relay

UGS Unsolicited Grant Service

VDC Volts Direct Current

VS Visualizer

W Watts

WADs Wireless Access Devices

WiFi Wireless Fidelity

WiMAX Worldwide Interoperability for Microwave Access

WLANs Wireless Local Area Network

WWAN Wireless Wide Area Network

ZC Zero condition

This page is intentionally left blank